FACTORS INFLUENCING SEISMICITY IN SOUTH-CENTRAL KANSAS AND NORTHERN OKLAHOMA

A Thesis by

Tyler Selves

Bachelor of Arts, Wichita State University, 2015

Submitted to the Department of Geology
and the faculty of the Graduate School of
Wichita State University
in partial fulfillment of
the requirements for the degree of
Master of Science

May 2017

FACTORS INFLUENCING SEISMICITY IN SOUTH-CENTRAL KANSAS AND NORTHERN OKLAHOMA

The following faculty members have examined the final copy of this thesis for form and content, and recommend that it be accepted in partial fulfillment of the requirement for the degree of Master of Science with a major in Earth, Environmental, and Physical Sciences.

Bill Bischoff, Committee Chair

Keith Gray, Committee Member

David Hughes, Committee Member

Andrew Swindle, Committee Member

ABSTRACT

Waste water injection and seismicity in south-central Kansas and northern Oklahoma increased dramatically from 2010 to 2016. Areas with increased well counts, elevated disposal pressures, and elevated injection volumes correlate with locations of seismic activity. The locations, history of injection, and seismic activity in three areas of interest (AOI) were examined with the aid of aeromagnetic maps to determine if seismic activity was induced by well activity in close proximity. A major northeast-southwest trend is observed in disposal well locations, earthquakes, and NewMag residual aeromagnetic maps. Moment tensors (focal mechanisms) from 180 earthquakes were obtained and detected strike-slip, normal, and reverse faulting. Eight of the strongest earthquakes (4.5-5.8 magnitude) were located along the margins of seismically active areas in Kansas and Oklahoma. A vast majority of earthquake foci are within Precambrian basement rock. The largest increases in both, seismic activity and injected volumes occurred in Harper County, Kansas as well as Grant and Alfalfa County, Oklahoma. Disposal well count increased after 2011, and by 2013 a majority of the new wells in Alfalfa, Grant, and Harper Counties disposed between 1 million barrels (MMBBL) to approximately 17MMBB per well/per year. Some of these wells also used injection pressures in excess of 300 pounds per square inch (PSI) per well/per year. By applying proper disposal practices, obtaining in-situ reservoir properties of the injection interval, and avoiding areas susceptible to seismic events, a reduction in seismic activity could occur.

TABLE OF CONTENTS

LIST OF TABLES

LIST OF FIGURES

LIST OF FIGURES (continued)

LIST OF ABBREVIATIONS

AOI	Area of Interest
PSI	Pounds per Square Inch
MMBBL	Millions of Barrels
SCP	Southern Central Plains Orogen
SGR	Southern Granite – Rhyolite Province
SWD	Salt Water Disposal Well(s)
UIC	Underground Injection Control Well(s)
MCR	Midcontinent Rift System
U-Pb	Uranium – Lead
Rb-Sr	Rubidium – Strontium
Sm-Nd	Samarium – Neodymium
mW/m2	milliWatt per Square Meter

GLOSSARY LIST OF TERMS

Residual Aeromagnetics – Measurement of the magnetic susceptibility of Earth's magnetic field in a given area, flown by an aircraft at a known elevation, in a known flight path.

Magnetic susceptibility – a dimensionless proportionality constant that indicates the degree of magnetization of a material in response to an applied magnetic field.

Basement – Precambrian crystalline, igneous, and/or metamorphic rock underling Cambrian to Tertiary sedimentary cover.

Shear Zone – An area in Earth's crust and upper mantle that forms as a response to deformation that partitions fault blocks of varying magnetic susceptibility in high strain zones, and can be 1-6 miles wide.

Suture Zone – A joining together along a major fault zone, of separate terranes, tectonic units that have different plate tectonic, metamorphic and paleogeographic histories.

Induced Seismicity – Earthquakes and tremors that are caused by human activities and alter the stress and strain on and within Earth's crust.

NewMag – An aeromagnetic map developed by Applied Geophysics Inc.

Moment Tensor – A mathematical representation of the type of movement on a fault during an earthquake. Describes the deformation in the source region that generates the seismic waves. Also called a focal mechanism.

Fault Block Pattern – Sets of parallel to sub-parallel fractures (shear zones) that strike in different directions and bound fault blocks within basement rock.

Terrane – A fragment of crustal material formed on, or broken off from, one tectonic plate and accreted or "sutured" to crust lying on another plate.

INTRODUCTION

Seismic activity in the central midcontinent region has increased dramatically in recent years. The study area is located in the following Kansas counties: Comanche, Kiowa, Barber, Pratt, Kingman, Sedgwick, Sumner, and Harper, as well as the following Oklahoma counties: Woods, Alfalfa, Grant, and Kay (Fig. 1). The Sedgwick Basin, Pratt anticline, Anadarko shelf, and Nemaha Uplift represent major tectonic elements of the study area (Fig. 2). From 1980 to 2012, 18 earthquakes (>2.0M) occurred within the study area, while 5,837 events (>2.0M) span 2013 to 2015 (Fig. 3). Waste water injection has also increased by approximately 450 million barrels (MMBBL) from 2012 to 2014, suggesting a possible correlation between the data (Fig. 4). Seismic activity is not uncommon in Oklahoma; however, since 2009, Oklahoma and Kansas have experienced over 9,000 earthquakes (>2.0M). By 2013, activity migrated north into the study area (USGS earthquake Catalog, accessed March, 2017). From 2013 to 2016, 6,153 earthquakes (>2.0M) occurred in the study area alone. The most frequent hypocenter depths recorded were between 5 and 7 km (Fig. 5). In 2005, 108 MMBBL of waste water were disposed in the study area and by 2015, 763 MMBBL of waste water were disposed in the study area (Fig. 4) (Appendix 1). Oklahoma injected approximately 68% of all waste water into the Cambrian-Ordovician aged Arbuckle Group in 2014 (Murray, 2015). The Kansas Corporation Commission (KCC) did not record injection intervals until 2014-2015, when the Arbuckle Group was primarily targeted for injection (Kansas Corporation Commission, 2016). In the present study, three areas of interest will be evaluated to determine possible factors influencing seismic events in the area. Based on these evaluations, suggestions of how to safely reduce the amount of earthquakes are offered.

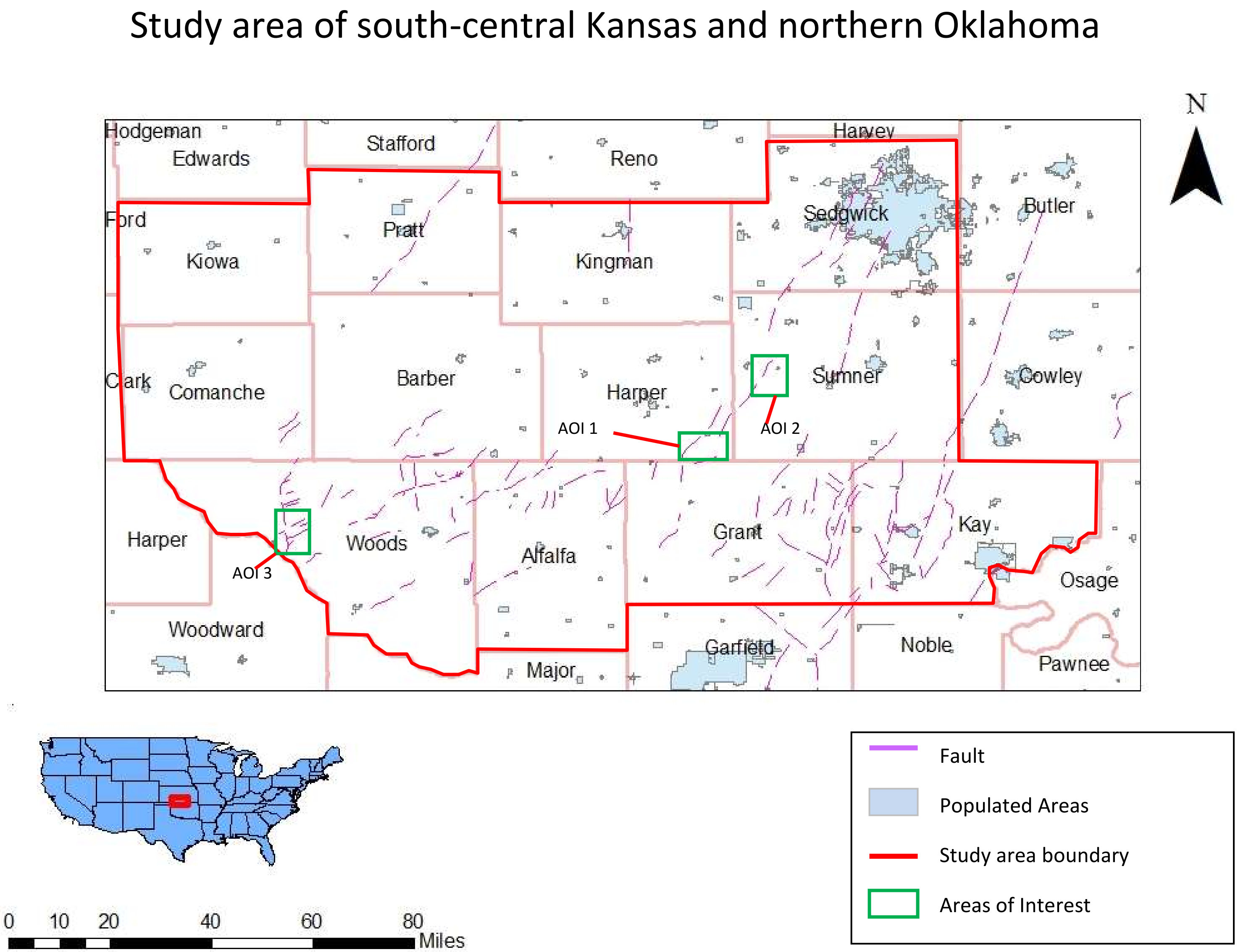

Figure 1: Study area with inset map of the study area. Study area outlined in red. Areas of interest (AOI) in green. Faults in Oklahoma modified by Holland (2015).

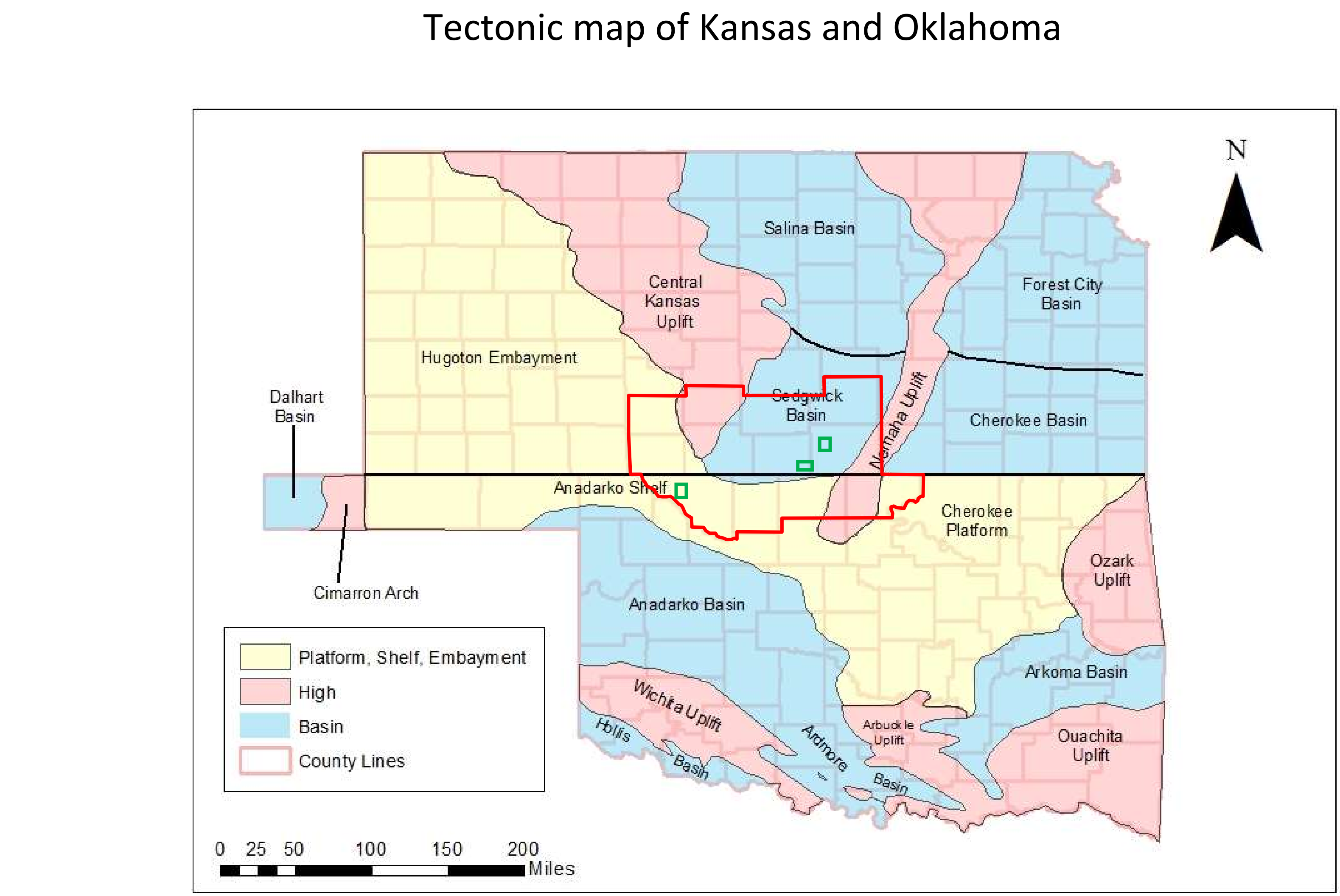

Figure 2: Tectonic map of Kansas and Oklahoma. Outlined in red is the study area, with AOI's in green. (Modified from KGS, accessed 2017 and OGS, accessed 2017).

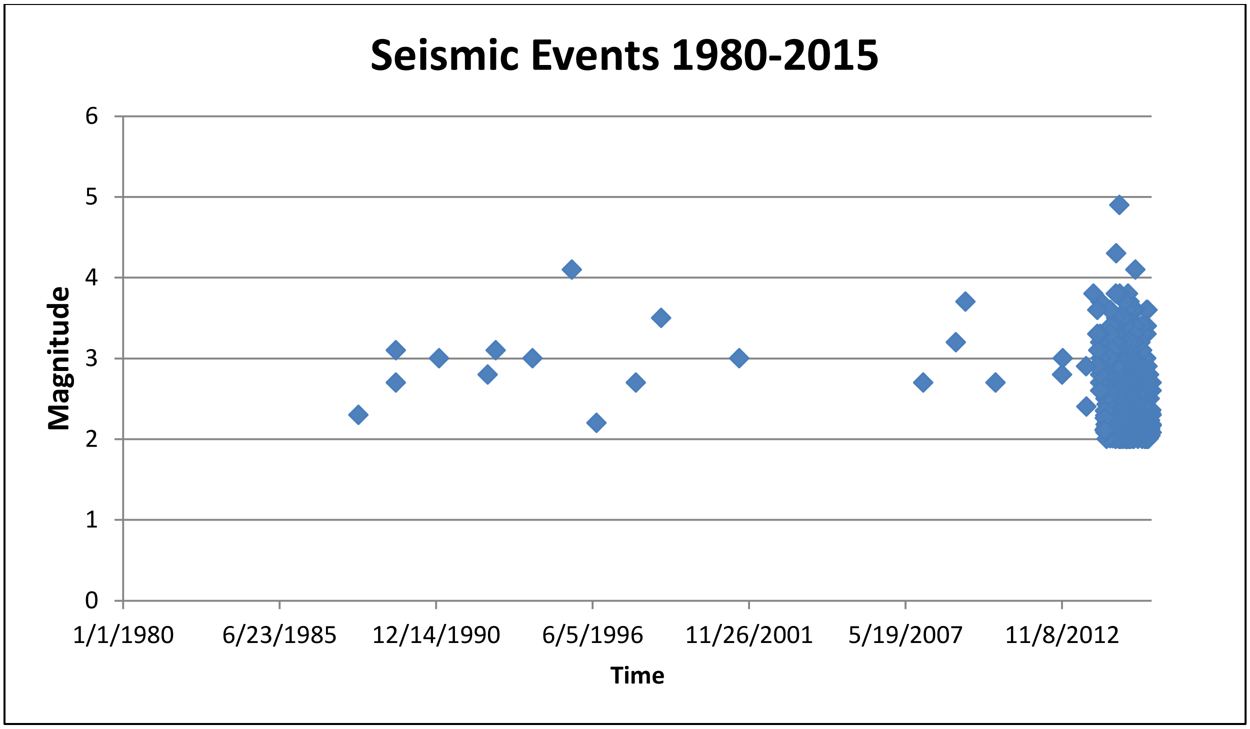

Figure 3: Distribution of earthquake magnitudes (>2.0M) from 1980-2015 in the study area.

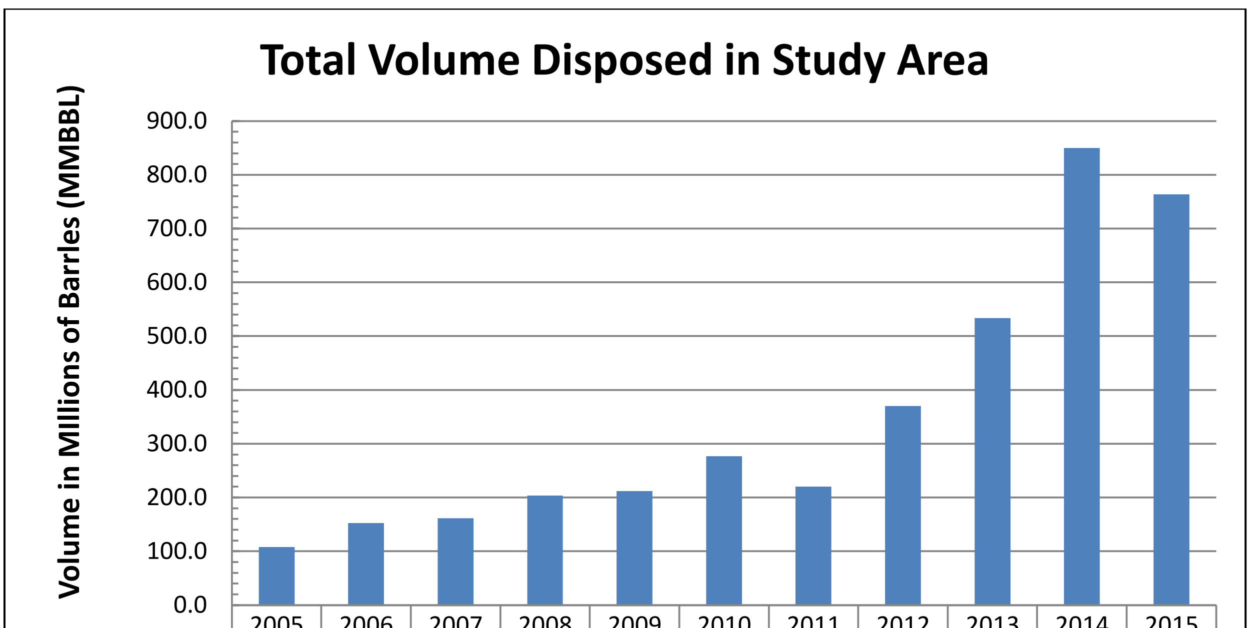

	2005	2006	2007	2008	2009	2010	2011	2012	2013	2014	2015
Total Volume	108.2	152.7	161.4	203.7	211.7	276.6	220.4	369.8	533.7	849.7	763.4

Figure 4: Total volume of disposed waste water from 2005-2015 in the study area. Values in millions of barrels.

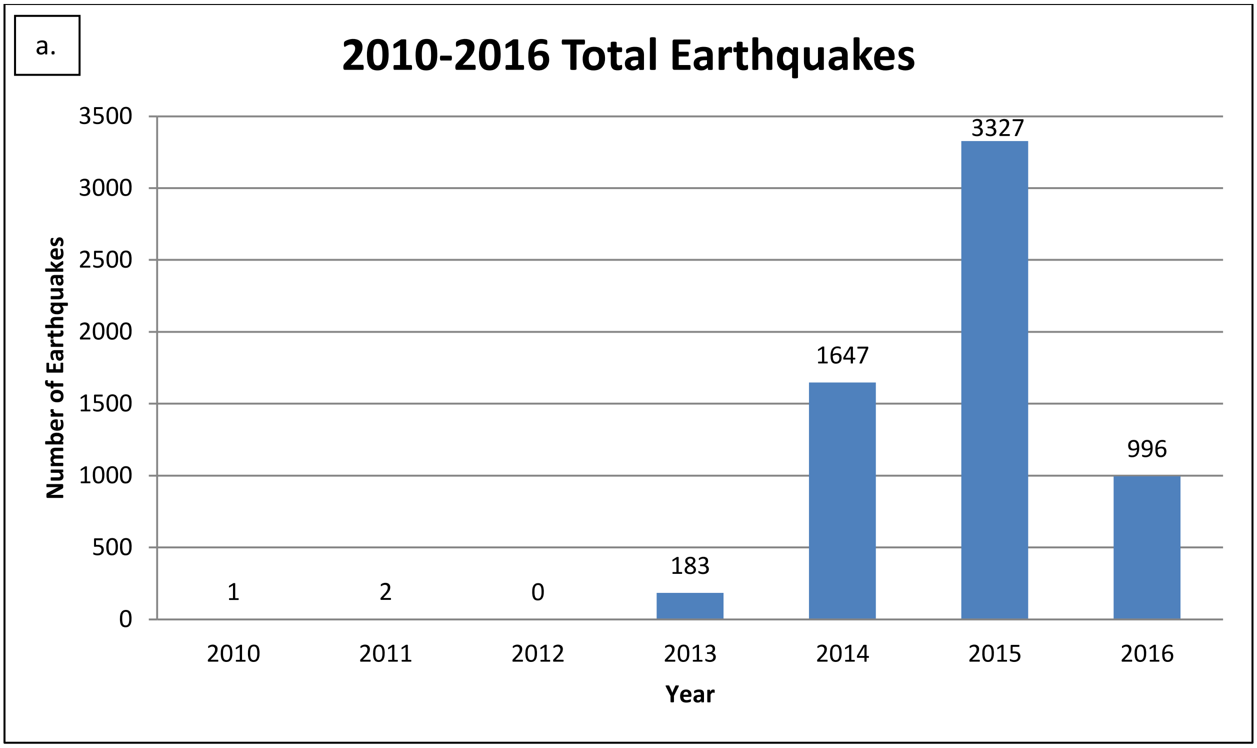

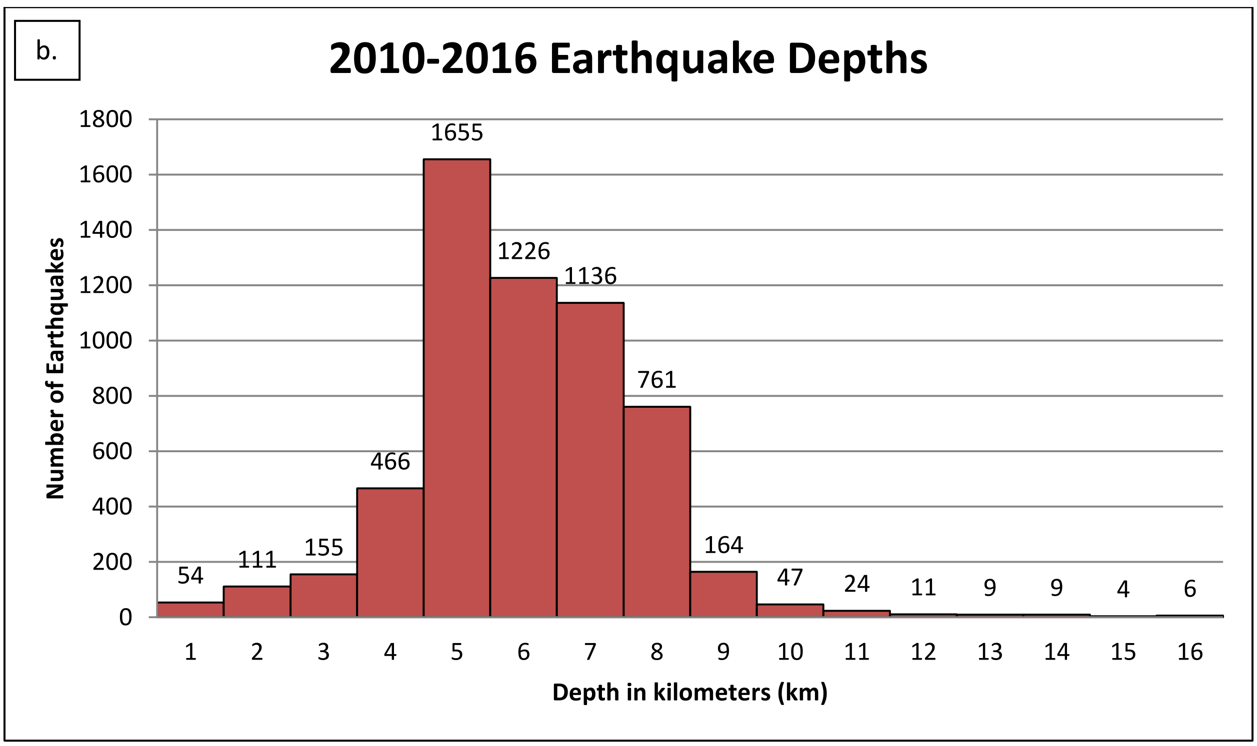

Figure 5: Earthquakes (>2.0M) are from 2010-2016. a) Number of earthquakes in the study area by year. b) Histogram of focal point depth in kilometers (km).

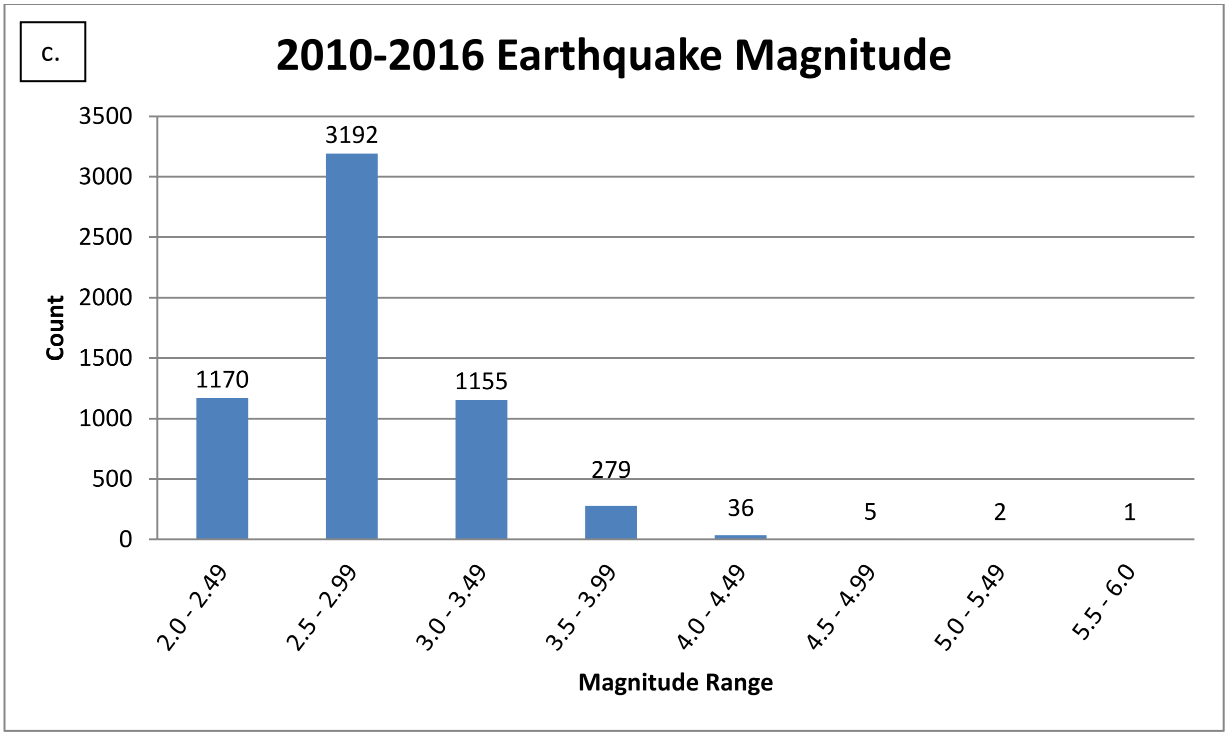

Figure 5 continued: c) Number of earthquakes by magnitude in the study area.

1.1 Previous Studies

Several studies propose a causal link between an individual or series of injection wells to a series of earthquakes. An injection well in Paradox Valley, Colorado, was determined to be the cause of the seismic activity in the area from 1996-2013. Some of these events were detected up to 16 km (9.9 miles) from the injection well (Ake and others, 2005). Another study examined potential induced seismic activity in Prague, Oklahoma that produced a swarm of earthquakes, including a 5.7M (Keranen and others, 2013). An experiment in Rangely, Colorado observed the effects of controlling seismic activity by injecting and recovering the injected water from wells (Raleigh and others, 1976). Other studies of possible induced seismicity include Rooks County, Kansas (Armbruster and others, 1989) and Youngstown, Ohio (Holtkamp and others, 2015). Research has been conducted by the Oklahoma Geologic Survey (OGS) over seismicity in Oklahoma (Darold and others, 2015), injection well data by geologic zone in Oklahoma (Murray, 2014, 2015), and a regional study over Nebraska, Kansas, and Oklahoma injection well volumes (Murray and Holland, 2014). This study will focus on injection volumes, pressures, and possible relations to seismicity in south-central Kansas and northern Oklahoma.

The Southern Granite-Rhyolite province (SGR), a Mesoproterozoic terrane (Fig. 6), comprises the basement rock which underlies all sedimentary cover from Cambrian Reagan Sandstone and Arbuckle Group to Permian rocks in some areas along the Nemaha Uplift (Kelly and Merriam, 1964); (McBee, 2003) (Fig. 7). Residual aeromagnetic maps measure the magnetic susceptibility of basement lithology in the study area. Based on the juxtaposition of magnetic high and low readings, a basement fault block pattern is interpreted. Fault blocks are separated by shear zones approximately 1 to 6 miles wide and occur in parallel and sub-parallel sets that are orthogonally cut by other shear zone sets. The locations of the interpreted shear zones coincide with faults mapped in the overlying sedimentary section (Gay, 1986) (Fig. 8). Shields are large areas of exposed Precambrian crystalline igneous and metamorphosed rocks that form tectonically stable areas. The Canadian Shield in southern Quebec also depicts abundant basement fractures that lack in the Paleozoic onlap of the Ontario Basin (Appendix 5). The Guyana Shield in Venezuela and Brazil also reveals 4 facture directions that fall into 2 orthogonal sets (Appendix 6) (Gay, 2009). These areas resemble the shear zones sets identified in aeromagnetic maps of the study area (Fig. 9). Gay (1986) identifies several tectonic boundaries in Kansas and separates them into five terranes. These terranes are groups of fault blocks and shear zones trending in similar directions (Fig. 9). Earthquake focal points are located along magnetically mapped shear zones that outline basement fault blocks.

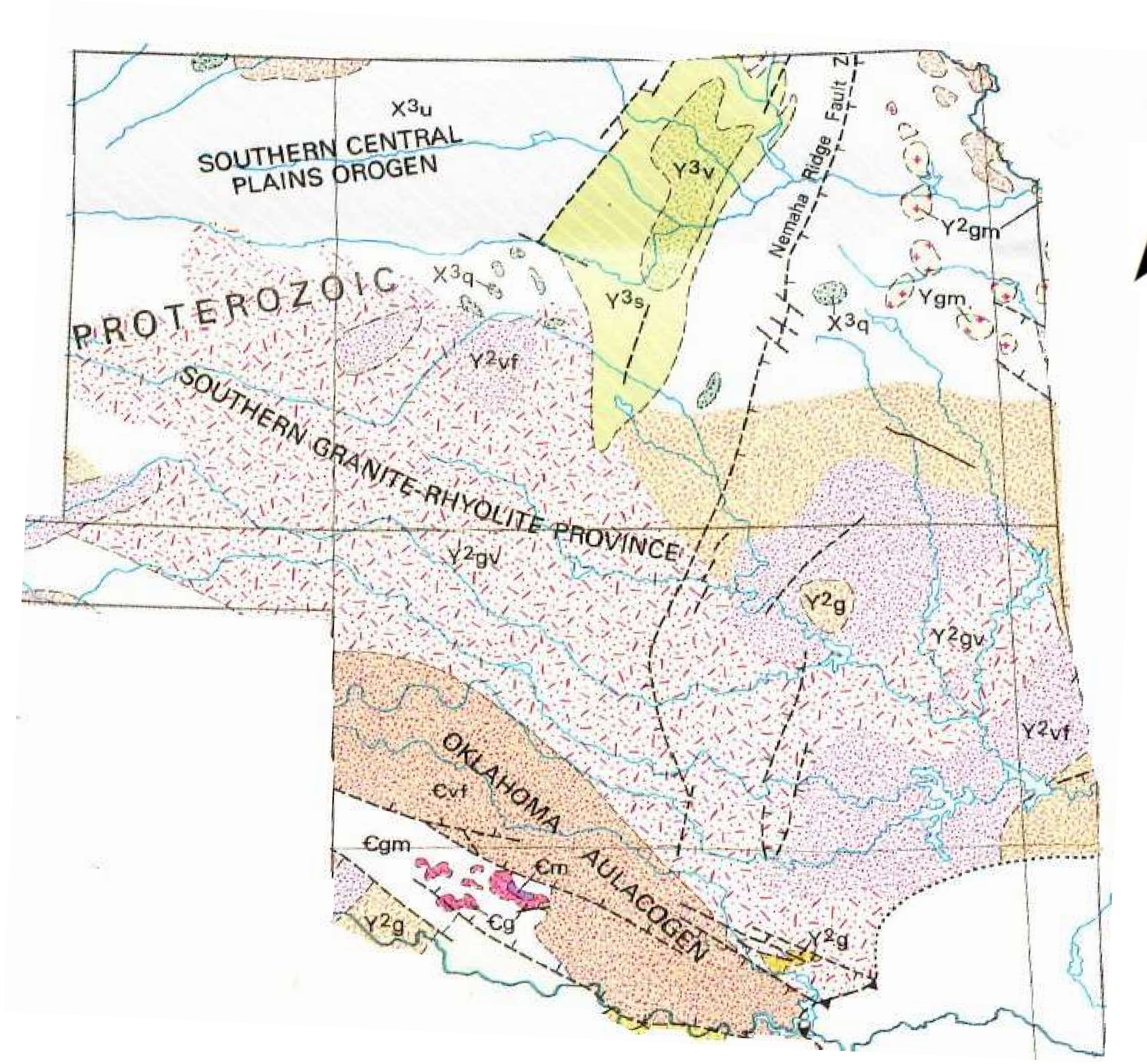

Figure 6: Kansas and Oklahoma map from; Map of Precambrian rocks of the conterminous United States modified from Reed (1993). Lithology types as follows; (Y2vf) Rhyolite and associated rocks of the 1.34-1.4 Ga suite in the Southern Granite-Rhyolite Province. (Y2gv) Granite and volcanic rocks of the 1.34-1.4 Ga suite in the Southern Granite-Rhyolite Province. (Y2g)Granitic rocks of the 1.34-1.4 Ga suite –Plutons in the Southern Granite-Rhyolite Province. (Y3s)(Y3v) Rocks associated with the MCR. (Cvf) Carlton Rhyolite Group and related rocks in the southern Oklahoma aulacogen. (Cm) Gabbro of the Wichita Granite Group. (Cg) Granite and anorthosite of the Wichita Granite Group. (Cgm) Granite, gabbro, and associated rocks of the Wichita Granite Group. (X3q) Quartzite-Sioux Quartzite, Baraboo Quartzite, and related rocks. (Ygm) Magnetite-bearing anorogenic granites. (Y2gm) Magnetite-bearing granitic rocks in the Southern Granite-Rhyolite Province. (X3u) Metasedimentary and metaigneous rocks of the Central Plains orogeny.

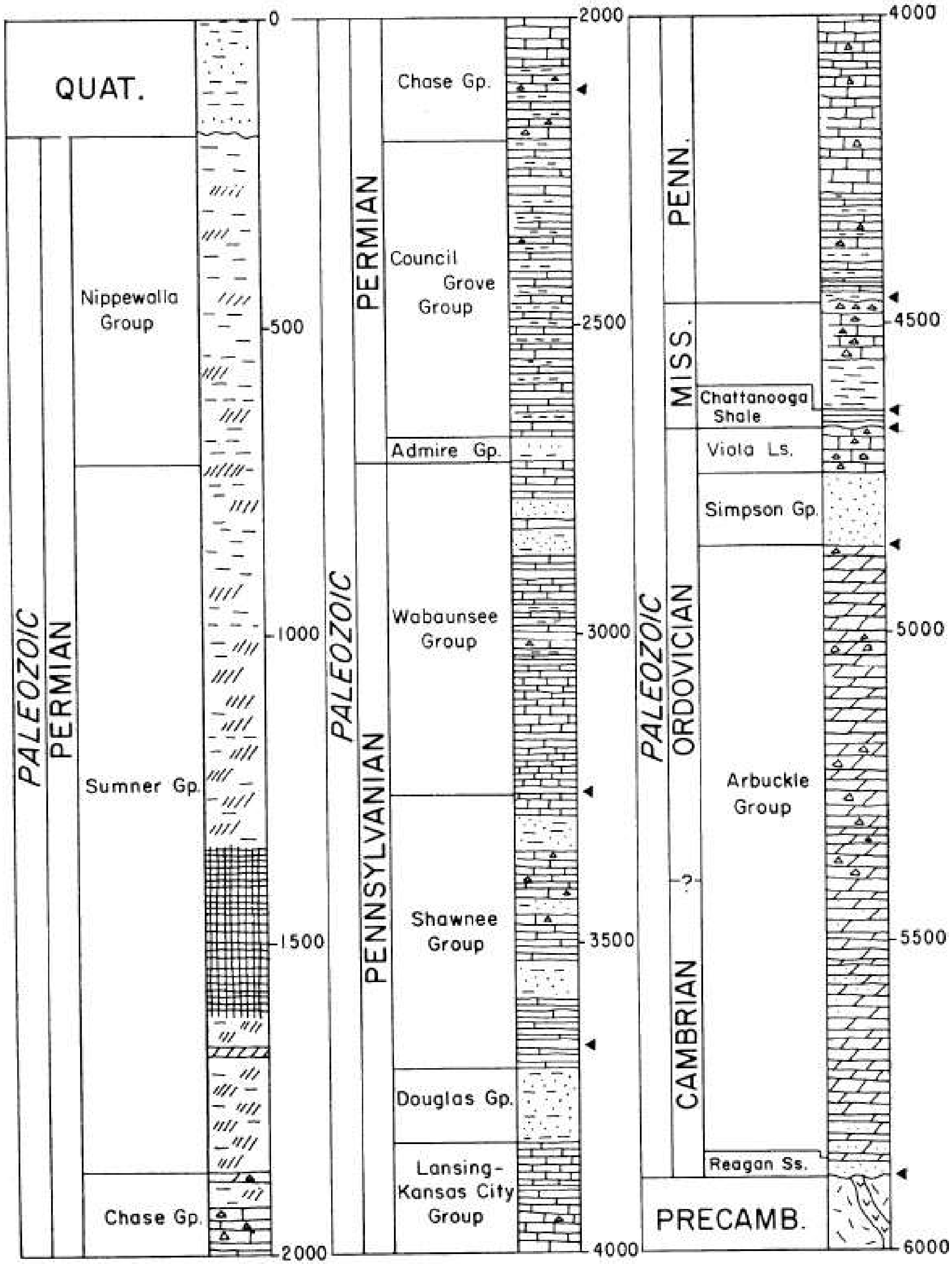

Figure 2. Generalized stratigraphic column showing major rock units present in Sedgwick Basin. About 6,500 feet of sedimentary rocks overlie Precambrian basement complex in deepest part of basin. Arrows indicate limits of isopachous intervals described. Conventional stratigraphic symbols are used.

Figure 7: Stratigraphic column of the Sedgwick Basin (Kelly and Merriam, 1964).

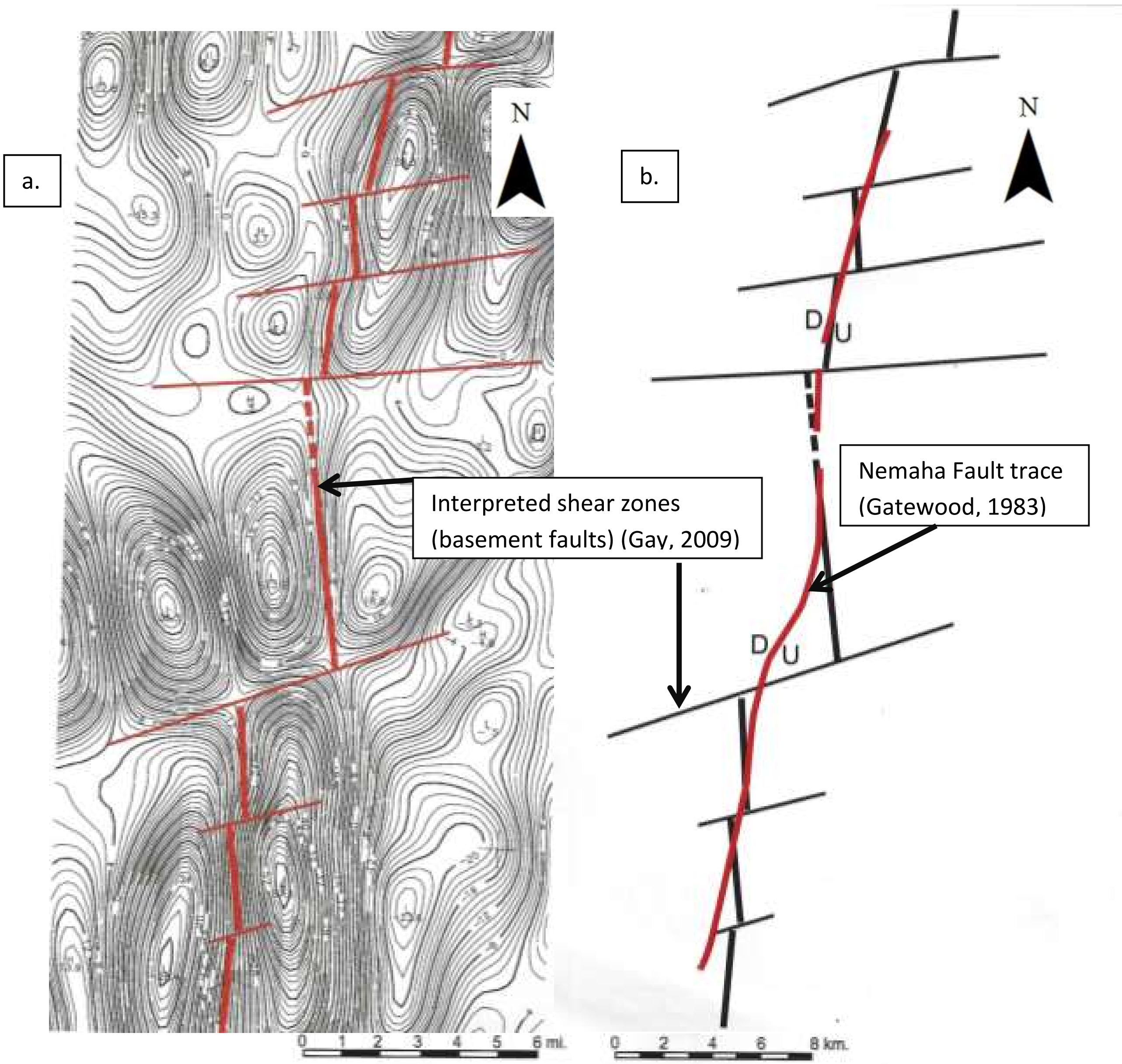

Figure 8: a) An example of a NewMag residual magnetic map of a portion of the Nemaha Uplift in Kay County, Oklahoma. A few proposed basement faults are superimposed in red. b) West bounding Pennsylvanian-age Nemaha fault (red) vs. basement fault system interpreted from aeromagnetic data. The Nemaha fault trace is from Gatewood (1983). Figures from Gay (2009).

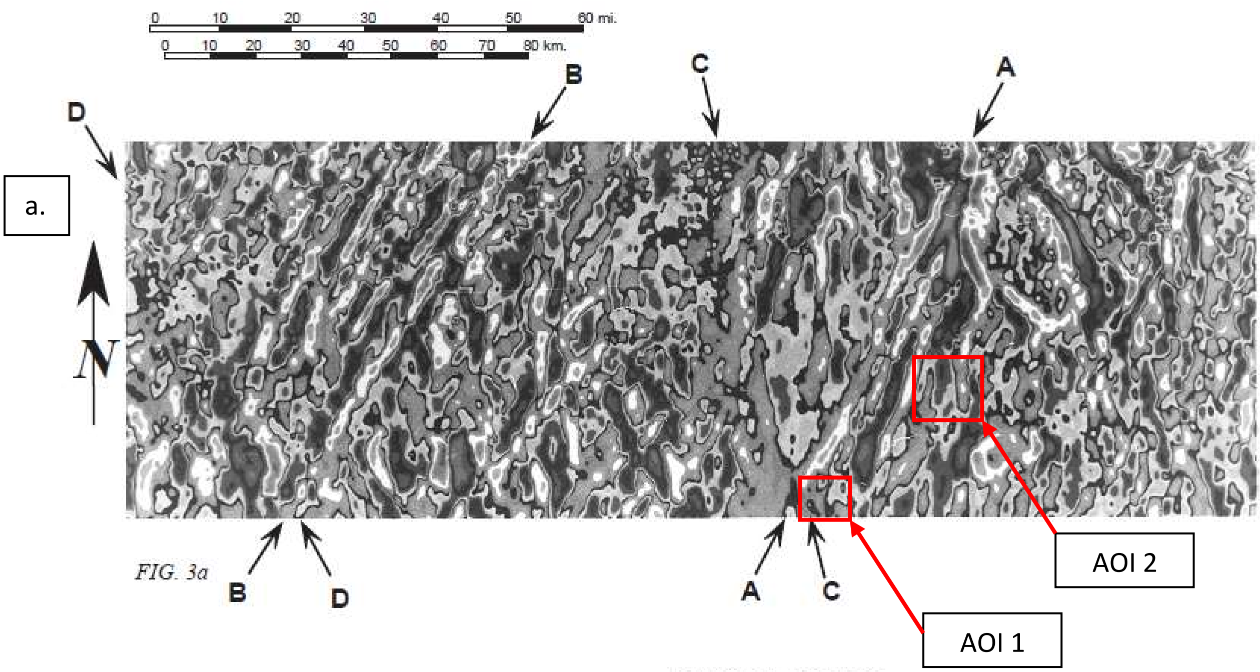

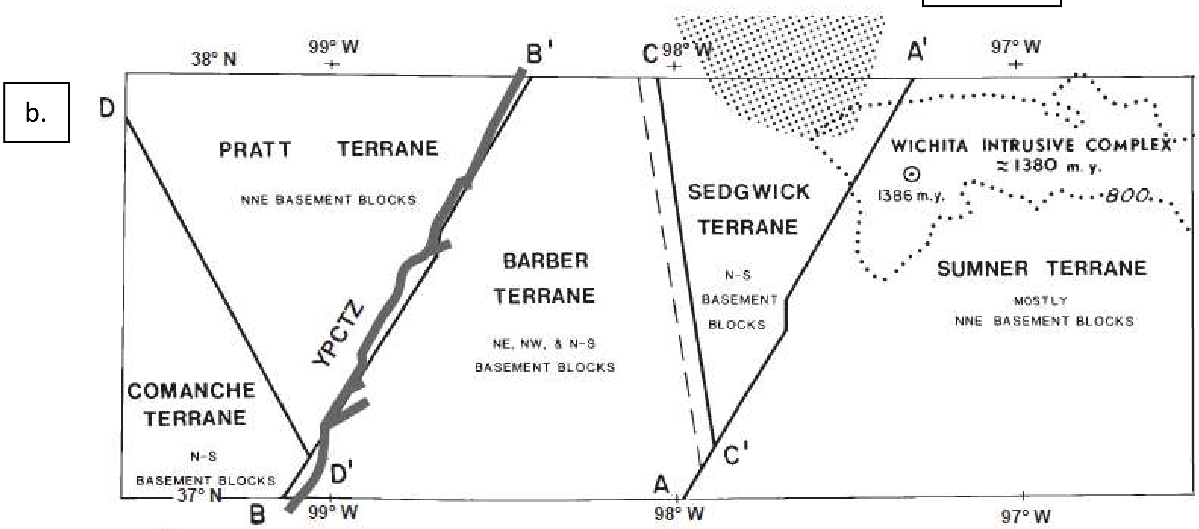

Figure 9a: Banded residual magnetic contours of south-central Kansas. Note the four basement sutures (tectonic boundaries), as indicated by the arrows. Red boxes show locations of AOI 1 and AOI 2. No residual magnetic data was available for AOI 3, located in west Woods County. Figure description modified from Gay (1986)

Figure 9b: Names are given for the various Precambrian terranes that are separated by the indicated sutures. A-A': Argonia Suture, B-B': Pratt Suture, C-C': Pretty Prairie Suture, D-D': Joy Suture. Note the close correlation of the "Yellowstone - Peace Creek Tectonic Zone" (YPCTZ) with the Pratt Suture. Description from Gay (1986).

The discussion will focus on the interpretation of merged injection well and earthquake data sets for south-central Kansas and northern Oklahoma on residual aeromagnetic maps. Determining what mechanisms affect earthquake locations and migration habits will be attempted by evaluating three areas of interest (AOI) (Fig. 1). Advancements in collecting earthquake data, monitoring, and cataloging injection well activities have been made in recent years by the addition of seismographs in the area; however, a full understanding of the relationship between physical properties of the injection interval, injection volumes, pressures, and locations still eludes researchers. In this review, results from computer modeling, spatially referenced data, magnetic maps, structure maps of pre Pennsylvanian formations, and literature on Precambrian terranes are combined to provide an up-to-date understanding of the mechanisms affecting seismicity in the midcontinent. Best practices for injection of waste water will also be discussed.

BACKGROUND

2.1 Seismicity

Interplate earthquake activity can be found along divergent, convergent, and transform plate boundaries. Normal fault movement is usually associated with divergent plate boundaries. An example of a divergent plate boundary is along the Mid-Atlantic Ridge, where the North American Plate and the Eurasian Plate are spreading apart from one another. Along the west coast of the United States, the Washington-Oregon coastline is an example of a convergent plate boundary, of which some normal fault movement is found as the oceanic plate bends just before it subducts beneath a continental plate. Thrust faulting is the primary fault movement found in convergent plate boundaries as the continental plate rides above the subducting plate. The Alpine Fault of New Zealand is an example of a transform plate boundary where strike-slip fault movement is detected. Intraplate earthquakes occur less frequently than interplate earthquakes, but the New Madrid seismic zone in Arkansas, Missouri, and Tennessee is an area known to have earthquakes with large magnitudes (>7.0M). This seismic zone lies within the Cambrian Reelfoot Rift (Hildenbrand and Hendricks, 1995). Right lateral and thrust (reverse) focal mechanisms characterize the New Madrid seismic zone at depths of 3 to 14 km (Herrmann and Canas 1978); (Andrews and others, 1985).

Between 1980 and 2012, 18 seismic events were recorded in the study area (USGS, accessed 2017). Over 880 seismic events have occurred in the Anadarko Basin from 1897 to 2008. "Most are constrained to an area nearly parallel to a deep, subsurface fault zone in west McClain and Garvin Counties and southeast Grady County" (Luza, 2008). McNamara and others (2015) found that 195 of the largest and best recorded earthquakes in Oklahoma from 2009 to 2014 were near-vertical, oriented NE-SW and NW-SE, and strike-slip fault movement in the crystalline basement (6 km). Over 90% of the earthquakes in this zone have occurred since 1977 (Luza, 2008) (Appendix 7). Central Oklahoma's recent seismic activity began north of Garvin, McClain and Lincoln Counties, Oklahoma, in 2009. Improvements in earthquake detection have been made in recent years that may be adding to the earthquake count, but central Oklahoma began experiencing a significant increase in seismic activity in 2009 (Appendix 8-10). Over the following years, activity has migrated to the north into Harper County, Sumner County, and Sedgwick County, Kansas, where seismic activity seems to have terminated. From 2010 to 2012, 6 earthquakes were produced in the study area. Major increases in seismic activity occurred from 2013 to 2016, with 6,153 events occurring. Average depths of the earthquakes are ~5km, but range from approximately 0.5-16 km (Fig. 10). Magnitudes in this study ranged from 2.0-5.1M; however, a 5.8M event was recorded just southeast of the study area. Figure 11 highlights the locations of earthquakes measured in the range of 4.5-5.8M.

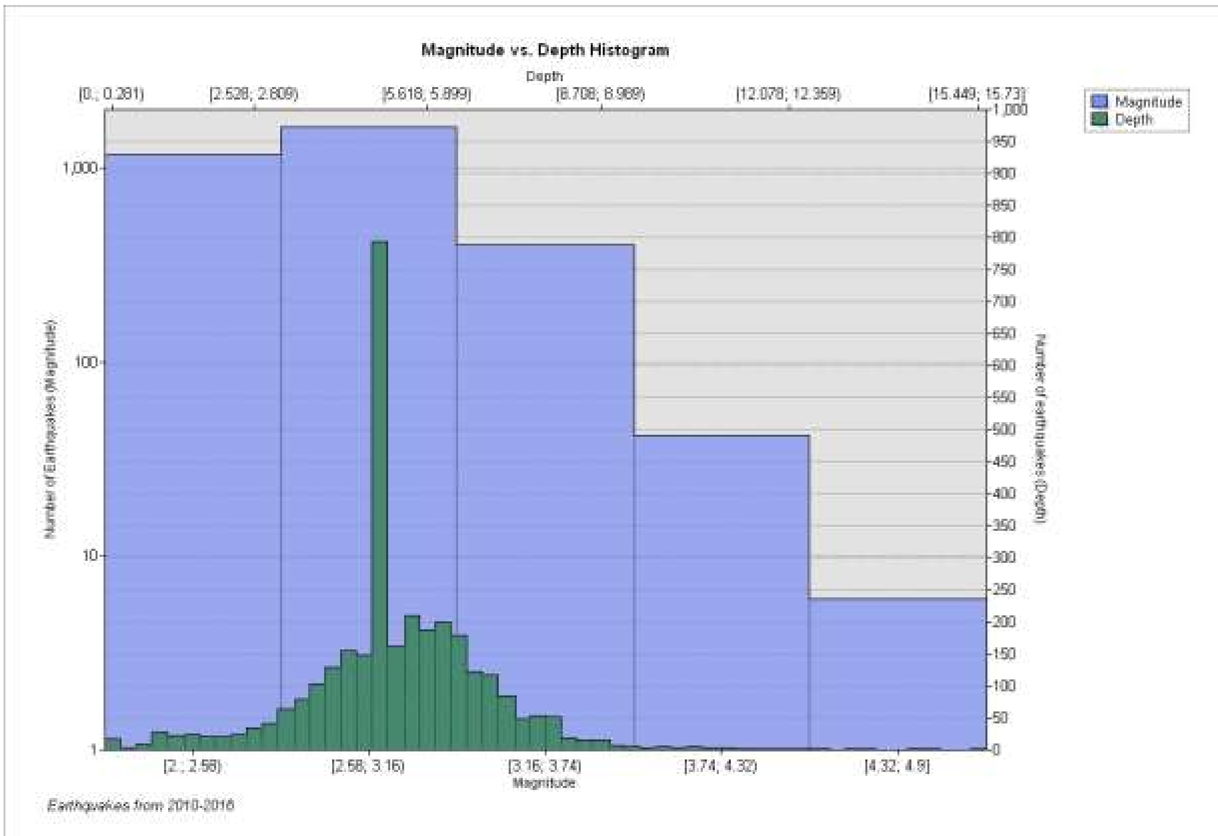

Figure 10: Histogram of magnitude (bottom and left axes) vs. depth (top and right axes) from 2010-2016.

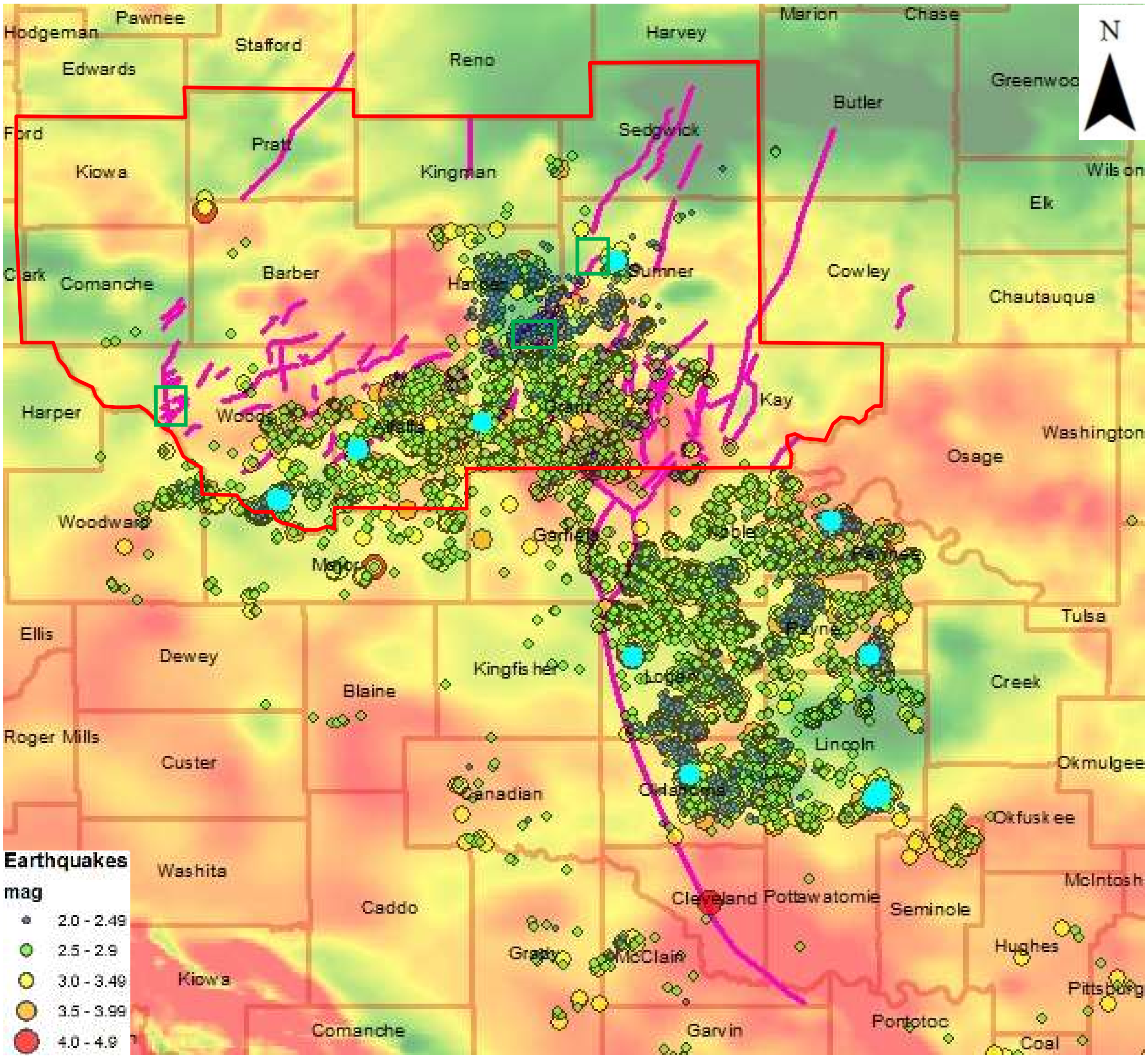

Figure 11: All earthquakes in south-central Kansas and Oklahoma from 2010-2016. Light blue dots highlight the locations of earthquakes 4.5-5.8 magnitude. Notice the locations tend to occur along the margins of seismically active areas. Aeromagnetic map from Sweeney and Hill (2005). Higher magnetic readings are red, yellow are median magnetic readings, and greens are low magnetic readings.

2.2 Salt Water Disposal Well Activities (SWD)

Waste water, brine, hazardous material, or any substance that is used or co-produced with oil and gas from unconventional wells is disposed of using salt water disposal wells (SWD) or underground injection control wells (UIC). Some wells use injection to improve the production of nearby wells. Other methods of treatment, (e.g., desalinization) exist, but underground injection is the most economical solution with present technology and infrastructure. Overwhelmingly, the Arbuckle Group receives the most of this disposed fluid (Murray, 2014). The Arbuckle Group of late Cambrian to early Ordovician age is dominated by highly permeable and porous dolomite and interbedded shale sequences of low permeability (Franseen and others, 2004). This Group is approximately 1,000 feet thick and 3,000 to 4,000 feet below sea level in the study area (Fig. 12). These characteristics make it an ideal Group in which to dispose waste water. The database logs 765 SWD wells operating on a gravity drain that require no pressure to receive the injected fluid (2015), and in many cases found in this research, areas that are associated with increased seismic activity use pressure to inject waste water. In 2014 approximately 850 million barrels of waste water was injected into the study area. Figure 13 details disposed volumes from 2005 to 2015 per county.

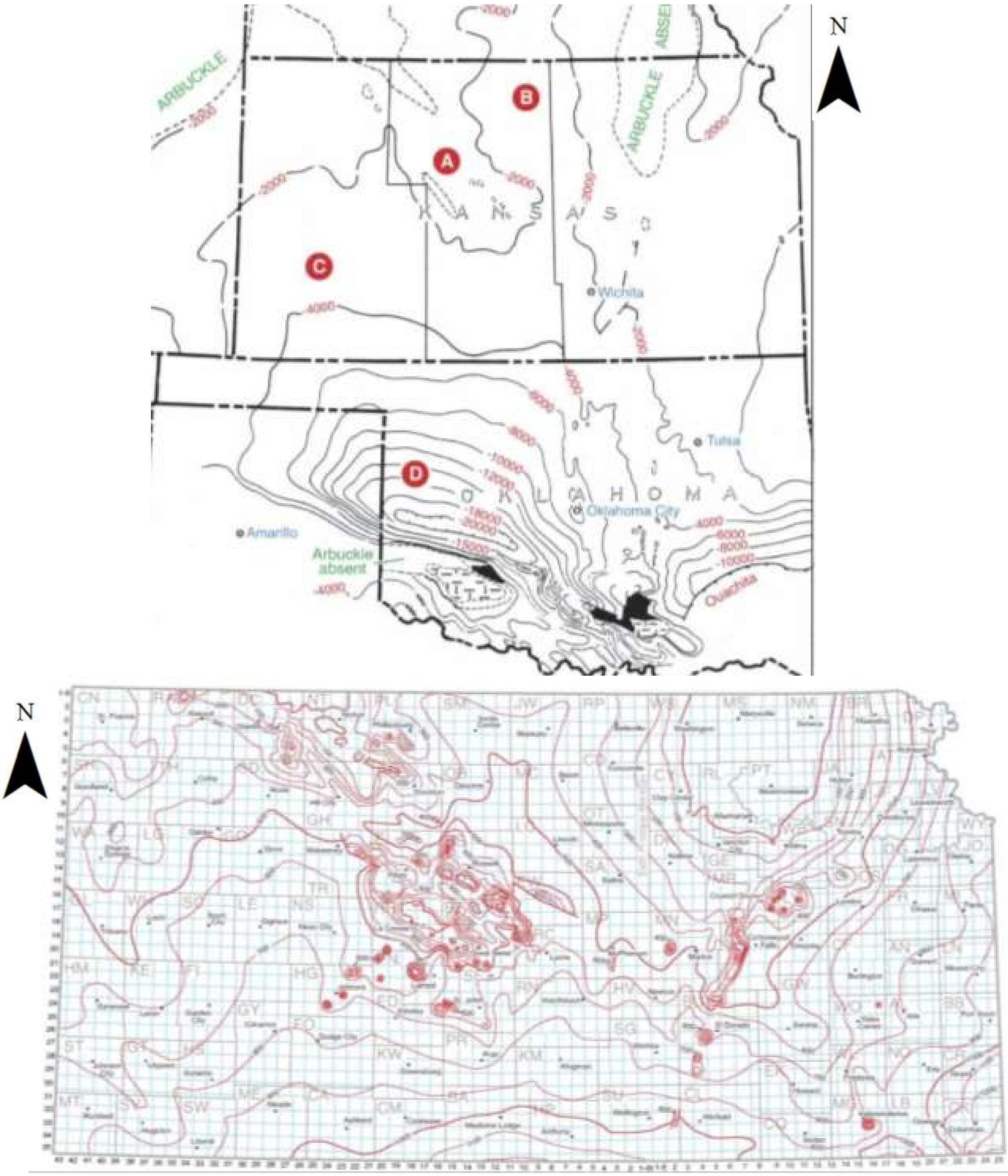

Figure 12: a) Structural contour map showing the top of Arbuckle Group. Contour interval 2,000 ft. A. Central Kansas Uplift, B. Salina Basin, C. Hugoton embayment of the Anadarko Basin, D Anadarko Basin (Bartram and others, 1950). b) Isopach map of the Arbuckle Group in Kansas. From well data up to 1965. Contour interval 100ft (Cole, 1975).

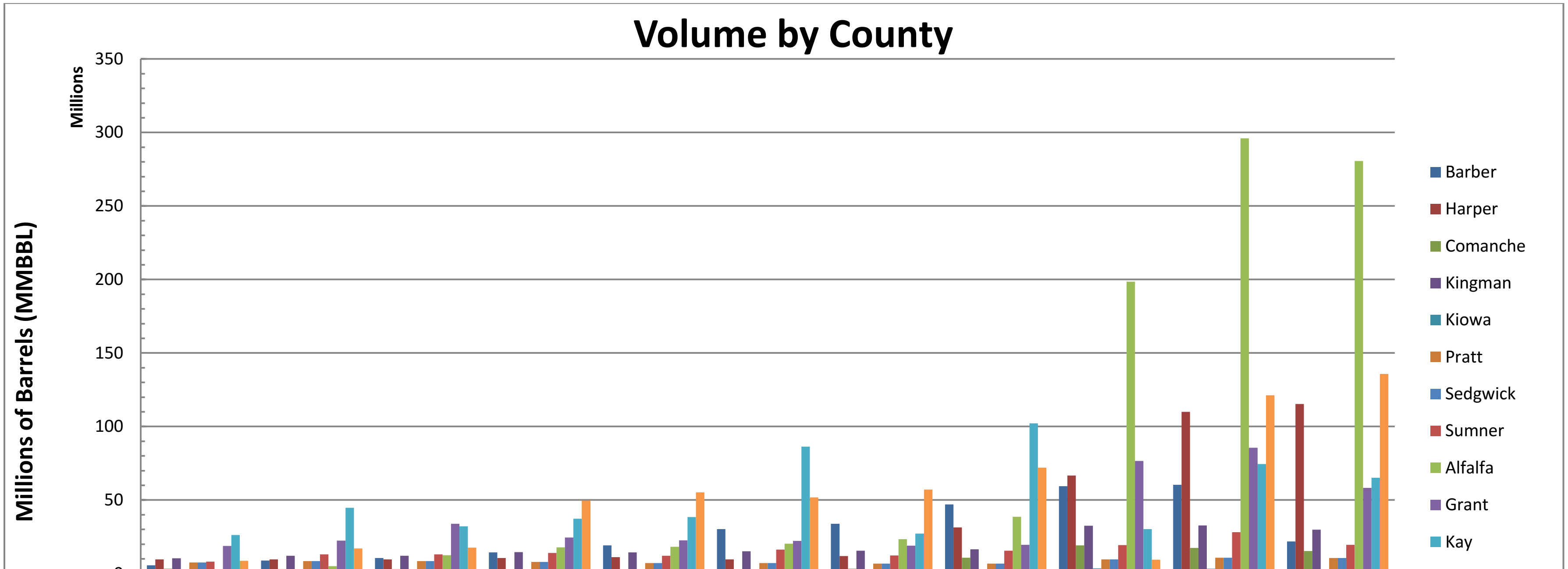

	2005	2006	2007	2008	2009	2010	2011	2012	2013	2014	2015
Barber	5,633,230	8,791,791	10,521,713	14,481,073	19,240,080	30,166,948	33,908,374	47,120,955	59,495,994	60,444,651	21,824,038
Harper	9,705,352	9,673,624	9,673,624	10,599,551	11,226,365	9,589,839	11,938,031	31,334,206	66,754,240	110,031,050	115,412,975
Comanche	3,305,695	3,230,186	3,230,186	2,994,498	2,675,292	2,800,225	3,423,742	10,757,810	19,219,054	17,419,690	15,349,281
Kingman	10,407,467	12,138,280	12,138,280	14,589,147	14,374,536	15,246,413	15,567,979	16,573,717	32,542,368	32,733,467	29,932,873
Kiowa	1,291,008	2,069,958	2,069,958	1,741,465	1,773,665	1,667,799	1,881,925	2,106,985	3,561,525	3,400,824	2,925,473
Pratt	7,561,371	8,497,343	8,497,343	7,970,620	7,215,197	7,154,872	6,827,941	6,760,389	9,552,266	10,689,899	10,533,063
Sedgwick	7,561,371	8,497,343	8,497,343	7,970,620	7,215,197	7,154,872	6,827,941	6,760,389	9,552,266	10,689,899	10,533,063
Sumner	8,023,018	13,084,366	13,084,366	14,095,586	12,136,033	16,301,177	12,322,207	15,541,415	19,359,192	28,113,422	19,552,884
Alfalfa	2,407,689	4,994,602	12,446,852	17,889,747	18,180,673	20,415,318	23,299,059	38,564,464	198,601,791	296,107,960	280,691,843
Grant	18,855,903	22,379,964	33,775,279	24,605,587	22,608,603	22,238,002	18,986,865	19,520,607	76,523,054	85,616,428	58,265,431
Kay	26,272,180	44,726,641	32,234,046	37,240,236	38,467,228	86,255,043	27,099,558	102,258,597	30,220,985	74,496,389	65,243,314
Woods	8,694,133	17,114,623	17,709,199	49,650,484	55,265,342	51,846,874	57,082,042	72,099,631	9,489,203	121,293,754	135,817,194

Figure 13: Total volume injected by county with inset table.

2.3 Precambrian Geology

Geochronological and geochemical analysis of U-Pb zircon, Rb-Sr whole rock samples, and Sm-Nd were used to determine the age range of 1.34 – 1.44 Ga for rhyolite and granite within the study area recorded by Van Schmus and others (1993). Rocks of this age and composition are found throughout the central and southeastern United States and depict widespread magmatism stitching together older coherent continental plates to the north with oceanic crust to the south (Bickford and others, 2015). Rhyolite and granite make up the basement rock in the study area. Northeast-southwest striking faults are interpreted from structure maps derived from oil and gas formation top data (Appendix 2 and 3). North-south trending faults have also been identified by subsurface mapping in the Oklahoma counties (Holland, 2015). In the present study, banded NewMag residual aeromagnetic maps of south-central Kansas help identify possible faults found on the generated structure maps in the Kansas Counties (Fig. 9a). Four basement suture zones are depicted and resemble conjugate shear zones separating five Precambrian terranes made up of individual fault blocks (Gay, 2009) (Fig. 9b). It is important to note that magnetic data measures the magnetic susceptibility of rock, not topography. The juxtaposition of fault blocks with different magnetic readings may indicate an active structural past. In an analysis of magnetic basement mapping in north-central Oklahoma and south-central Kansas, Gay (1986) has identified eight sets of magnetic lineaments that he relates to major tectonic events interpreted by magnetic maps of the region (Gay, 1986). Appendix 5 and 6 resemble the pattern Gay is identifying. The Precambrian basement of Kansas and northern Oklahoma is currently separated into three major features;

the Southern Central Plains orogen (SCP), the Southern Granite-Rhyolite Province (SGR), and the Midcontinent Rift System (MCR) (Fig. 6 and 14).

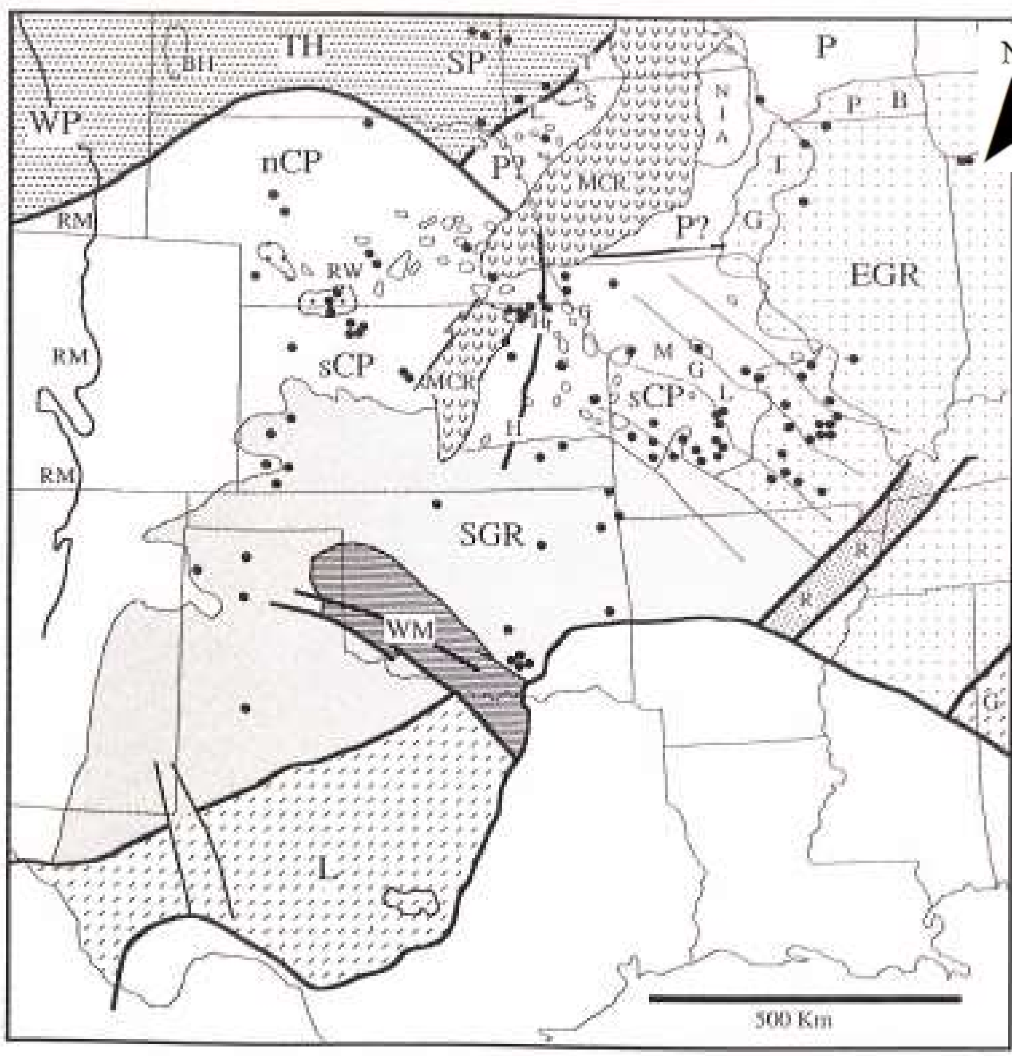

Figure 21. Major geologic features of the western Midcontinent region. WP, Wyoming province; BH, Black Hills; TH, southern end of Trans Hudson orogen; SP, southwestern corner of Superior province; SLT, Spirit Lake trend; P, Penokean province; P?, possible Penokean basement; nCP, northern Central Plains orogen; sCP, southern Central Plains orogen; NIA, Northeast Iowa anomalies; S, Spencer Plutonic Complex, RW, Red Willow batholith; EGR, Eastern Granite-Rhyolite province; GIPB, Green Island plutonic belt; SGR, Southern Granite-Rhyolite province; MGL, Missouri gravity low; R, Reelfoot rift; MCR, Midcontinent rift; WM, Wichita Mountains magmatic province; G, Grenville province; L, Llano province; RM, eastern edge of Rocky Mountains uplift; H, Humboldt fault zone (Nemaha uplift). Unlabeled open units represent many of the anorogenic plutons which have been identified from magnetic maps. Solid dots are locations of drill hole and outcrop samples for which U-Pb ages are available (see Fig. 22).

Figure 14a: Originally from *Transcontinental Proterozoic provinces*, in Reed and others, eds., *Precambrian:* Conterminous U.S. (Van Schmus and others, 1993).

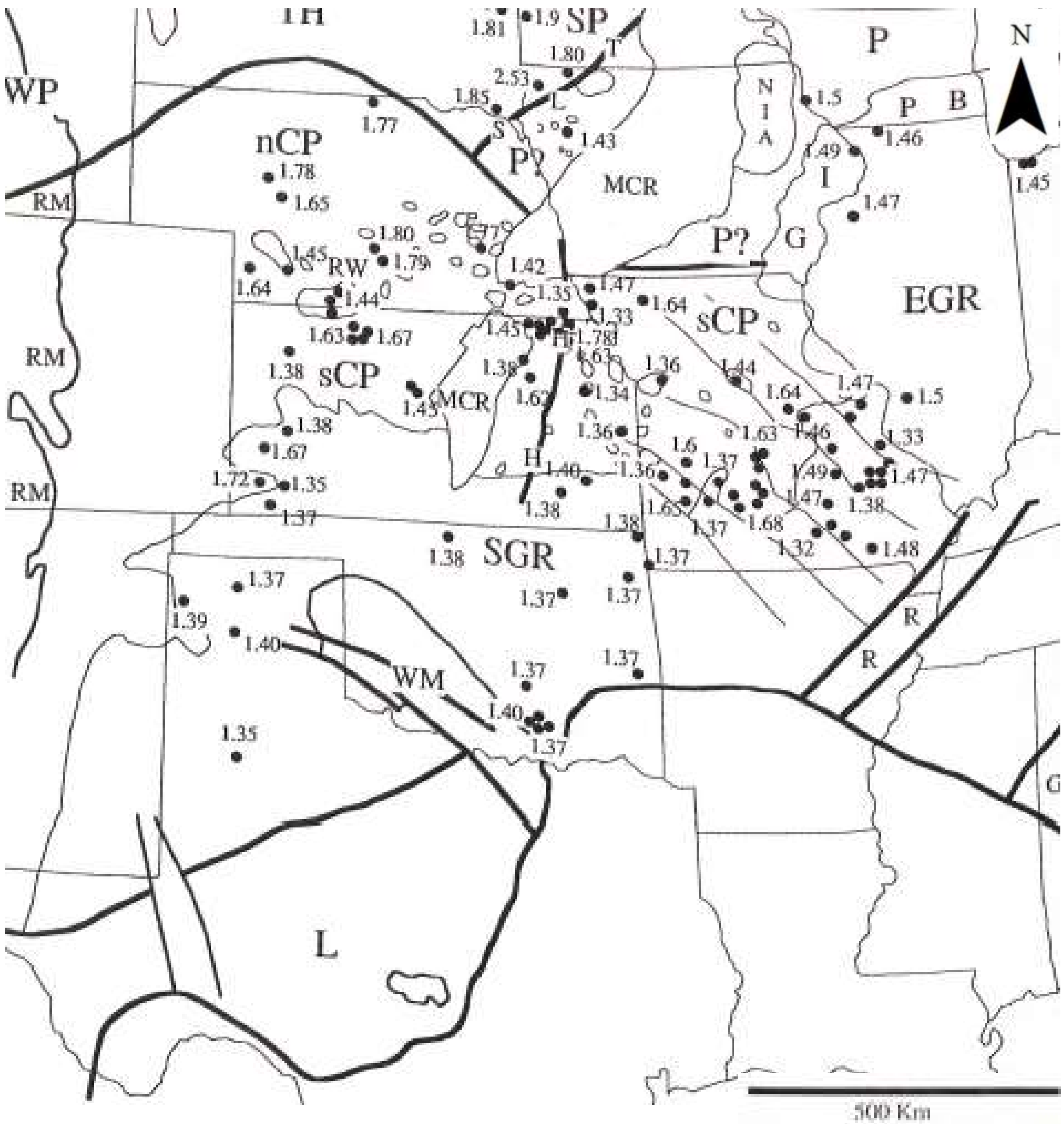

Figure 14b: U-Pb ages on zircons in the midcontinent. Ages in northwestern and northeastern Kansas may yield slightly younger ages due to zircon overgrowths in association with a later thermal event (Van Schmus and others, 1987). Abbreviations on Figure 14a.

2.3.1 Southern Central Plains Orogen

This feature of the midcontinent region is located across the upper two thirds of Kansas and portions of Missouri and Colorado (Fig. 6 and 14). Primary U-Pb ages derived from zircons indicate ages around 1.65 Ga with some slightly younger samples of 1.58 – 1.62 Ga (Van Schmus and others, 1987) (Fig. 14b). Composition of 1.65 granites show characteristics for volcanic-arc granites and intraplate granites, but a Nb versus SiO2 ratios indicate a stronger correlation with volcanic/continental collision environments (Pearce and others, 1984). Older ages of 1.72 Ga have been reported and are similar to southern Colorado's volcanic and plutonic rocks that are intruded by 1.65 Ga granites, which support the possibility of much of Kansas may have zircons with similar U-Pb ages. The 1.67-1.65 Ga volcanic plutonic suite, possibly classified as an arc complex, was intruded by a batholithic complex of plutons with ages of 1.62 Ga. A suggestion for the age difference may be a deeply eroded surface, exposing the younger batholith. With 1.65 Ga plutons identified as far north as Nebraska, intruding 1.75-1.8 Ga crust of the Northern Central Plains orogen, any possible subduction zones associated with the 1.65 Ga suite of plutons must have been dipping to the north and located to the south of these plutons (Van Schmus and others, 1987).

2.3.2 Southern Granite – Rhyolite Province

This province of granite and felsic volcanic rock, with U-Pb ages of 1.34-1.4 Ga, lies buried beneath southwest Missouri, southern Kansas, Oklahoma, and the Texas Panhandle (Van Schmus and others, 1987) (Fig. 14b). Exposures of the SGR are located in the eastern Arbuckle Mountains of southern Oklahoma and along the Spanivaw Creek in northern Oklahoma.

Transcontinental Proterozoic provinces must have been subject to a major thermal event that stretched from the western to the eastern midcontinent. Isolated plutons of the same age are found in the SCP orogen and intrude the St. Francois Mountains of southeastern Missouri (Bickford and others, 1981b; Thomas and others, 1984; Latham and others, 1988). The St. Francois Mountains are defined as a part of the eastern Granite-Rhyolite province, but bear a very similar chemical makeup and age (~1.47 Ga) to the SGR province. Sm-Nd crustal ages from samples in Oklahoma, (Nelson and DePaolo, 1984), indicate that these samples were derived by partial melting of older crust (Thomas and others, 1984; Van Schmus and others, 1987). Partial melting of older crust suggests that the SGR province may be a layer of shallow plutonic rocks that lie above older Proterozoic crust. To date, no wells have been drilled completely through this veneer of volcanic rock, but the rock below the SGR province may likely be related to the SCP orogen.

Pratt (1989) provides a maximum thickness of 11 km for the SGR province. Several wells have drilled into felsic volcanic rocks to depths of 1.1 km in the Texas Panhandle (Denson, 1966); 1.4 km in southwestern Oklahoma (Ham and others, 1964); 1 km in the Ozark Uplift (Snyder, 1968); and 3 km have been mapped in the St. Francois Mountains (Sides and others, 1981). Using a standard heat flow equation of 33mW/m2 for the eastern United States and assuming typical values of heat generation in the SGR province, a thickness of 4 to 7 km is assigned (Roy and others, 1968); (Sass, 1981). Deformation is expressed by block faulting and metamorphism is absent or limited to the minimal greenschist facies (Van Schmus and others, 1987).

2.3.3 Midcontinent Rift System

One of Kansas most prominent tectonic features is the Midcontinent Rift System (MCR), a 1.1 Ga extensional structure stretching from the Great Lakes region through southeast Nebraska, and reaches its most southern extent into north central Kansas (Van Schmus and others, 1982). Aeromagnetic data suggest fracture systems associated with the MCR reach as far as northern Oklahoma (Yarger, 1985). The rift system segmented near the Kansas – Nebraska border by a NW-SE striking sinistral strike-slip fault zone associated with an anomaly called the Missouri Gravity Low. Mafic igneous rocks comprise the central portions of the rift, along with post rift basins filled with mainly red clastic rocks. These clastic rocks from the MCR are likely found as far south as Harper County. Rifting may have terminated due to compressive forces associated with the Grenville Orogeny to the east (Van Schmus and others, 1987).

2.4 Paleozoic Geology

Sedimentary units in the Sedgwick Basin range from Cambrian Reagan formation and Arbuckle Group to Permian and Tertiary sediments at surface. The sedimentary cover is in excess of 5,500 feet in the study area. The basin strata are characterized by facies changes and increased thickness to the south from the shelf area into the deeper part of the Anadarko Basin. The Sedgwick Basin is characterized as a pre-Desmoinesian post-Mississippian structural feature bounded to the east by the Nemaha Uplift, the Pratt Anticline to the west, and the Anadarko shelf to the south. A saddle separates the Sedgwick Basin from the Salina Basin to the north (Fig. 2). The Bluff City-Valley Center and Pratt anticlines are north-northeast trending folds oriented parallel to the MCR and the Nemaha Uplift. Reverse faulting is documented in Harvey and Reno Counties north of Sedgwick County (Fig. 15a), and south of Kay and Grant County along the Nemaha Uplift (Fig. 15b). The Arbuckle and Simpson Groups were utilized to determine the structure and thickness of sedimentary rocks in the Sedgwick Basin. Structure maps were derived from Kansas Oil and Gas formation data (Appendix 2 through 4). The Arbuckle Group is a Cambrian-Ordovician age collection of mostly dolomites and shales whose structure deepens and thickens to the south into the Anadarko Basin. The Simpson Group is middle Ordovician in age and includes shale and sandstone. The Simpson sits stratagraphically above the Arbuckle Group. The Viola Group, (Ordovician) sits stratigraphically above the Simpson Group and is carbonate dominated. The Viola Group was removed in many portions of the Sedgwick Basin and is absent in southeast Kansas (Adkison and other, 1972).

The Nemaha Uplift comprises a series of uplifted fault blocks. It is a pre-Desmoinesian post-Mississippian structure that runs from the Central Plains Megashear in Nebraska, through the southeast corner of Sumner County, Kansas and into south-central Oklahoma where it terminates against the Oklahoma Megashear (McBee, 2003) (Fig. 16). The Nemaha Uplift has been expressed as having compressional, extensional, left-lateral, and right-lateral features. Its current right lateral motion is likely a result of left lateral displacement along both mega-shears (McBee, 2003). The Springer onlap in the southern terminus of the Nemaha Uplift in southern Oklahoma is offset by the Nemaha Fault (Humboldt fault), providing evidence for right-lateral movement in mid-Pennsylvanian time (Friess, 2005). Gay (1999) illustrates the Nemaha Uplift as having a series of compressional features associated with left-lateral movement (Fig. 15). The Wichita Intrusive Complex, just west of the Nemaha, shows 6 km of left-lateral offset (Gay,

S. P. Jr., 1999) (Fig. 17a and b). Extensional deformation towards the end of this left-lateral fault has also been proposed by Blair and Berendsen (1988) and Gay (1999). These examples show how the Nemaha Uplift, as well as other portions of the study area, has experienced several phases of deformation.

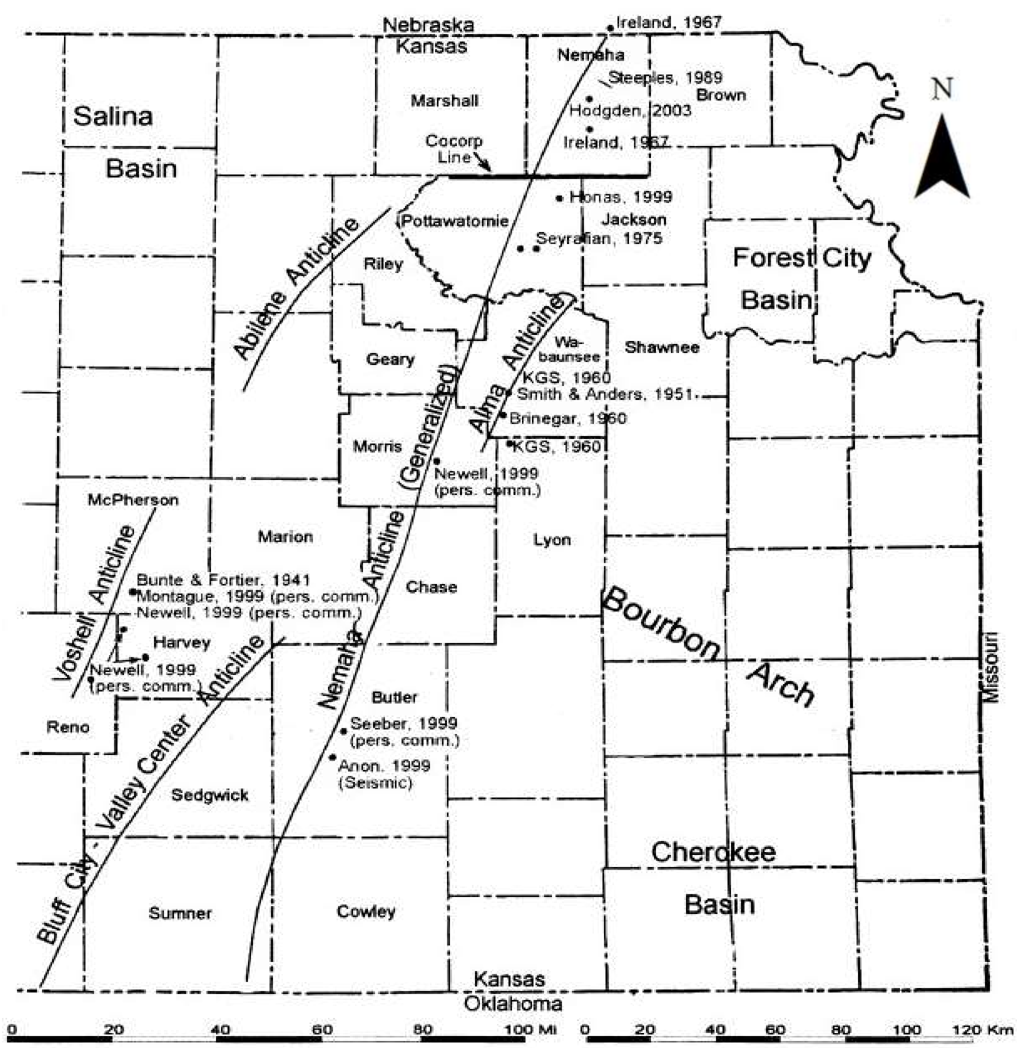

Figure 15a: Anticlinal features with dots indicating areas of documented reverse faulting in eastern Kansas (Gay, 1999).

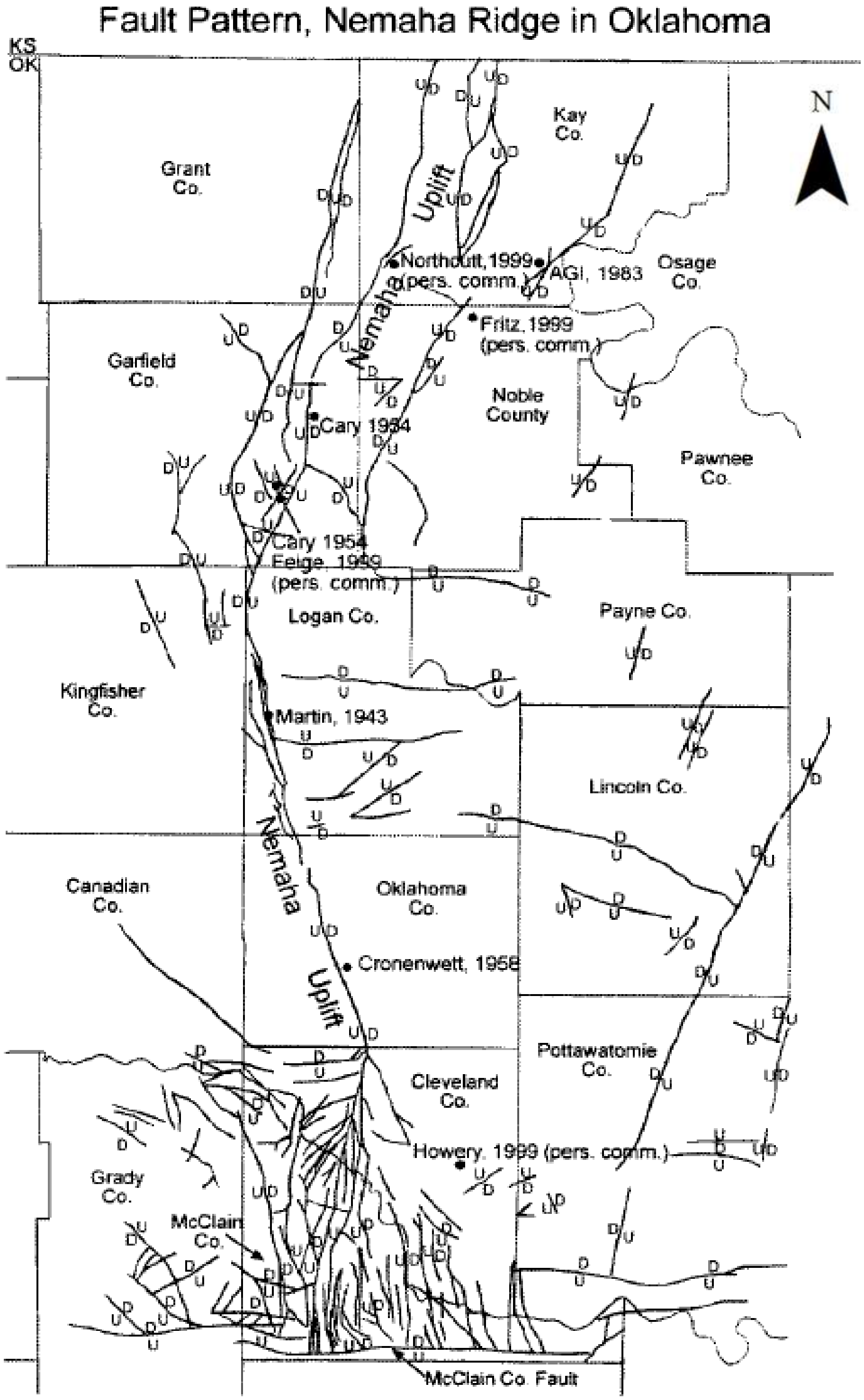

Figure 15b: Fault map of north-central Oklahoma. Proprietary mapping by Lloyd Gatewood (personal communication with Gay, 1983) and places where reverse faulting has been documented shown by dots (Gay, 1999).

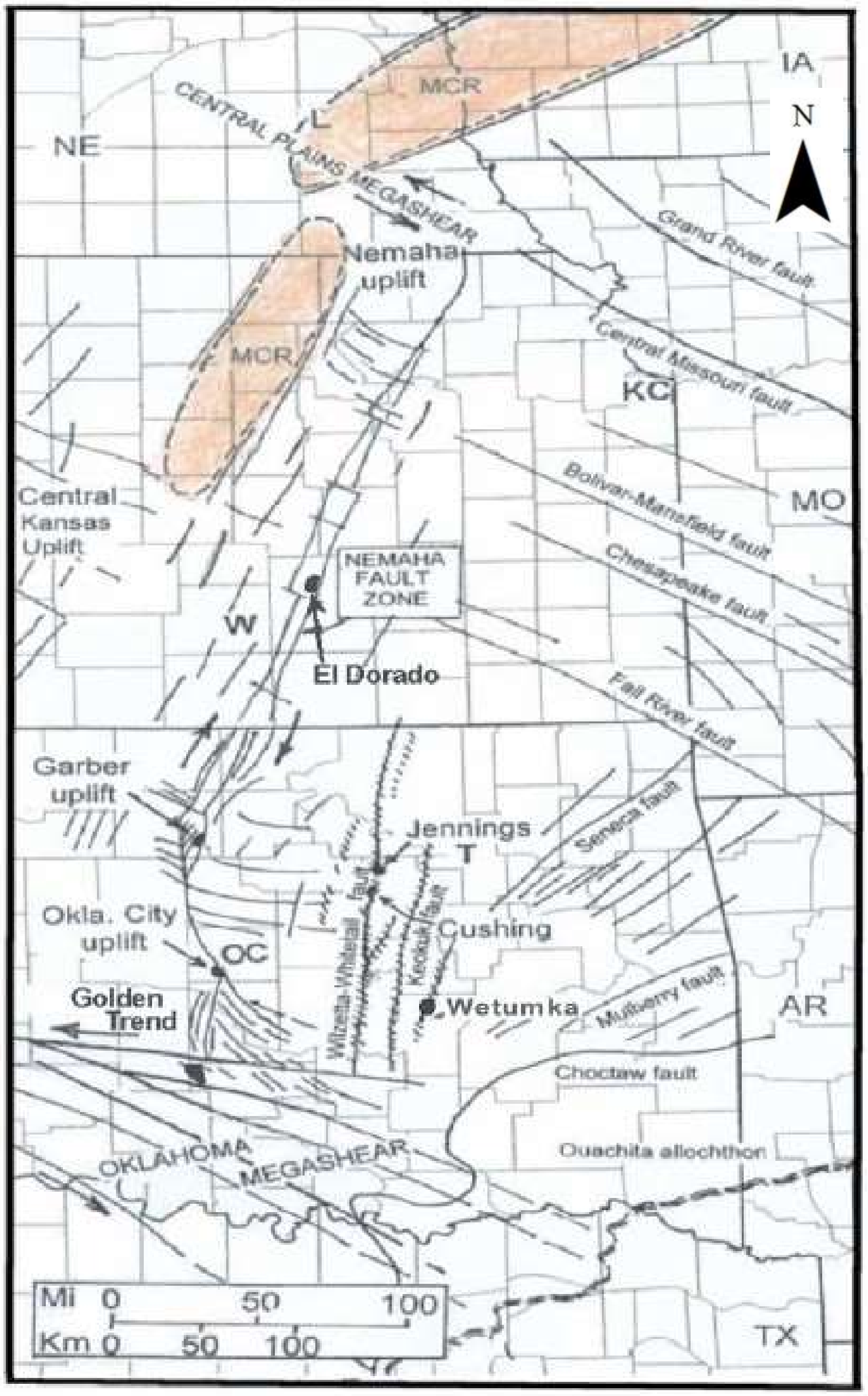

Figure 16: Fault map depicting the present day motions of the Central plains Megashear, Oklahoma Megashear, and the Nemaha Fault Zone (McBee, 2003).

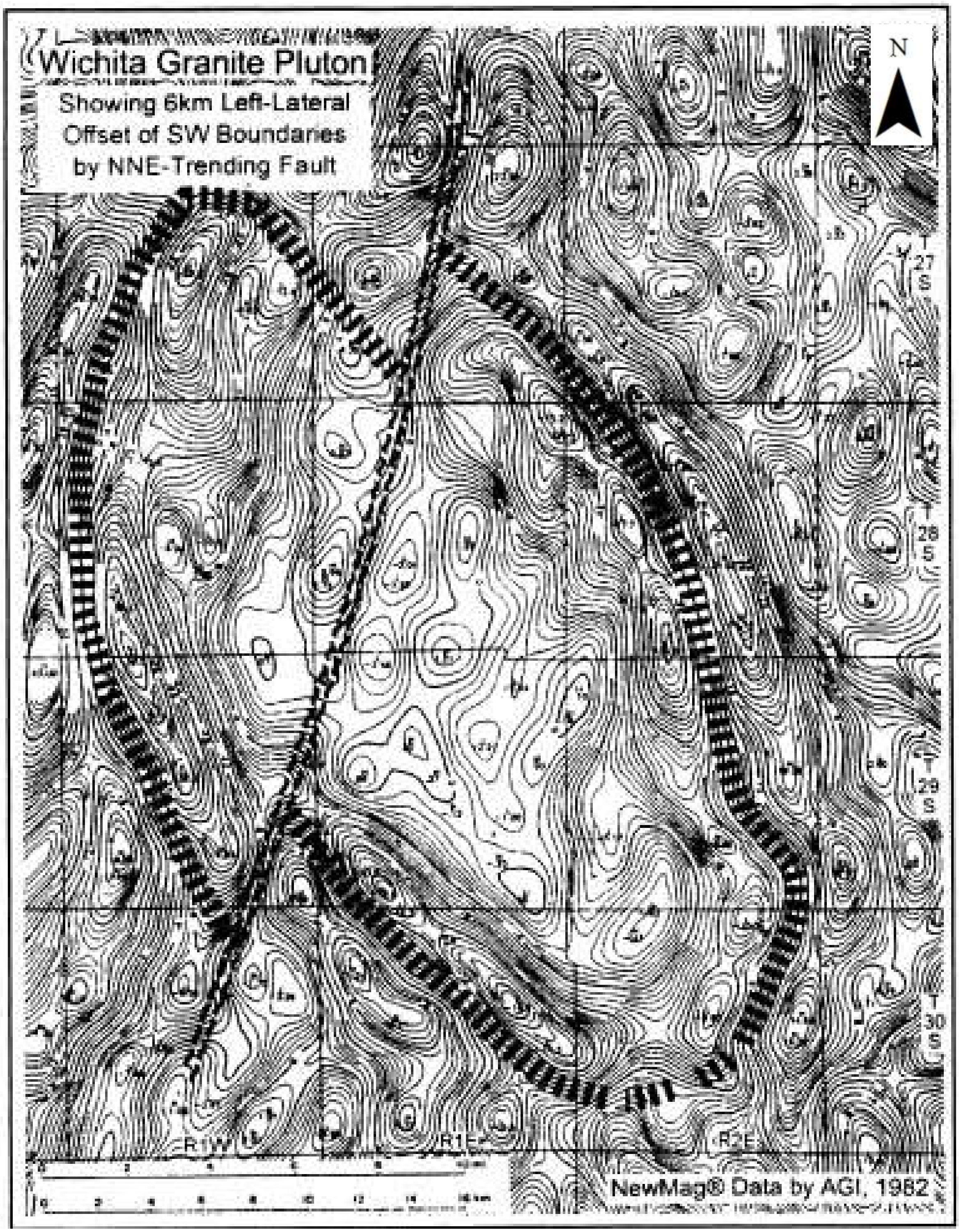

Figure 17a: Wichita Granite Pluton of northeast Sumner County (Gay, 1999).

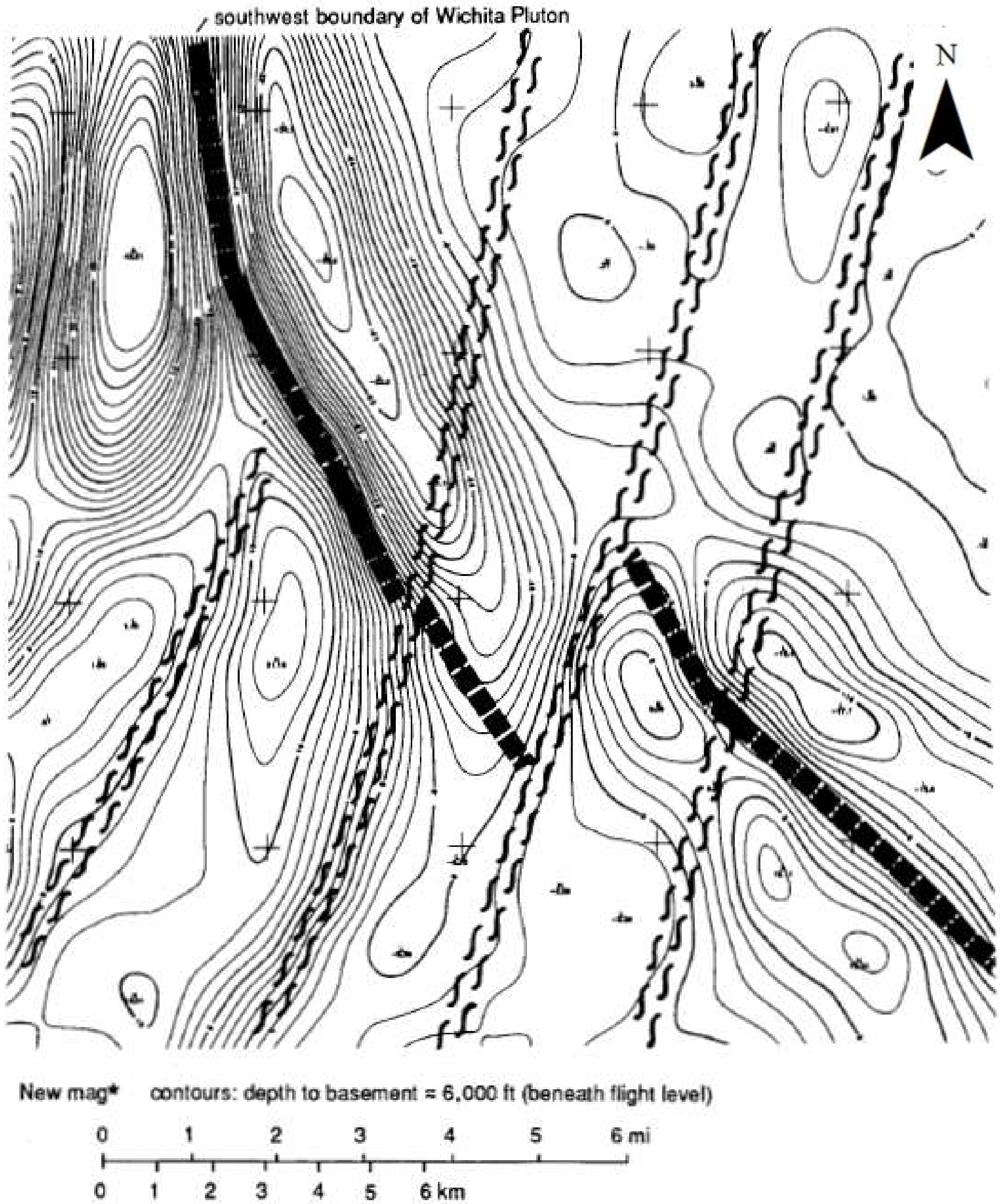

Figure 17b: A closer look at the southwest portion of the Wichita Granite Pluton depicting a series of left-lateral faults (~) interpreted by Gay (1989).

MATERIAL AND METHODS

Geographix and ArcGIS 10.4 software applications were used to generate and compare SWD well attributes, earthquake locations, aeromagnetic maps, and structure maps. Methods used to conduct this study involved the integration of Oklahoma and Kansas SWD well and Class II underground injection control (UIC) well datasets. These databases came from several sources, including the Oklahoma Corporation Commission (OCC), the Oklahoma Geologic Survey (OGS), the Kansas Corporation Commission (KCC), and the Kansas Geologic Survey (KGS). These databases provided the study with unique American Petroleum Institute (API) well numbers for all wells in the study area. Using the API numbers as reference allowed each well to be characterized with its associated attributes, including latitudes and longitudes, well status, annual pounds per square inch (PSI), total injected volume monthly and annually in barrels (bbl) when applicable, injection zones when applicable, and formation tops. Formation tops were made available by the Kansas Geological Survey and vetted for accuracy in the Viola, Simpson, and Arbuckle Groups in south-central Kansas using wire log data. Formation tops in Oklahoma were not included in the study due to unavailability of data. Geographix was used for the generation of structure maps of Cambrian to Mississippian age formations in Kansas. In the Geographix database, Kansas and Oklahoma SWD well datasets range from 2005 to 2015. The ArcGIS database uses available PSI readings and annual injection volumes for each well from 2010 to 2015. The Kansas SWD wells from 2005-2014 only contain annual injection volumes for each well and the maximum PSI recorded. SWD wells in 2015 recorded injection volumes and average PSI measured per month. No injection zones were recorded in the Kansas database. Wells in Harper and Sumner County, Kansas were manually checked and compared to scanned copies of Form 1012A: ‘Annual Fluid Injection Reports’ that may or may not list each formation receiving the injected fluid or gas. The Oklahoma report year for 2011 did not include any PSI readings or injected formations, but did include monthly injection volumes. In years 2012-2015, Injection formation, injection interval, injection volume, and psi reading for each well was reported. Class II UIC well data for Kansas and Oklahoma were filtered for statistical analysis or represented on a map by county, year, injection volume, PSI, and injection zone when applicable.

The USGS earthquake catalog provided a query of the study area’s earthquake epicenters, depth, magnitude, and date of event from January 1st, 2010 to December 31st, 2016. In some cases a moment tensor is assigned to an event. Earthquakes are numbered to assign an individual ID to the event. ArcGIS was used to make a time laps video of UIC well volumes/PSI from 2010 to 2015 and earthquakes from 2010 to 2016. NewMag residual magnetic maps of south-central Kansas and portions of Grant County and Kay County, Oklahoma, were provided by Applied Geophysics Inc., and only portions of those maps were used to create three areas of interest. These maps were georeferenced in both software applications. ArcGIS also includes entire Kansas and Oklahoma magnetic maps georeferenced from the USGS (Sweeney and Hill, 2005) and a fault map of Oklahoma (OGS, 2015).

The three areas of interest (AOI) were determined by the availability of NewMag Residual aeromagnetic data and quantity of earthquake activity in a given area. Analysis was conducted by; 1) creating graphs and tables of earthquake and SWD well data per AOI on an annual basis; 2) comparing active SWD well locations and the fluctuation in volume and pressure used to inject by year to shear zones where seismic activity followed after the injection increase or decrease in an area.

RESULTS

Appendix 1 displays a map view of annual volume per well, maximum pressure used per well by year, and earthquakes per year from 2010-2015 in the study area. Factors found to influence the locations of seismic events include the orthogonal fracture pattern of shear zones separating Precambrian basement fault blocks (Fig. 9), 33.9 billion barrels of fluid injected into the subsurface from 2005 to 2015 (Fig. 4 and 13), and wells using elevated injection pressures over stressed shear zones. In 2012, a noticeable increase in the number of injection wells (Fig. 18) and the number of wells using elevated pressures to inject waste water occurred (Appendix 1a-1c).

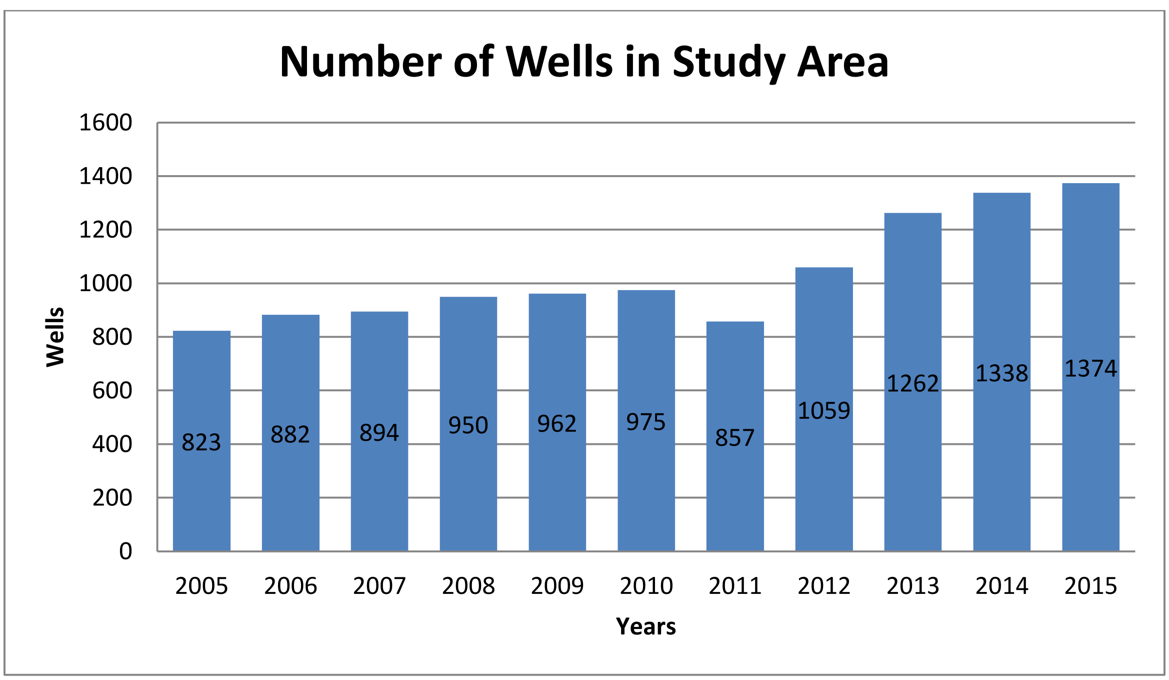

Figure 18: SWD well count from 2005-2015.

The following year, volumes and seismic activity increased (Fig. 4 and 5a). Of the 33.9 billion barrels of fluid disposed into the subsurface from 2005-2015, 63% of the total injected volume has been from 2013-2015. A total of 6,153 earthquakes were detected from 2013-2016 (Fig. 19). Ninety-four percent of seismic activity from 2013-2016 in Kansas occurs in Harper and Sumner Counties along the Argonia and Pretty Prairie suture zones (Fig. 20). A wide variety of fault movement was detected within the study area. Transtensional and strike-slip movement were the most detected moment tensors, although transpressional events did occur (Fig. 21). Appendix 11 defines moment tensors seen in the study area. The first occurrences of seismic activity were detected in Alfalfa County in September, 2010 and southern Kay County along the Nemaha fault system in November, 2012. The highest rates of seismic activity are seen in the Oklahoma counties of the study area. Depths ranged from approximately 0.5-16 km with a vast majority of the focal points within the Precambrian basement. The most common depths were 5-6 km, accounting for 1,048 of the 6,153 earthquakes in 2013-2016 (Fig. 10). Earthquake magnitudes within range of 2.5-3.0M were the most frequent of the 6,153 events (Fig. 5c and 10). Earthquake epicenters coincided with shear zones mapped by NewMag residual magnetics (Fig. 6 and 13), as well as faults in the sedimentary section (Fig. 6 and 13). Faults primarily strike to the northeast-southwest, but also run north-south and northwest-southeast (Fig. 1). Earthquakes have been detected as far northeast as Sedgwick County and as far west as Kiowa and Comanche Counties in 2015-2016 (Fig. 11). Earthquakes occurred within regional magnetic lows, and outlined regional magnetic highs. The western portion of a large magnetic high in Grant and Kay Counties is an exception to this observation as this correlates with the Nemaha

Uplift. SWD wells are found throughout the study area, but a long linear trend is found atop a magnetically high area in Woods, Barber, and Harper Counties (Appendix 1).

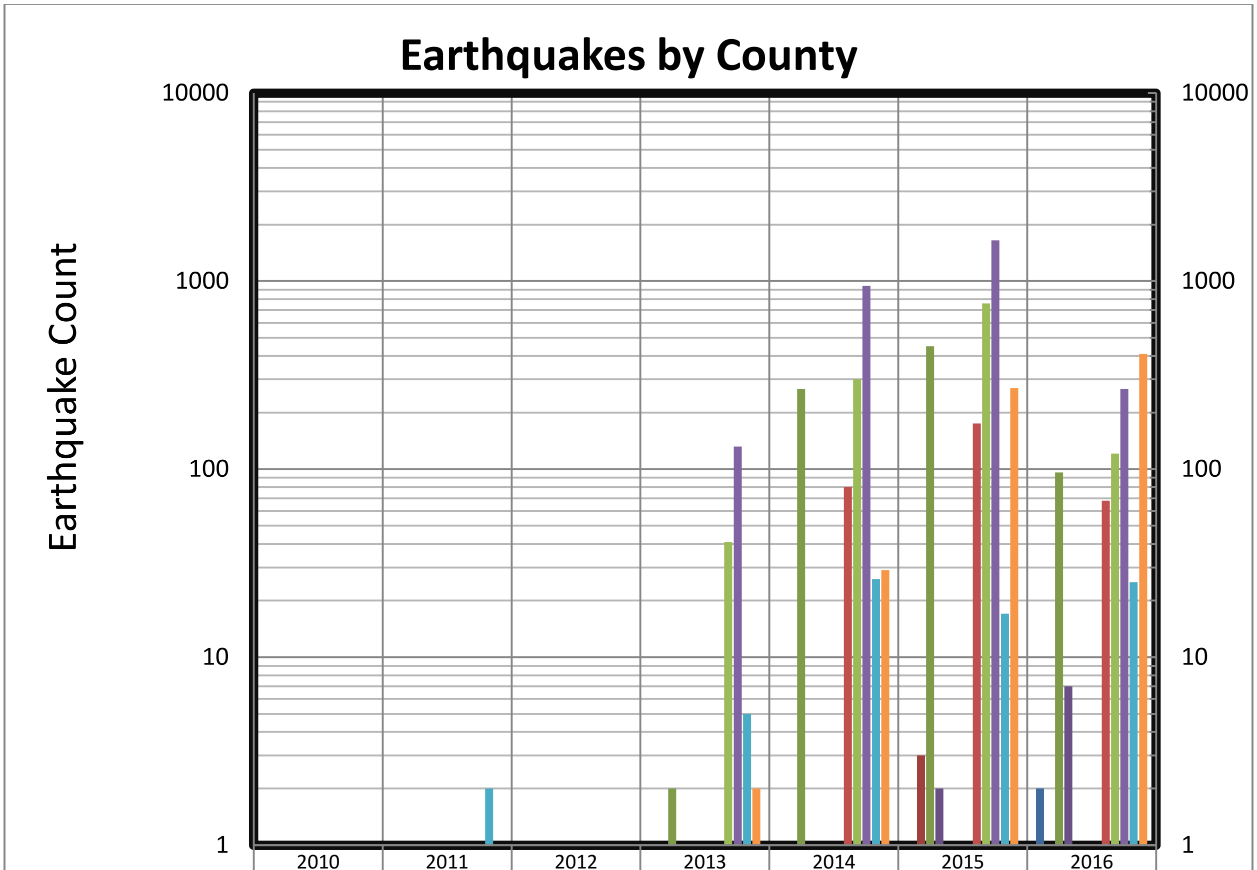

	2010	2011	2012	2013	2014	2015	2016
Barber	0	0	0	0	0	1	2
Comanche	0	0	0	0	0	3	0
Harper	0	0	0	2	267	450	96
Kingman	0	0	0	0	0	2	7
Kiowa	0	0	0	0	0	0	0
Pratt	0	0	0	0	0	0	0
Sedgwick	0	0	0	0	0	1	1
Sumner	0	0	0	1	80	175	68
Alfalfa	0	0	0	41	300	761	121
Grant	0	0	0	132	945	1648	267
Kay	0	2	0	5	26	17	25
Woods	1	0	0	2	29	269	409
Total Earthquakes	1	2	0	183	1647	3327	996

Figure 19: Total number of earthquakes by year and county.

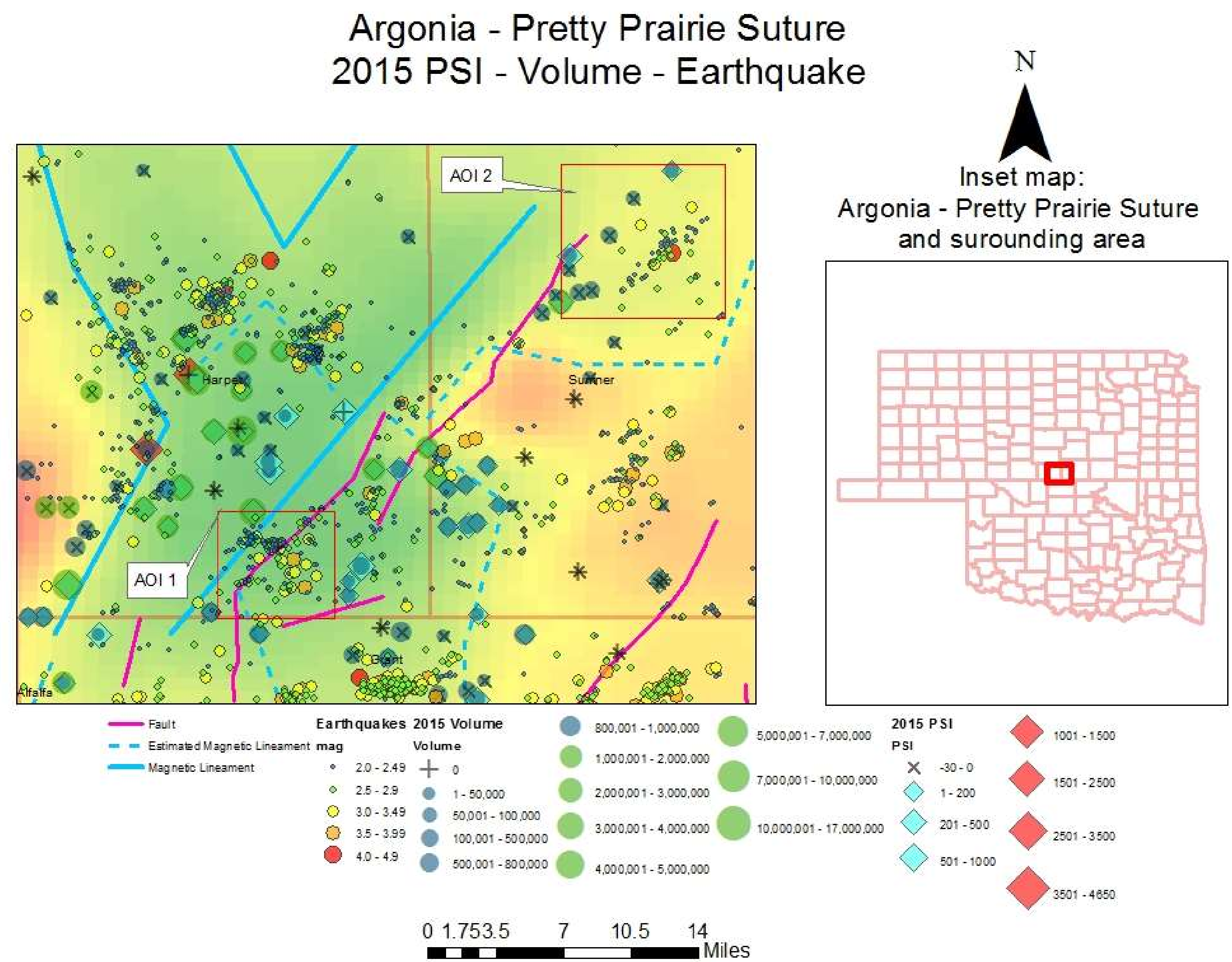

Figure 20: Magnetic map Of Argonia-Pretty Prairie suture with estimated lineament features. Aeromagnetic map from Sweeney and Hill (2005). Higher magnetic readings are red, yellow are median magnetic readings, and greens are low magnetic readings.

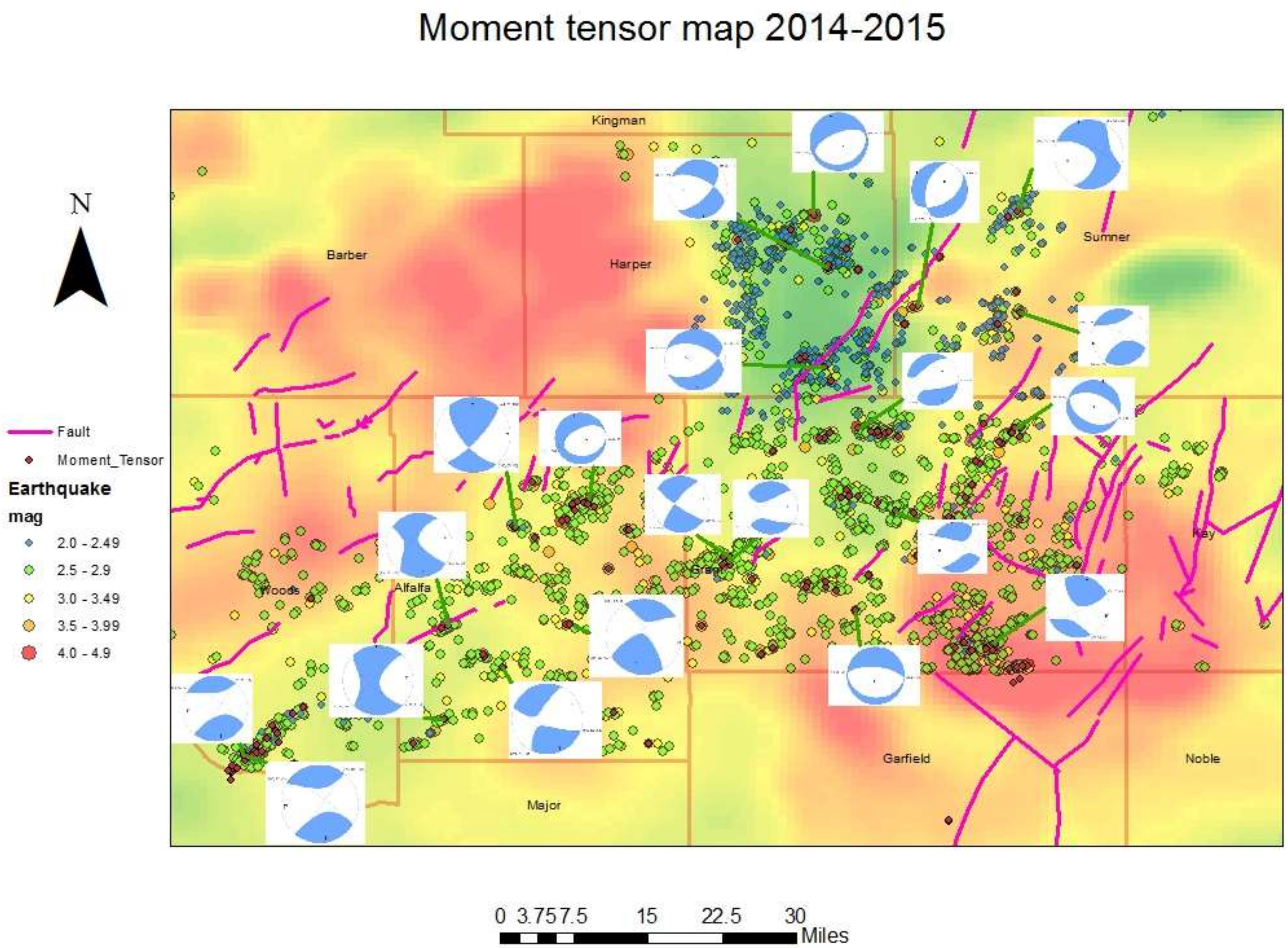

Figure 21: This is just a portion of the moment tensors recorded in the study area. Transtensional and strike-slip events are the dominant motion of the earthquakes. Aeromagnetic map from Sweeney and Hill (2005). Higher magnetic readings are red, yellow are median magnetic readings, and greens are low magnetic readings.

Limiting factors include the availability of aeromagnetic data, what injection well data was recorded, collection methods used by SWD well database sources, and any data describing stress and pressure systems within the injecting formations. The archiving of SWD well data is not formatted synonymously from year to year or across state borders. All Kansas SWD data, with the exception of the 2015 reporting year, is annual rather than monthly. This does not allow the monitoring of wells by month in relation to seismic events and provides a broader interpretation to the causes of seismic activity. The current database for 2011 Oklahoma injection wells did not provide any pressure readings. Considering these limitations, three areas of interest were examined. The first area of interest (AOI) is located in southeast Harper County, AOI 2 is located in west Sumner County, and AOI 3 is located in west Woods County (Fig. 1).

4.1 Area of Interest 1

AOI 1 represents a magnetically high basement block situated within the regional magnetic low in southeast Harper County (Fig. 22). This fault block is the southern hinge of the conjugate fault defined by Gay (1986) as the Argonia and Pretty Prairie suture zone. Two faults identified on the Simpson structure map (Appendix 2) strike northeast-southwest and bound the areas seismic activity. A total of 225 earthquakes occurred from 2013-2016; 200(2.0-2.9M) and 25 (3-3.9M). In 2015, 26 of the 156 seismic events registered as 3.0 magnitude or greater. The most frequent depths recorded were in the 4-5.9km range. Three moment tensors depicting transtensional strike-slip motions were recorded in 2015 as well as one transpressional event in the most southern portion of the AOI (Fig. 22f). Table 1 displays annual volumes and maximum PSI per year in each well. The injection of 180,000bbl of waste water from one well 5 miles south of the fault block began in 2011 and by 2013, 9 wells injected 18.8MMBBL. Two injection wells 2.5 miles north of the fault block were drilled a mile apart from one another and injected 48% of 2013's total volume and used maximum pressures of 480 and 472 PSI. Waste water injection increased to 26.3MMBBL in 2014 with 59 associated earthquakes. The volume of disposed waste water decreased in 2015 to 18.3 MMBBL but, pressures used to inject the volume remained consistent with the prior year.

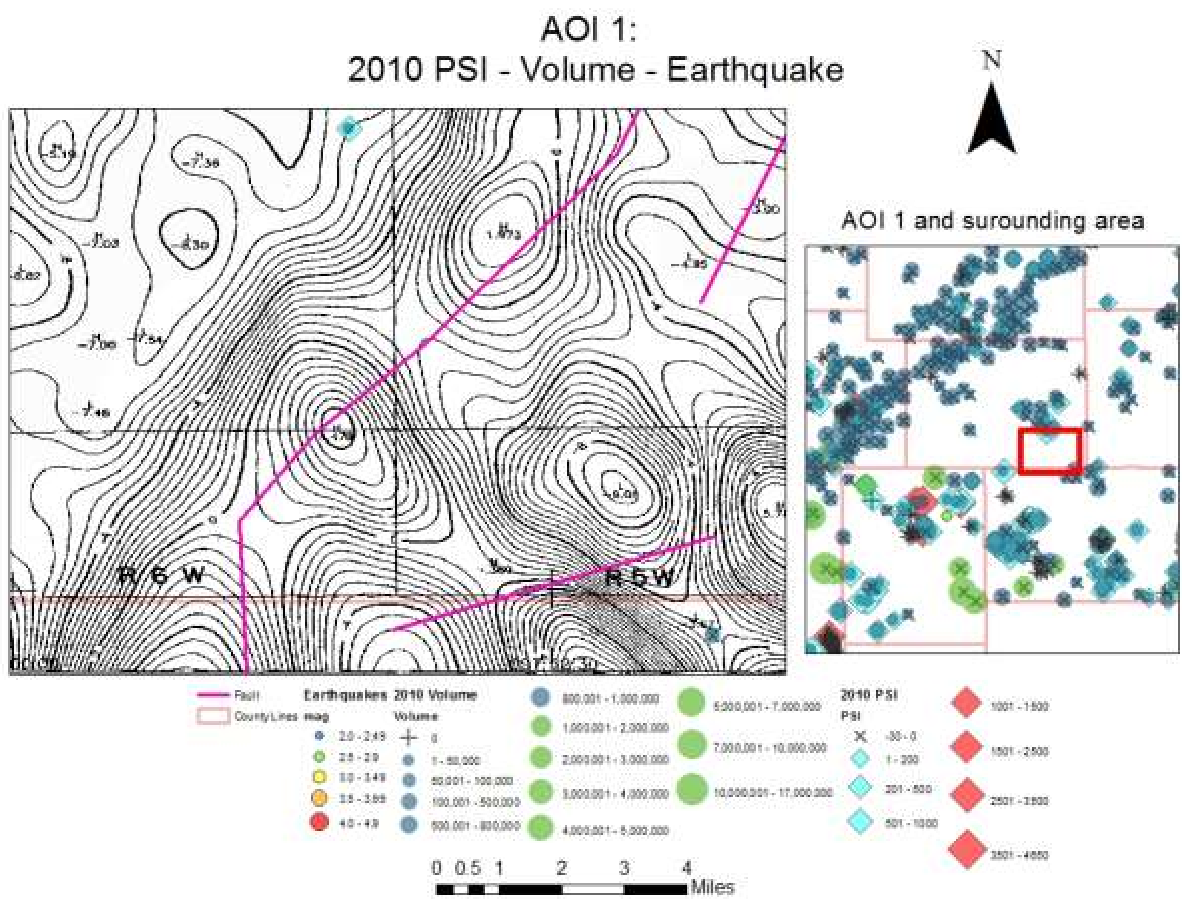

Figure 22a: The locations of SWD wells with their associated volumes (circles) and pressures (diamonds) in relation to the timing and locations of earthquakes. An inset map is provided to depict the evolution of the surrounding area. Magnetic contours provided by Gay.

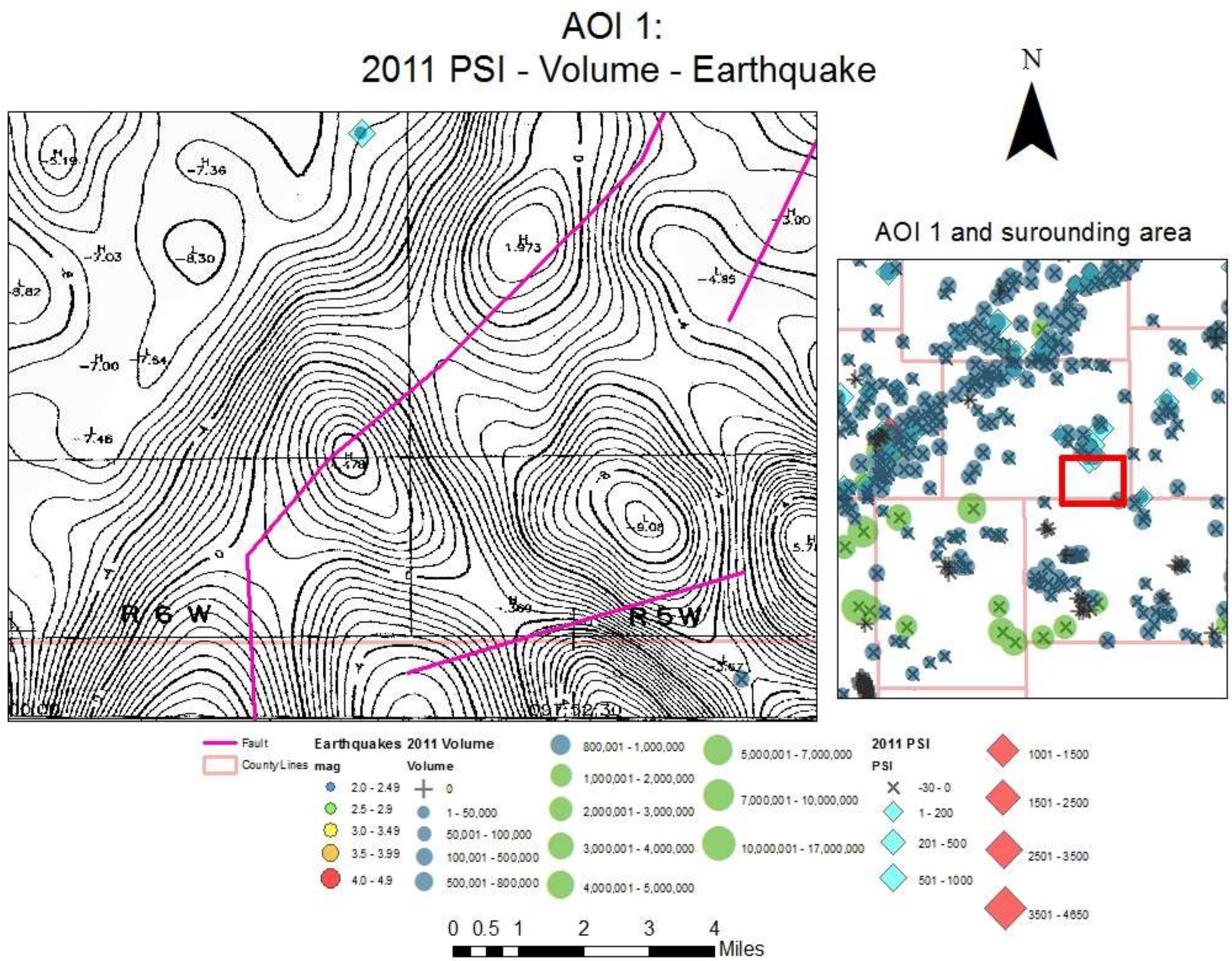

Figure 22b: The locations of SWD wells with their associated volumes (circles) and pressures (diamonds) in relation to the timing and locations of earthquakes. An inset map is provided to depict the evolution of the surrounding area. Note: SWD pressures were not provided for Oklahoma in 2011. Magnetic contours provided by Gay.

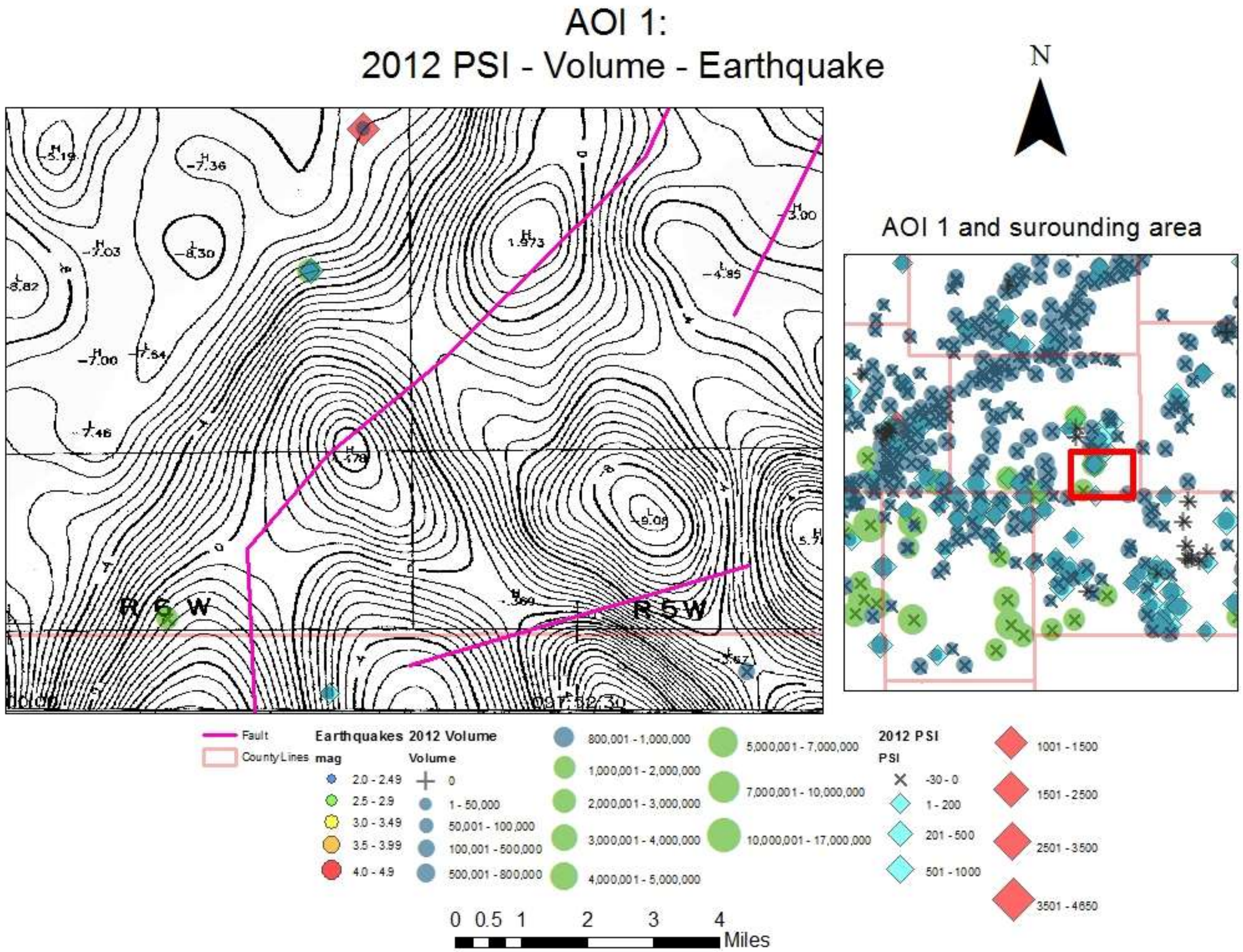

Figure 22c: Notice the increased well count and wells using 200-500 PSI around the AOI, especially to the southwest and north. The locations of SWD wells with their associated volumes (circles) and pressures (diamonds) in relation to the timing and locations of earthquakes. An inset map is provided to depict the evolution of the surrounding area. Magnetic contours provided by Gay.

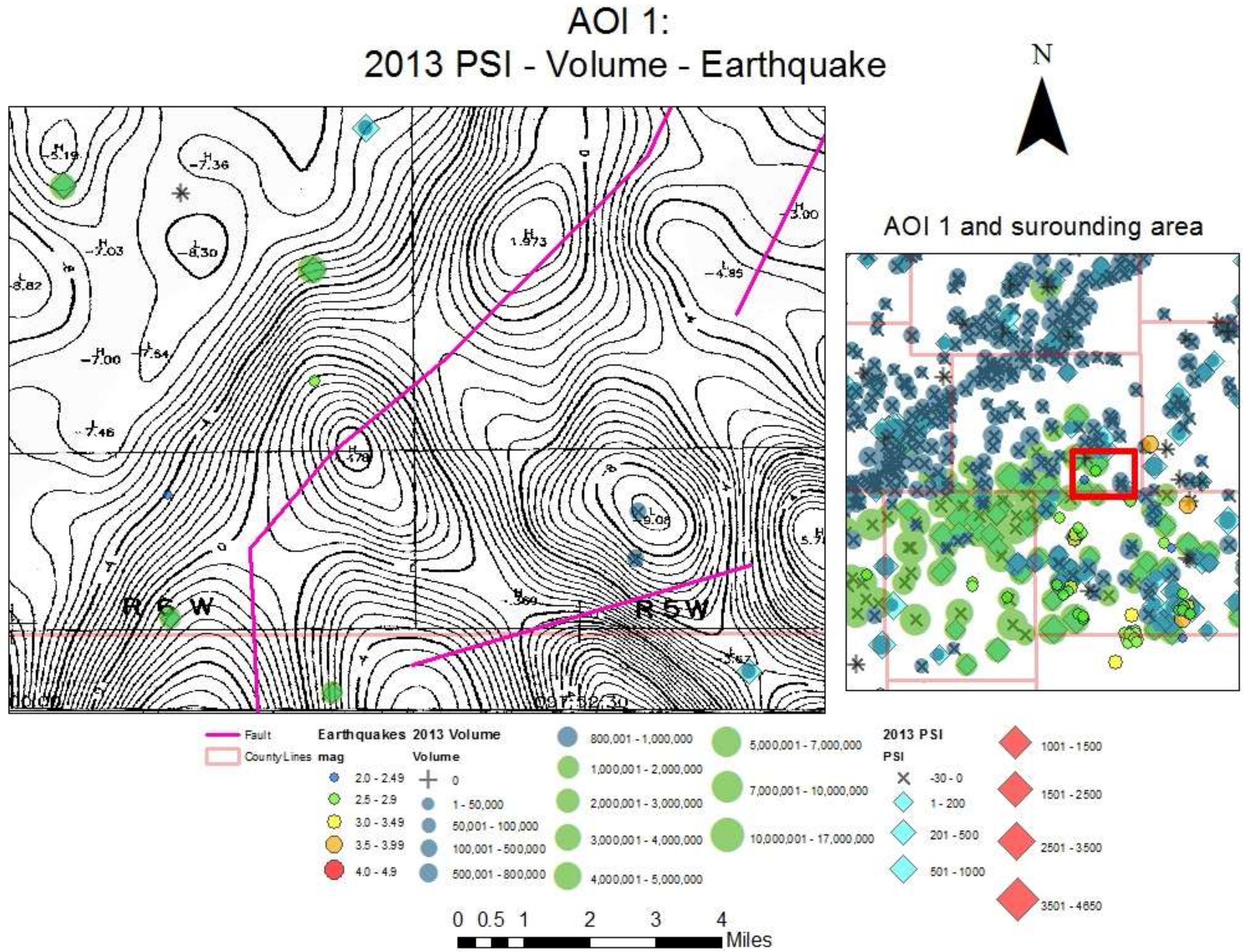

Figure 22d: Notice the increased well count, wells using 200-500 PSI, and major increase of wells injecting >1MMBBl around the AOI, especially to the southwest and north. The locations of SWD wells with their associated volumes (circles) and pressures (diamonds) in relation to the timing and locations of earthquakes. An inset map is provided to depict the evolution of the surrounding area. Magnetic contours provided by Gay.

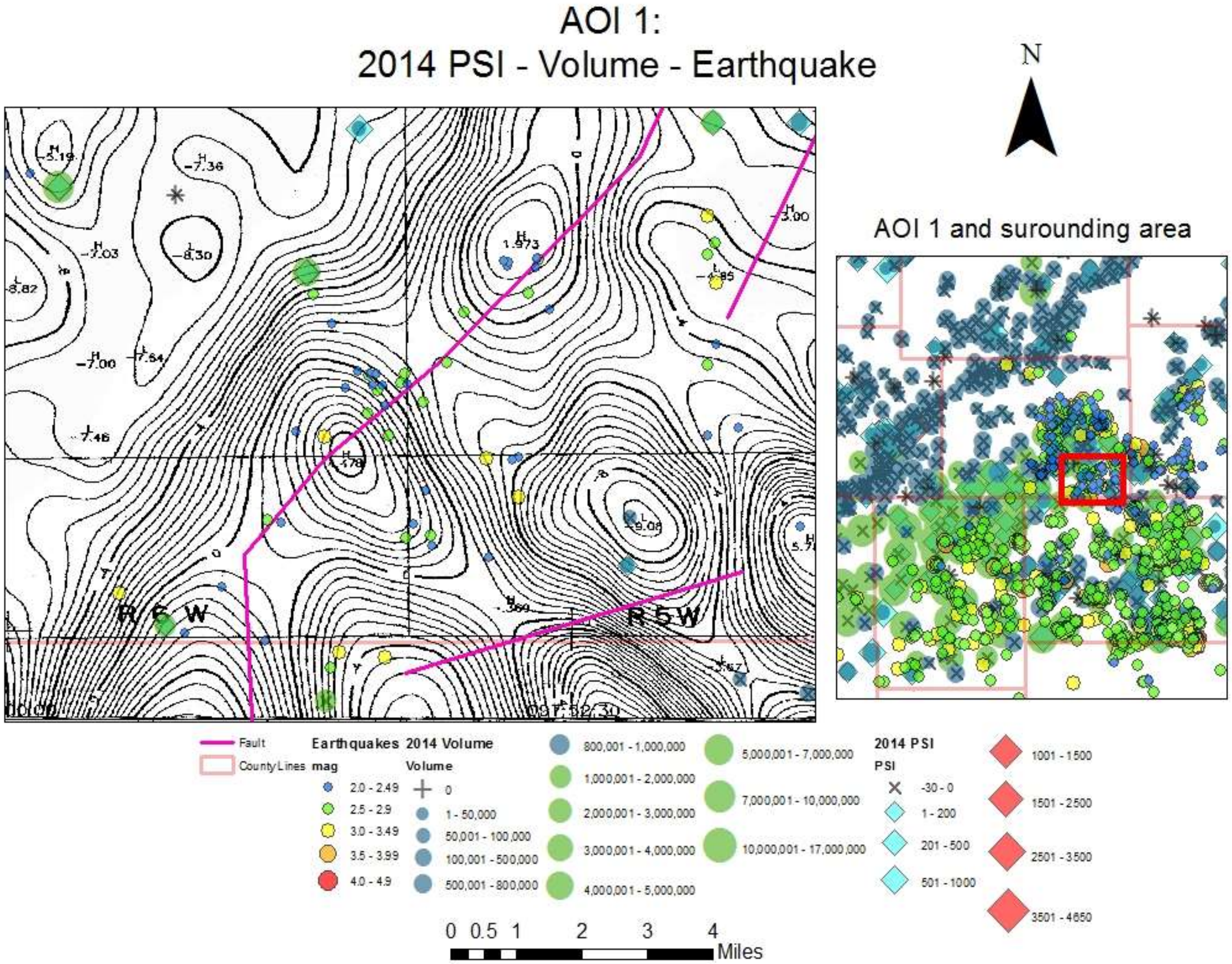

Figure 22e: Notice the increased earthquake activity is to the southeast of the largest injection plume. The locations of SWD wells with their associated volumes (circles) and pressures (diamonds) in relation to the timing and locations of earthquakes. An inset map is provided to depict the evolution of the surrounding area. Magnetic contours provided by Gay.

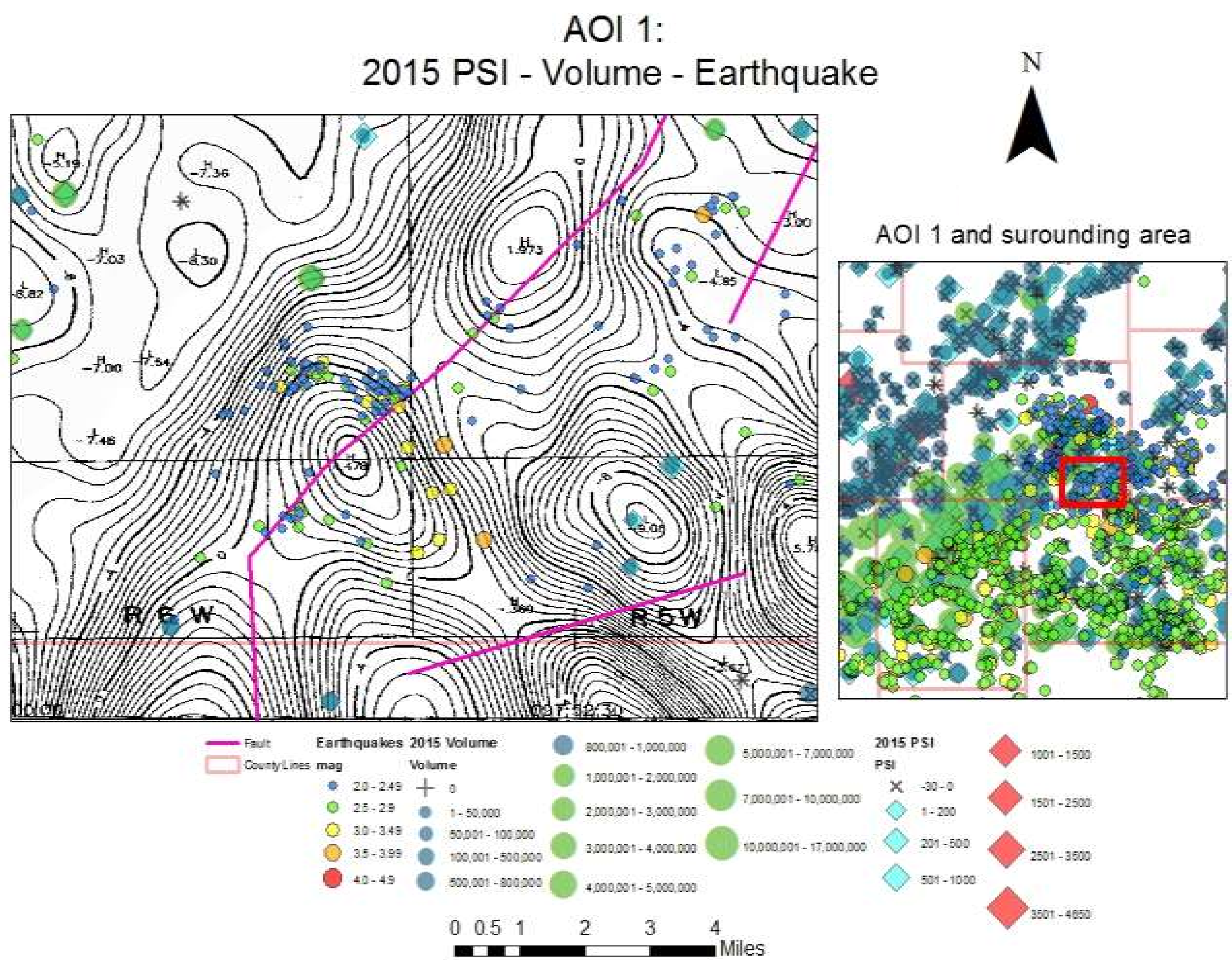

Figure 22f: Notice the increased earthquake activity all along the fault block. The three moment tensors depict transtensional movement. The farthest event to the south may be displaying transpression. The locations of SWD wells with their associated volumes (circles) and pressures (diamonds) in relation to the timing and locations of earthquakes. An inset map is provided to depict the evolution of the surrounding area. Magnetic contours provided by Gay.

Table 1: The (*) denotes twinned wells, or wells less than a mile apart.

AOI 1: Annual Volume and PSI

Well API	2011		2012		2013		2014		2015	
	Volume	PSI	Volume	PSI	Volume	PSI	Volume	PSI	Volume	PSI
15077001200001	0	0	0	0	107961	0	60284	25	70056	30
15077205040001	0	0	0	0	0	0	0	0	0	0
15077217430001	0	0	0	0	192190	0	64505	-12	35122	5
*15077217670000	0	0	2268365	140	4178686	480	3340210	393	3393422	385
*15077217770000	0	0	682530	454	4951528	472	4364707	395	3422442	389
15077217790000	0	0	1061114	0	1314649	118	1451992	125	572164	131
15077219100000	0	0	0	0	3420265	333	5837015	364	3462583	360
15077219260000	0	0	0	0	2892120	267	7750257	306	3545139	400
15077220140000	0	0	0	0	0	0	1127161	310	1451252	100
15077220160000	0	0	0	0	0	0	498924	248	345531	354
3505321127	182641	0	180424	0	99969	250	74401	0	0	0
3505322763	0	0	37489	24	0	0	0	0	237960	0
3505322764	0	0	456691	0	0	0	0	0	342855	142
3505322835	0	0	42356	57	1650071	10	1330274	0	648944	5
3505323364	0	0	0	0	0	0	365631	0	830022	-19
Total Volume	182641		4728969		18807439		26265361		18357492	

4.2 Area of Interest 2

AOI 2 is situated in west Sumner County along a knobby pattern within a regional transition of low magnetic susceptibility in the northwest to high magnetic susceptibility to the southeast. This example is a continuation of the Argonia suture zone to the northeast of AOI 1, whose reactivation begins in February, 2014. A fault is identified in Simpson age sediments and lies to the west of all injection wells and earthquake activity (Fig. 23). Table 2 shows wells through time with associated volumes and pressures used to inject. Injection volume increased 64% from 2013-2014. Four seismic events span from February-September, 2014 with three >3.0M occurrences. An earthquake measured at 4.9M occurred in November, 2014. This was followed by 35 earthquakes by the end of 2014, with another 23 occurring throughout 2015. A moment tensor was collected from one event in September, 2014 depicting a slightly transtensional motion. A second moment tensor recorded from the 4.9M event indicated transpressional movement (Fig. 23e).

4.3 Area of Interest 3

AOI 3 sits along an area of varying magnetic susceptibility similar to AOI 2. A fault running north-south bisects several northeast-southwest trending faults. Eleven operational SWD wells cover the area in 2010 and reduced to 2 wells in 2015 (table 3). Reduction was also seen in the volume of injected fluid from 21.5 MMBBL in 2010 to 8.5 MMBBL in 2015. Only one well used 13 PSI for injection in 2010. The remainder of the wells operated on a gravity drain from 2010-2015 (Fig. 24). The closest well with high volume and pressure is 5 miles to the north along the same fault system. There were no earthquakes detected in this area. The closest earthquakes are located 15 mile south and 10 miles to the northwest of the AOI.

DISCUSSION

The factors affecting seismicity in the study area include; 1) orientation of fracture sets and shear zones; 2) reservoir properties of the injection zone; and 3) method of injection used by individual or groups of SWD wells. There is a strong correlation between the increased numbers of SWD well locations, the volume of injected material, and the resulting high rates of seismic activity over a short period of time (Figs. 4 and 14). Areas with the highest increase in seismic activity are found in Alfalfa, Grant, Barber, and Harper Counties and were identified as using elevated annual maximum pressures in 2012 which persisted through 2015 (Appendix 1). Two wells in the most seismically active areas of Harper County, API numbers: 15077010450000 and 15077001460000, used 1500 and 1225 PSI respectively in 2015. Many other wells in the previously stated counties used a maximum injection pressure of 300-1000 PSI. Murray (2015) depicts Woods, Alfalfa, and Grant as counties with increased SWD volumes and increased earthquakes, while Kay County had a slight reduction of disposed volume with slight increase of earthquakes. Murray's results are very similar to the results of this research. Earthquake numbers in a study over Oklahoma seismicity in 2014 yielded similar results to those found in this research (Darold and others, 2014).

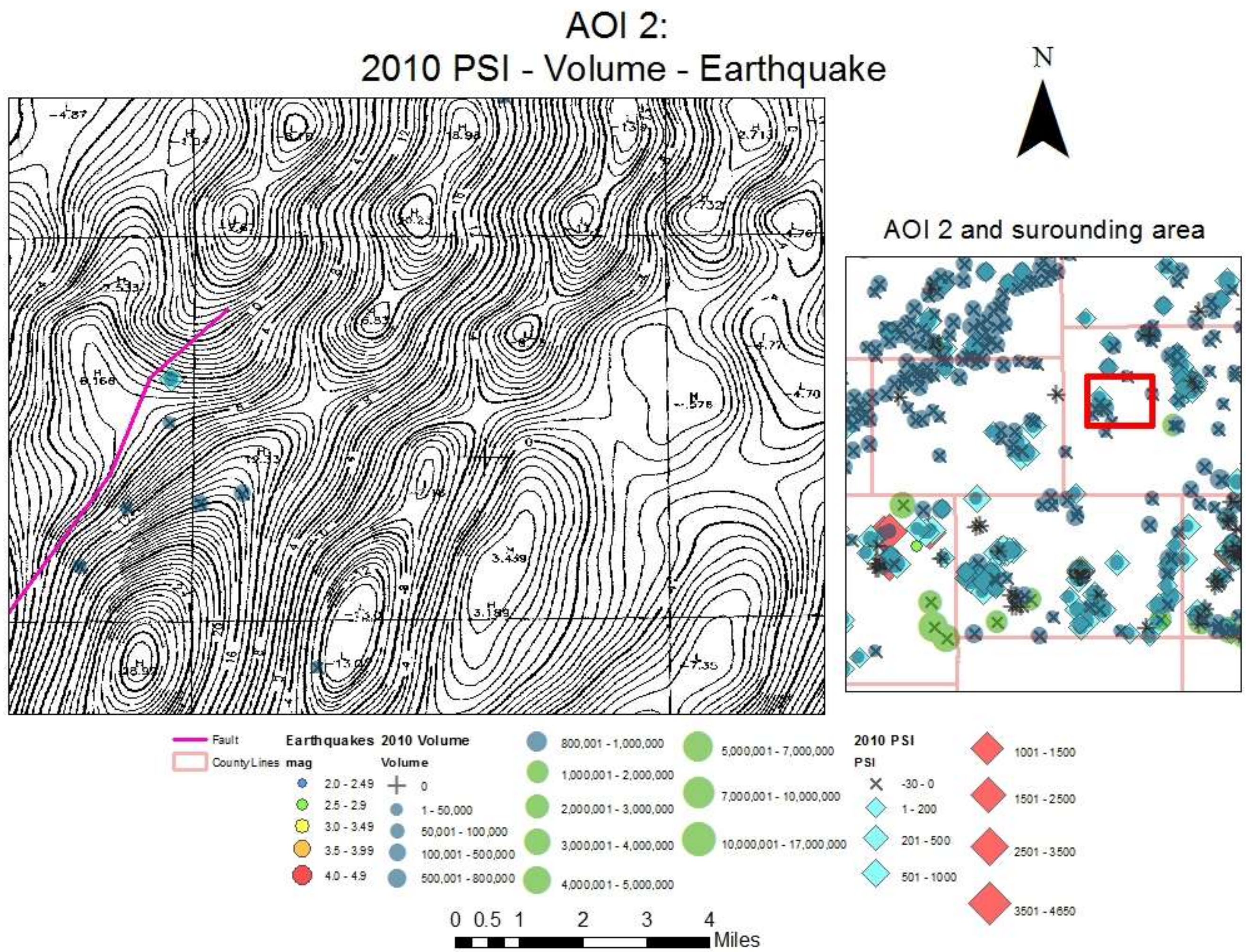

Figure 23a: The locations of SWD wells with their associated volumes (circles) and pressures (diamonds) in relation to the timing and locations of earthquakes. An inset map is provided to depict the evolution of the surrounding area. Magnetic contours provided by Gay.

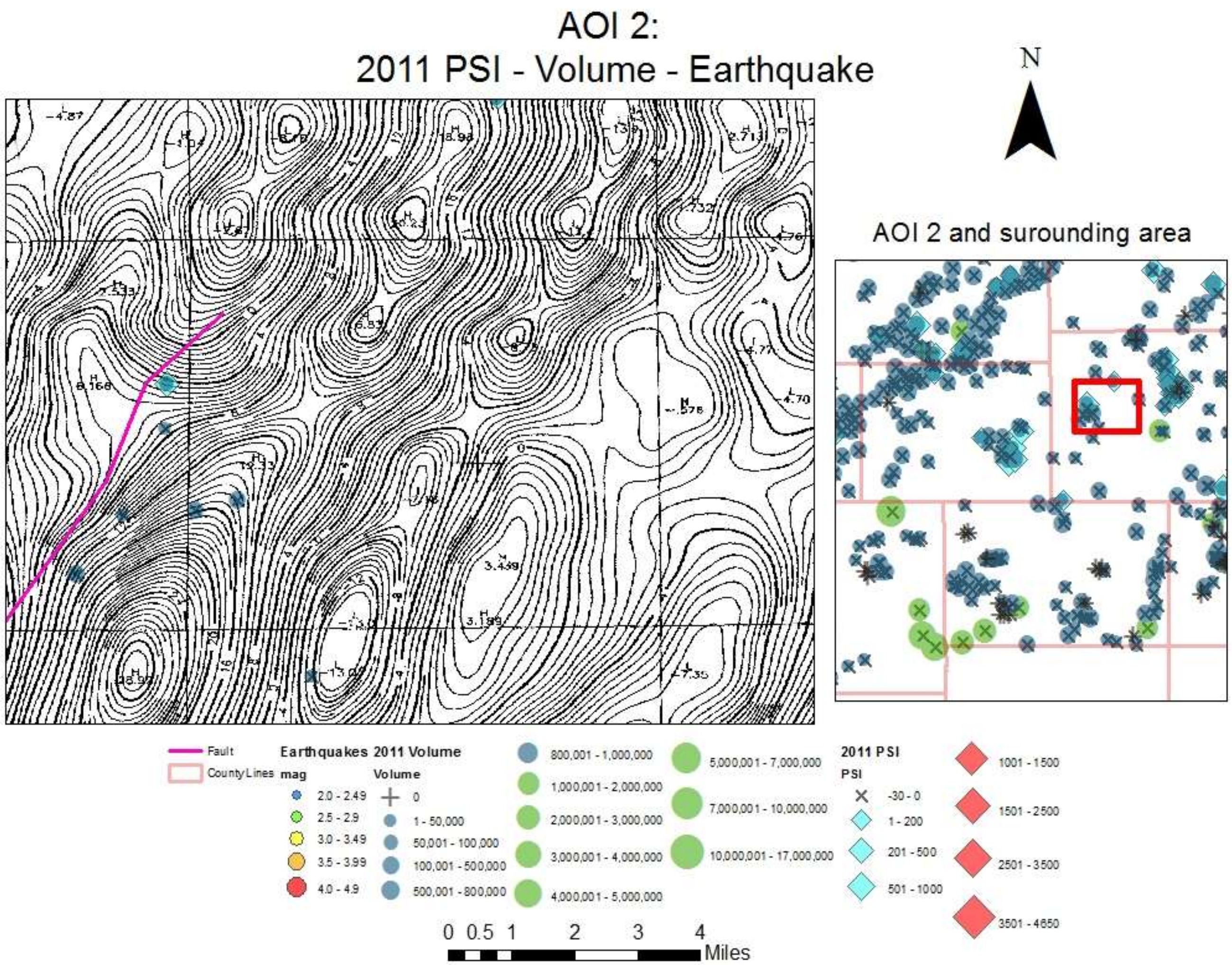

Figure 23b: The locations of SWD wells with their associated volumes (circles) and pressures (diamonds) in relation to the timing and locations of earthquakes. An inset map is provided to depict the evolution of the surrounding area. Magnetic contours provided by Gay.

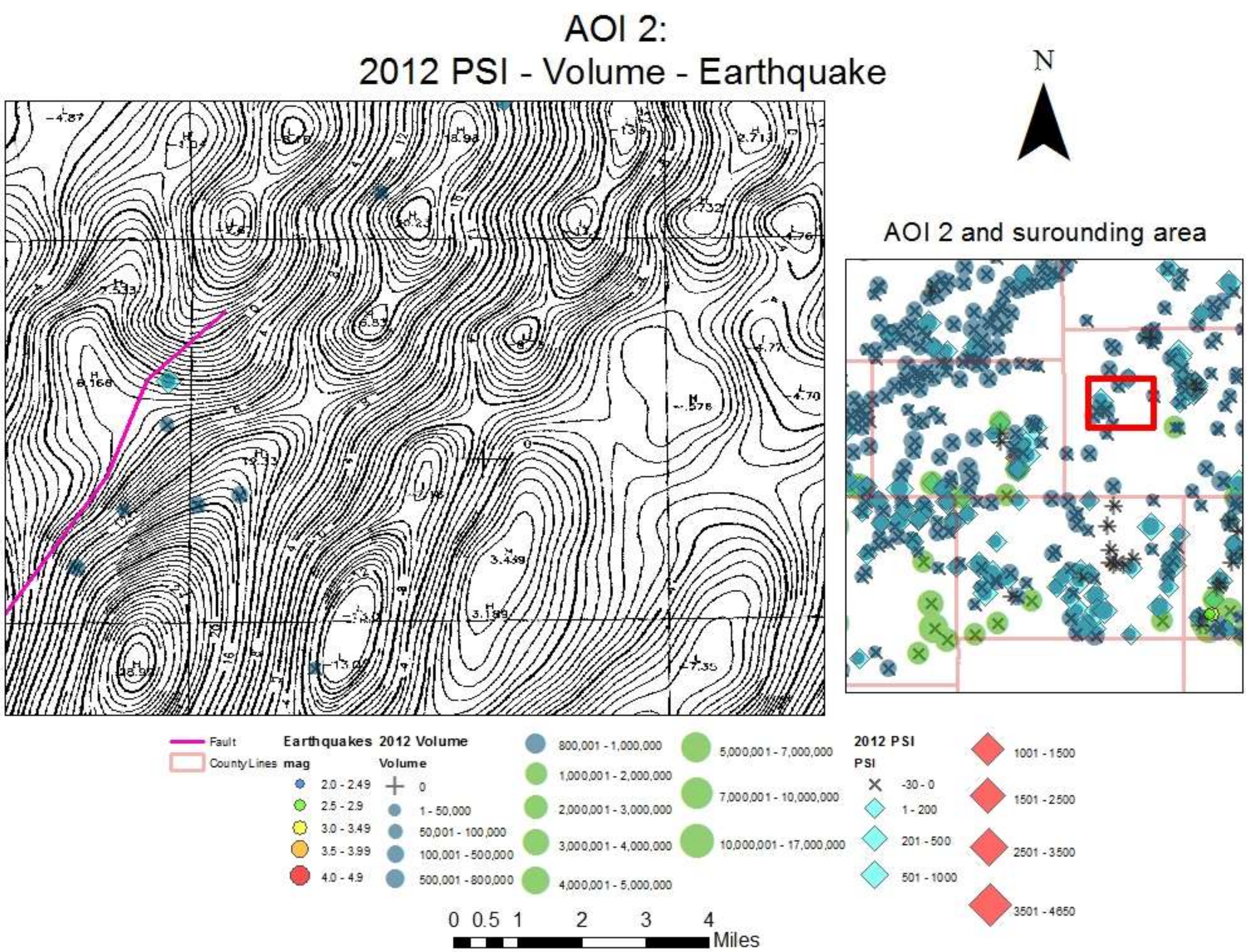

Figure 23c: The locations of SWD wells with their associated volumes (circles) and pressures (diamonds) in relation to the timing and locations of earthquakes. An inset map is provided to depict the evolution of the surrounding area. Magnetic contours provided by Gay.

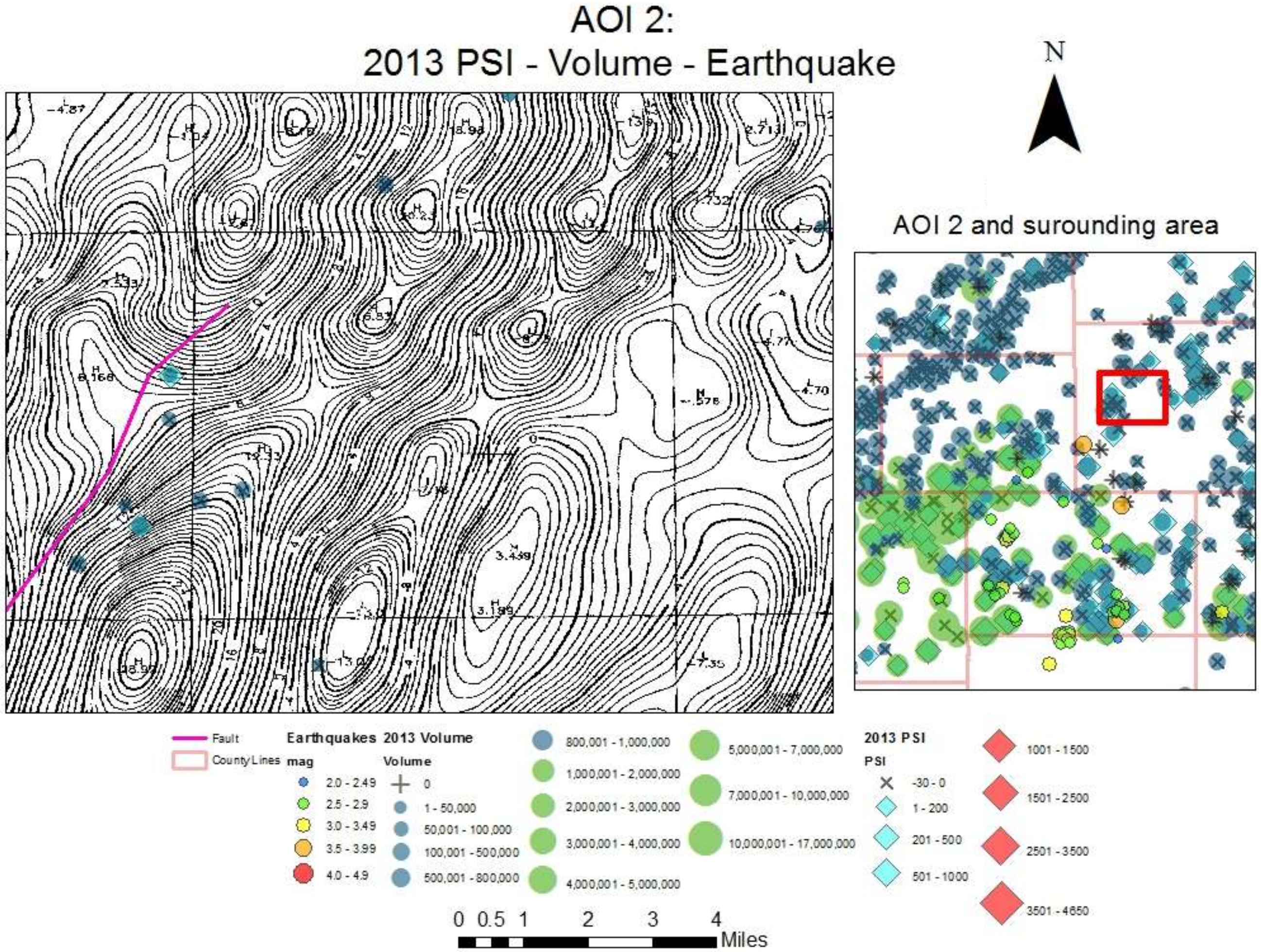

Figure 23d: The locations of SWD wells with their associated volumes (circles) and pressures (diamonds) in relation to the timing and locations of earthquakes. An inset map is provided to depict the evolution of the surrounding area. Magnetic contours provided by Gay.

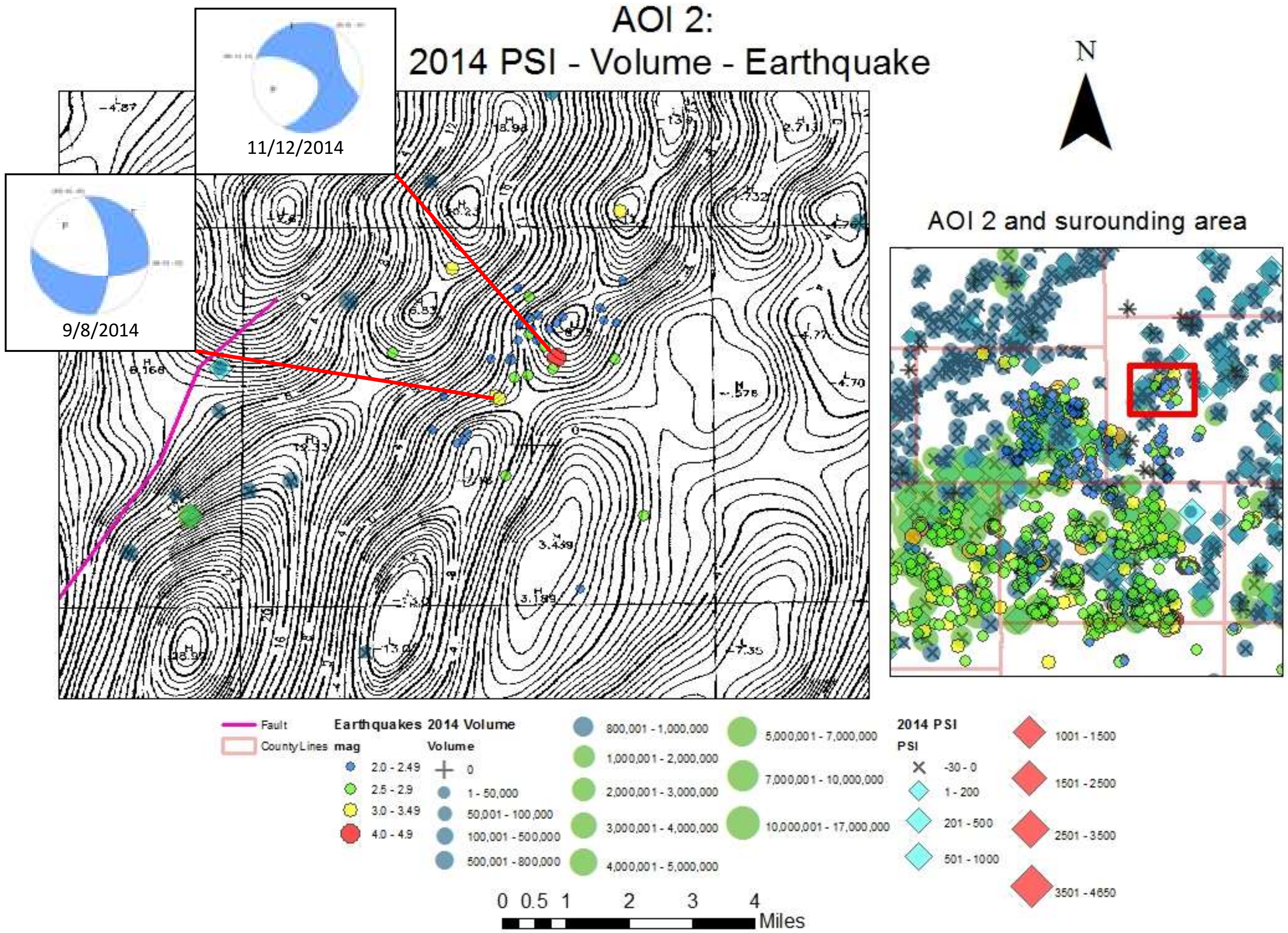

Figure 23e: Three >3.0M events occur with one moment tensor depicting transtensional movement prior to November, 2014. A 4.9M earthquake occurred in November, 2014 depicting transpressional movement followed by 35 earthquakes until the end of December, 2014. The locations of SWD wells with their associated volumes (circles) and pressures (diamonds) in relation to the timing and locations of earthquakes. An inset map is provided to depict the evolution of the surrounding area. Magnetic contours provided by Gay.

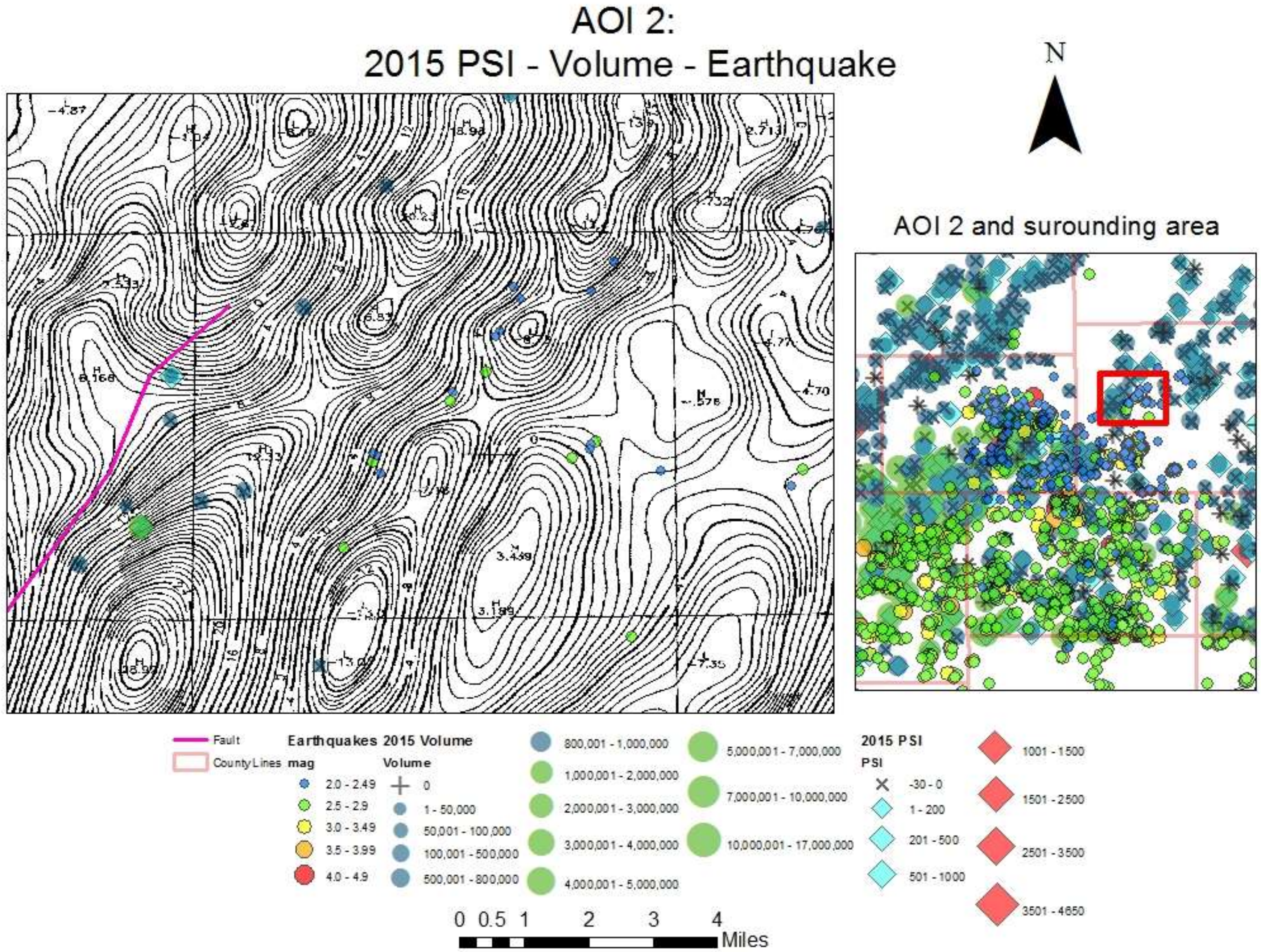

Figure 23f: 25 earthquakes recorded in all of 2015. None are above 3.0M. The locations of SWD wells with their associated volumes (circles) and pressures (diamonds) in relation to the timing and locations of earthquakes. An inset map is provided to depict the evolution of the surrounding area. Magnetic contours provided by Gay.

Table 2: Injection and volume of wells in AOI 2 by year.

AOI 2: Annual Volume and PSI

Well API	2010		2011		2012		2013		2014		2015	
	Volume	PSI	Volume	PSI	Volume	PSI	Volume	PSI	Volume	PSI	Volume	PSI
15191227260000	0	0	0	0	0	0	0	0	911013	0	263592	0
15191226860000	0	0	0	0	0	0	72228	210	12327	0	0	0
15191226820000	0	0	0	0	0	0	442951	210	2257853	330	2842674	460
15191304040000	90000	360	90000	360	90000	360	90000	300	90000	300	90000	300
15191205220000	64071	0	65961	0	61236	0	58779	0	54621	0	68985	0
15191206420000	0	0	0	0	0	0	36650	25	26260	25	24008	0
15191202240000	0	0	0	0	0	0	46789	0	124391	0	38475	0
15191015850000	0	0	0	0	0	0	3690	200	14895	200	17935	200
15191004490000	72907	0	113393	0	191237	0	141896	0	239268	0	114672	0
15191208690000	255500	0	255500	0	256200	0	109500	0	109500	0	109500	0
15191224810000	0	0	0	0	63519	0	120730	0	76741	0	71424	0
15191224410000	36500	0	36500	150	165710	150	158775	120	147825	120	98550	120
15191224050000	40150	0	45625	0	90155	0	80300	0	82125	0	78475	0
15191223410000	1620	0	7300	0	14280	0	13870	0	16425	0	18250	0
15191206710000	1081	0	1037	0	1163	0	796	0	858	0	981	0
15191212670000	335450	0	322390	0	291400	0	267820	0	387155	0	347395	0
15191000500000	47631	0	43327	0	41097	0	39707	0	60923	0	25930	0
Total Volume	944910		981033		1265997		1684481		4612180		4210846	

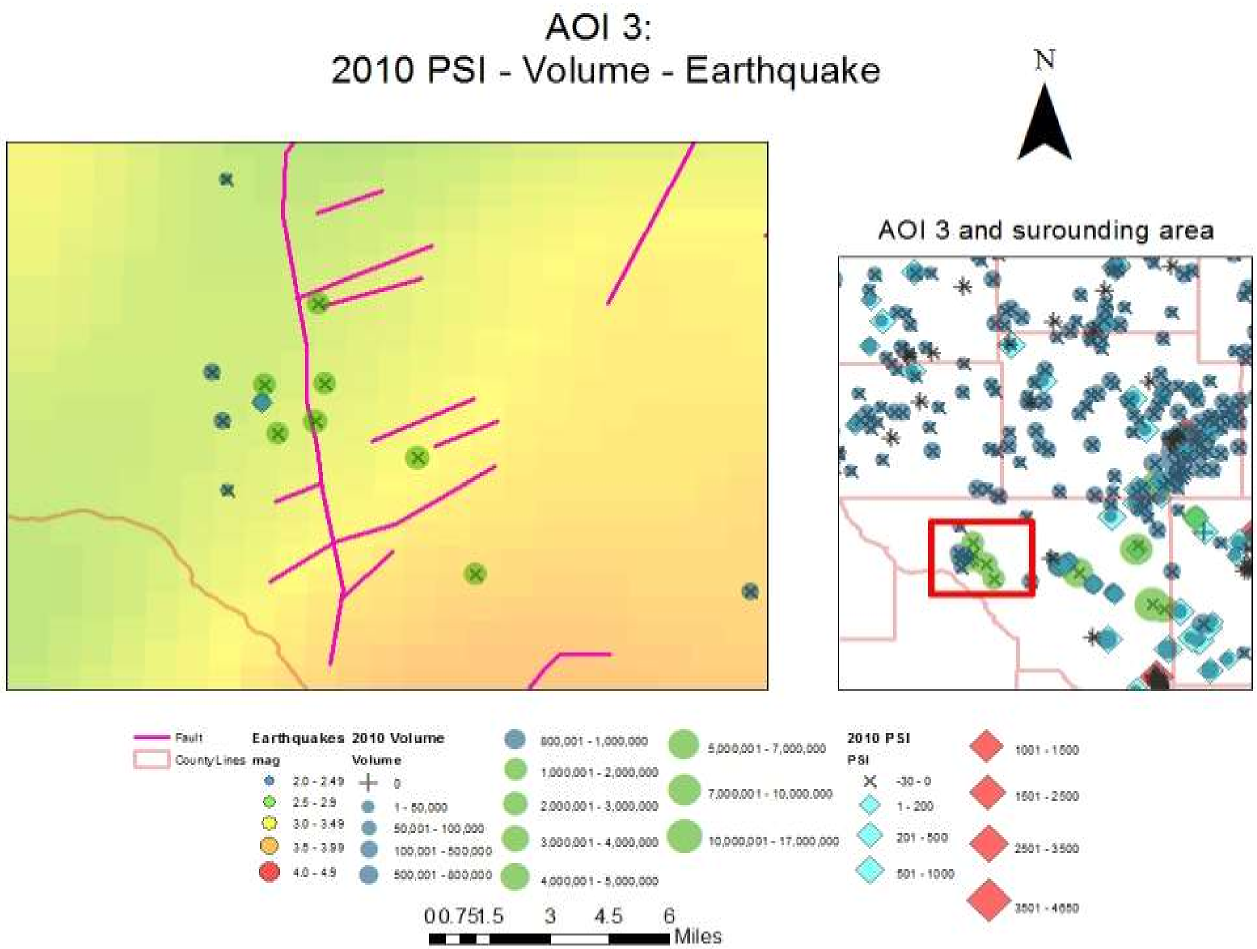

Figure 24a: Injection is at its highest in 2010. Six wells are injecting >1MMBBl of waste water. Note these wells are operating on gravity drain. Aeromagnetic map from Sweeney and Hill (2005). Higher magnetic readings are red, yellow are median magnetic readings, and greens are low magnetic readings.

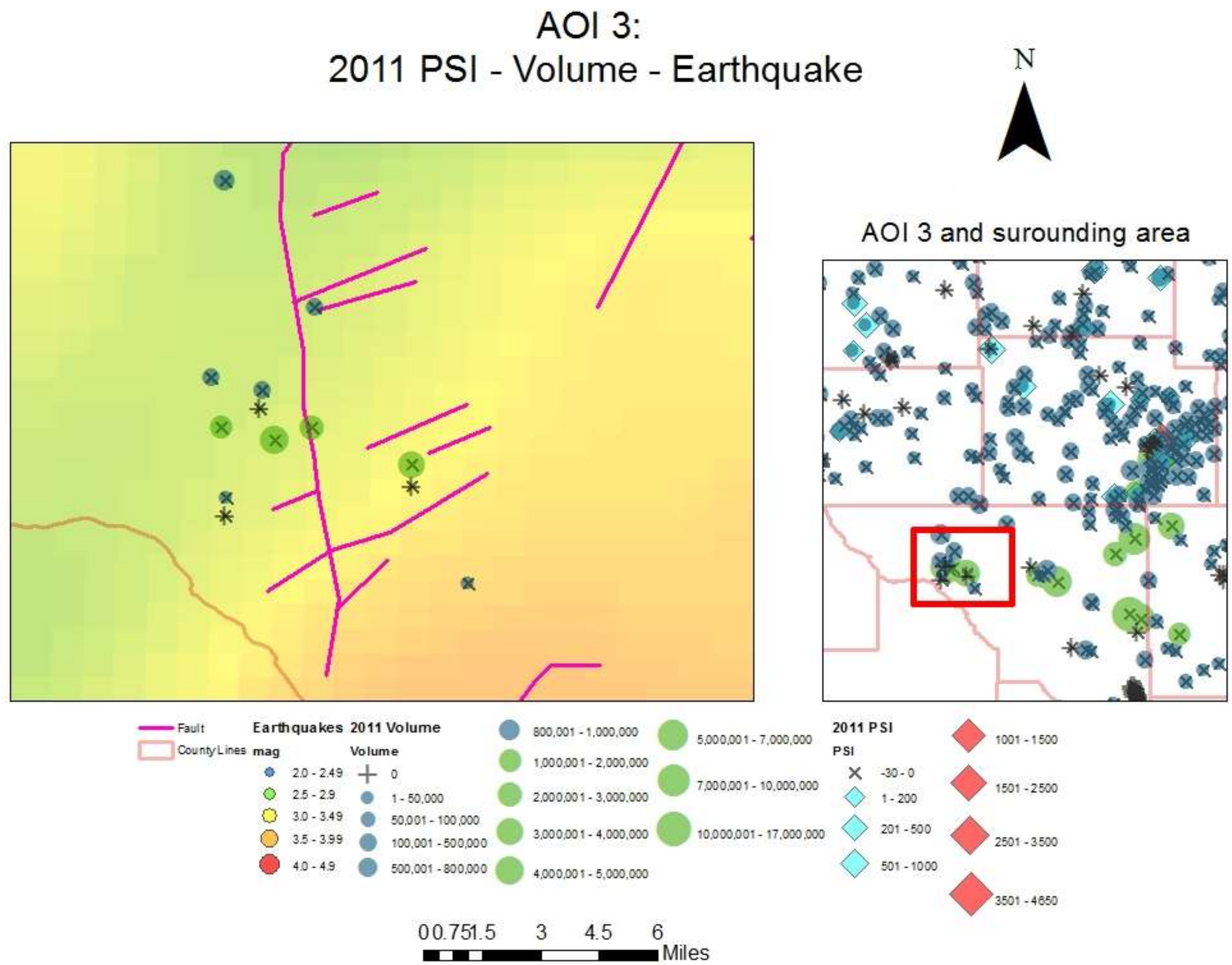

Figure 24b: A slight reduction in injected volume. Figure 24a: Injection is at its highest in 2010. Six wells are injecting >1MMBBl of waste water. Note these wells are operating on gravity drain. Aeromagnetic map from Sweeney and Hill (2005). Higher magnetic readings are red, yellow are median magnetic readings, and greens are low magnetic readings.

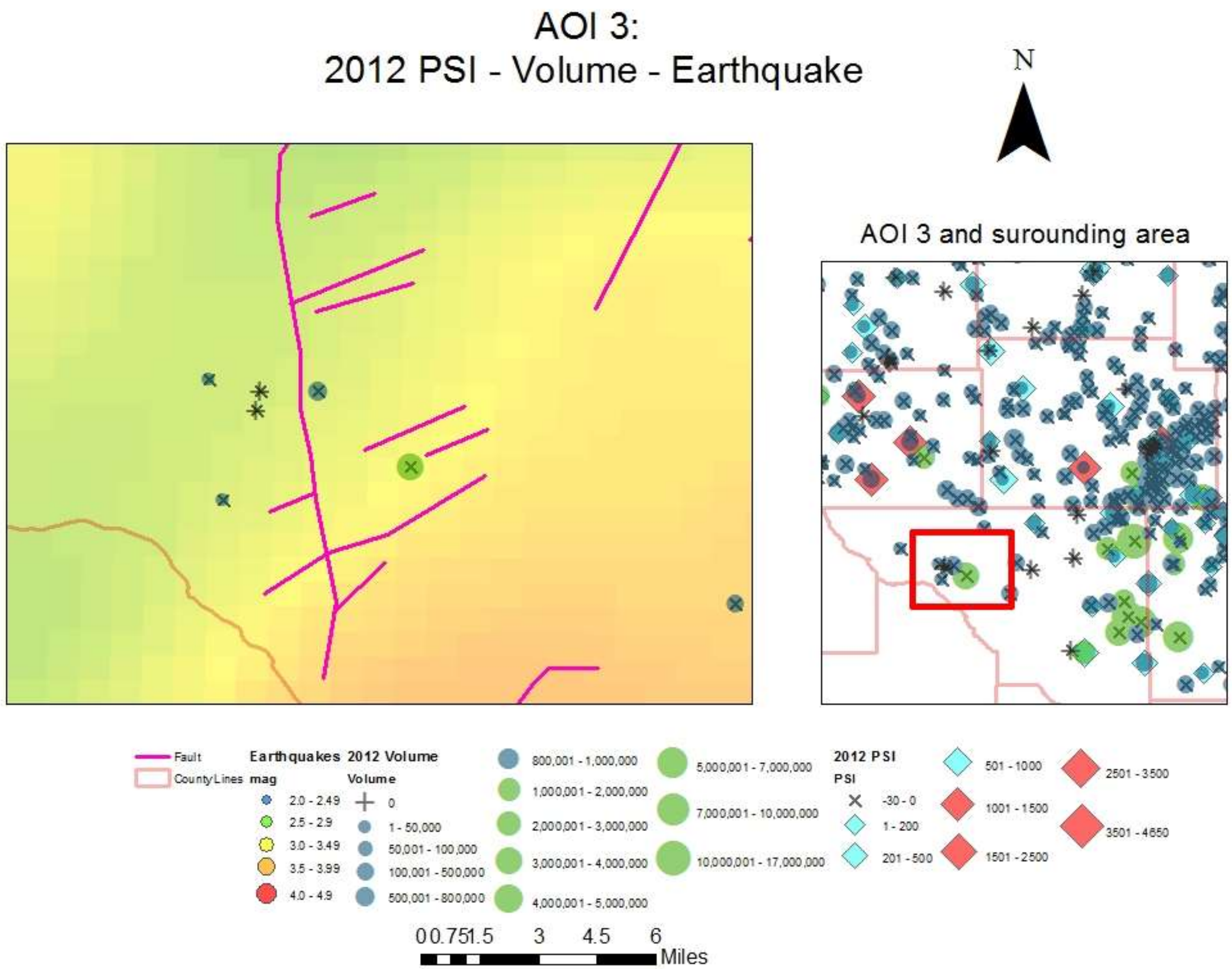

Figure 24c: Injection decreases in AOI 3 while well count increases to the east. Figure 24a: Injection is at its highest in 2010. Six wells are injecting >1MMBBl of waste water. Note these wells are operating on gravity drain. Aeromagnetic map from Sweeney and Hill (2005). Higher magnetic readings are red, yellow are median magnetic readings, and greens are low magnetic readings.

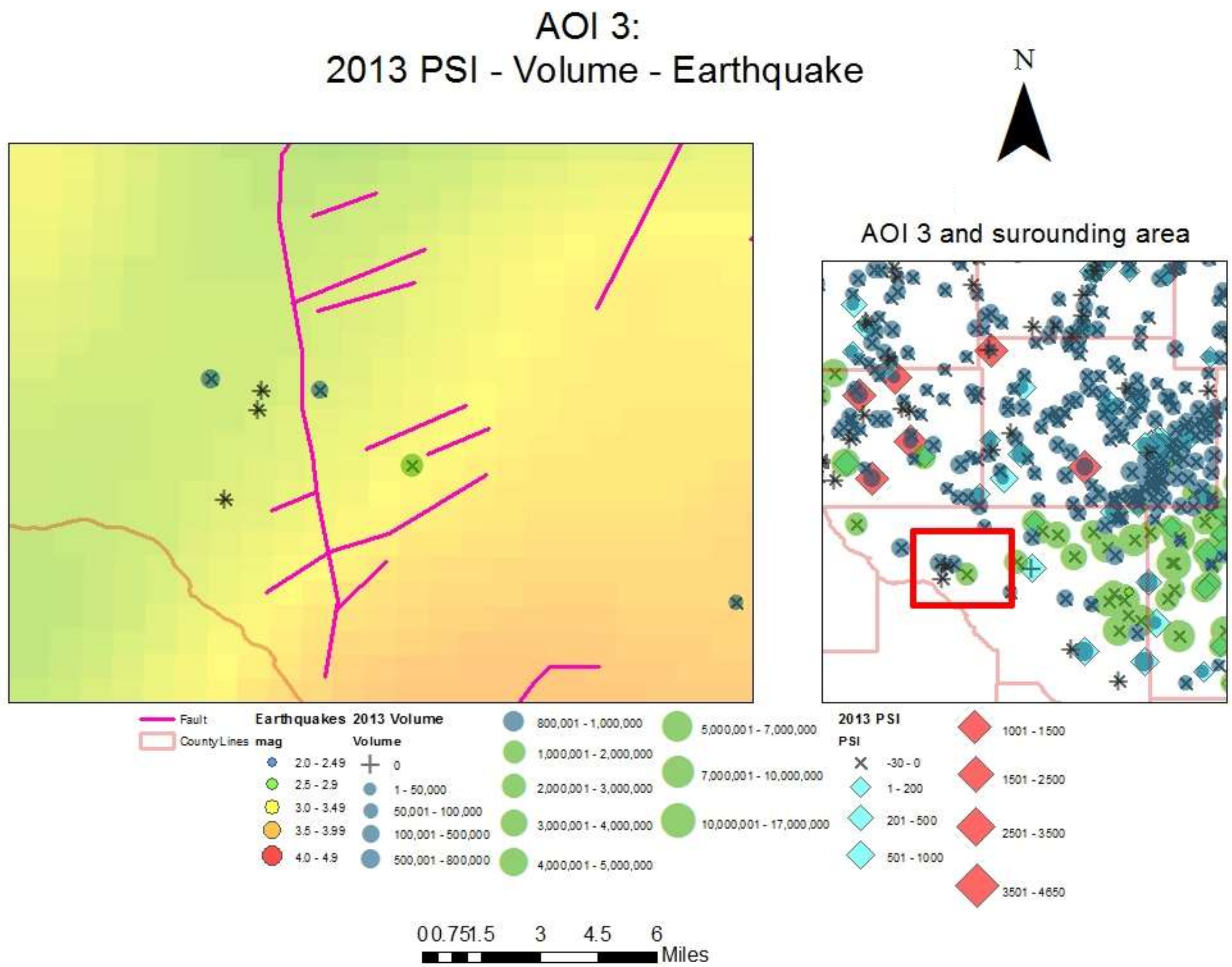

Figure 24d: AOI 3 in 2013. Volume decreases. Figure 24a: Injection is at its highest in 2010. Six wells are injecting >1MMBBl of waste water. Note these wells are operating on gravity drain. Aeromagnetic map from Sweeney and Hill (2005). Higher magnetic readings are red, yellow are median magnetic readings, and greens are low magnetic readings.

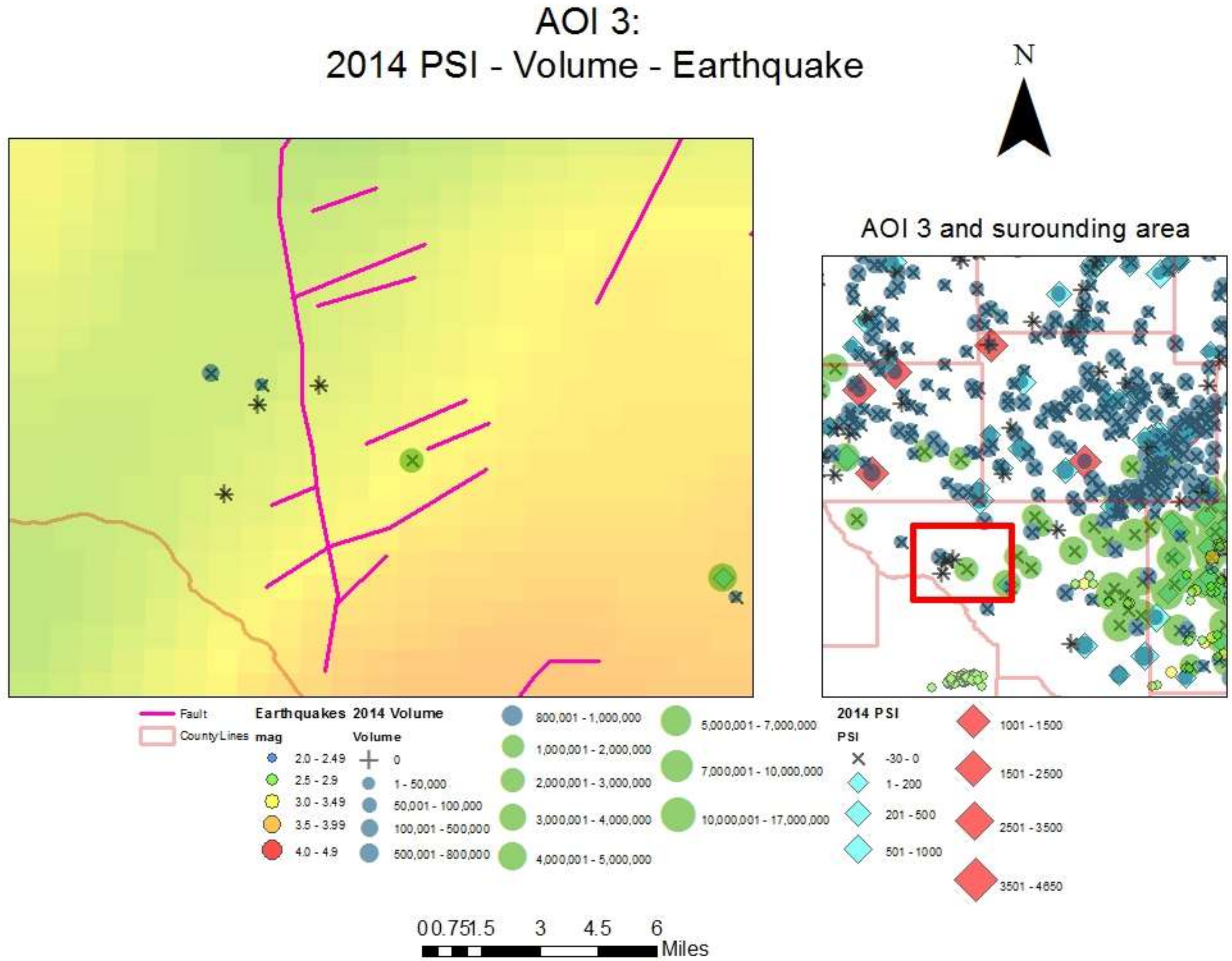

Figure 24e: AOI3 in 2014. Figure 24a: Injection is at its highest in 2010. Six wells are injecting >1MMBBl of waste water. Note these wells are operating on gravity drain. Aeromagnetic map from Sweeney and Hill (2005). Higher magnetic readings are red, yellow are median magnetic readings, and greens are low magnetic readings.

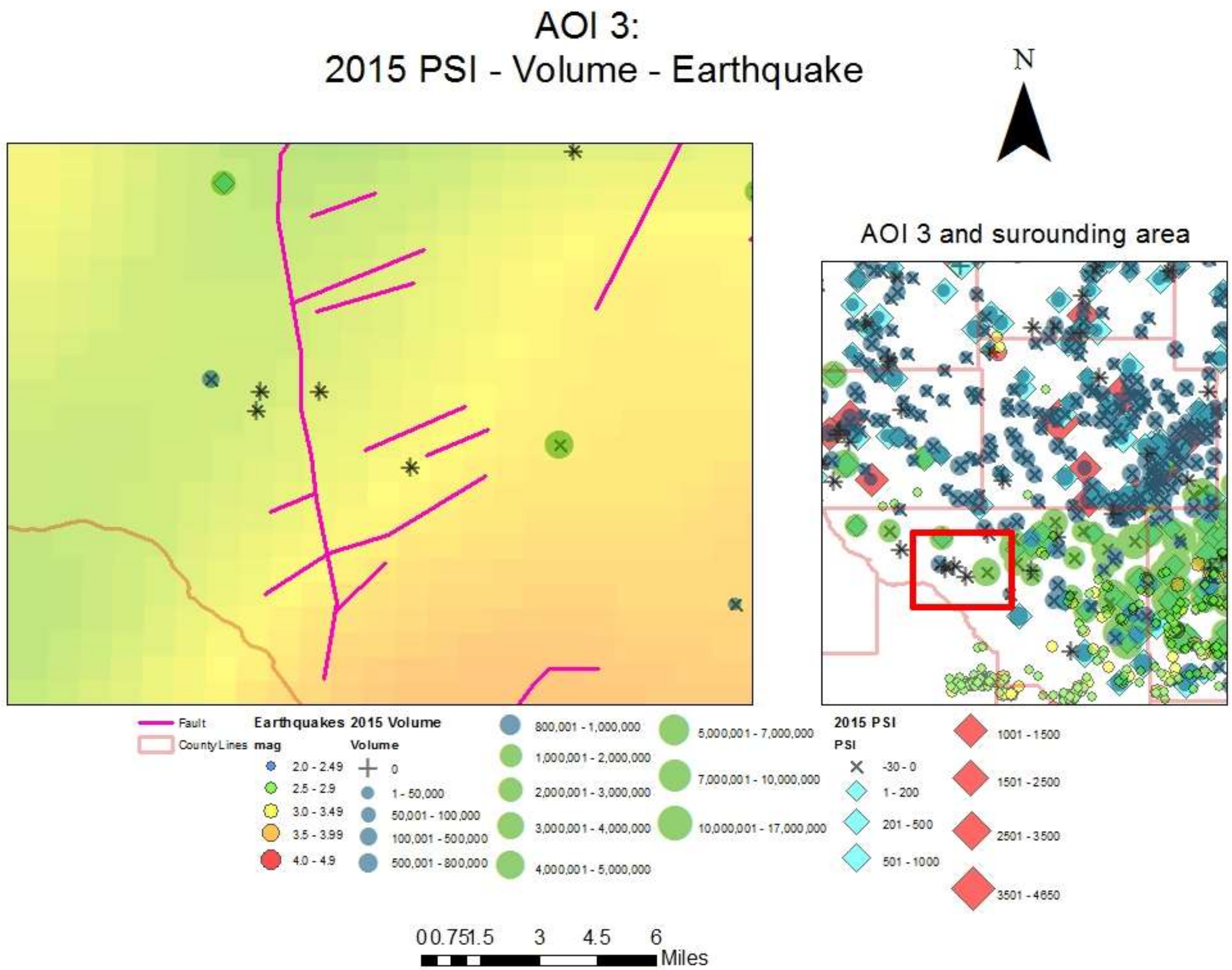

Figure 24e: AOI3 in 2015. Figure 24a: Injection is at its highest in 2010. Six wells are injecting >1MMBBl of waste water. Note these wells are operating on gravity drain. Aeromagnetic map from Sweeney and Hill (2005). Higher magnetic readings are red, yellow are median magnetic readings, and greens are low magnetic readings.

Table 3: Injection volume and pressures used in AOI 3.

AOI 3: Annual Volume and PSI

Well API	2010		2011		2012		2013		2014		2015	
	Volume	PSI	Volume	PSI	Volume	PSI	Volume	PSI	Volume	PSI	Volume	PSI
3515123146	1027009	0	482321	0	0	0	0	0	0	0	0	0
3515122776	24585	0	9694	0	11853	0	0	0	0	0	0	0
3515122757	2127414	0	3426932	0	3118898	0	1404940	0	2251342	0	0	0
3515123245	307849	0	183555	0	33805	0	533668	0	453229	0	184426	0
3515123023	1234275	0	190623	0	0	0	0	0	600	0	0	0
3515123194	306972	13	0	0	0	0	0	0	0	0	0	0
3515122602	2734478	0	2112874	0	0	0	0	0	0	0	0	0
3515123217	1676395	0	4551189	0	0	0	0	0	0	0	0	0
3515122847	237082	0	1985812	0	0	0	0	0	0	0	0	0
3515122834	1425989	0	567	0	0	0	0	0	0	0	0	0
3500335283	0	0	0	0	0	0	0	0	0	0	0	0
3500335291	0	0	0	0	0	0	0	0	0	0	0	0
3515122809	1245515	0	0	0	613158	0	173402	0	0	0	0	0
3515123737	0	0	0	0	0	0	0	0	0	0	4103124	-23
Total Volume	12347563		12943567		3777714		2112010		2705171		4287550	

It is difficult to correlate individual well injections with a single seismic event. AOI 1 could be identified as an area affected by induced seismicity. Wells in AOI 1 began injecting with elevated pressures in 2012 and continue with the elevated pressures though 2013 as the volume of waste water was increased. This activity persists into 2015 and seismic activity continues (Fig. 22). The Argonia and Pretty Prairie suture zones may represent areas of weakness in the geologic past, and are currently experiencing a dramatic change in normal and shear stress regimes. The stress regime changes are evident by the variety of fault movement seen around the study area. AOI 1's location on a conjugate suture zone and movement of seismic activity lead to the interpretation that this specific fault block is dropping and rotating. Normal displacement is represented by moment tensors and the rotational motion is based on the sequence of earthquake occurrences through time. It is likely that many of the earthquakes occurring in the study area reflect adjustments to several fault block motions. As weaker magnitude earthquakes rupture along and around fault blocks within the study area, the highest magnitude earthquakes are seen around the margins of the seismically active areas (Fig. 11). The margins may be experiencing higher magnitudes because shear stress acting on fault planes exceeded the normal stress, not by way of fluid injection and increase pore pressure, but by the increase in shear stress developed by the smaller earthquakes. This may hold true for events in AOI 2 and some smaller magnitude earthquakes elsewhere. However, the increased volume of disposed fluid is likely contributing as well. This method could be the driving force of seismicity in the area. As effective normal stress is reduced, the shear stress overcomes the effective normal stress resulting in an earthquake (Ellsworth, 2013) (Warpinski, 2012). Neither method requires direct contact with the fault plane.

Figure 20 shows earthquakes within the Argonia - Pretty Prairie suture zone from 2010 to 2016, as well as SWD well volumes and pressures of 2015. This area has been subject to fluid injection at elevated pressure prior to 2010. In 2015, 27 wells injected at high volumes and elevated pressures in the center of this suture zone. There are minimal earthquakes found between wells within the suture zone from 2010-2016, and much of the seismicity is located along the surrounding fault blocks and shear zones (Fig. 20). A pressure gradient likely exists reducing the effective normal stress in the pores and fractures of the upper Arbuckle and causing faults to reactivate. This method requires no direct connection between the reservoir rock and the fault plane.

AOI 2's location to the northeast of the Argonia- Pretty Prairie suture zone leads to the interpretation that this area could be naturally adjusting to shear stresses developed by other earthquakes in the south-southwest, rather than being induced by the injection wells within the area. The amount of injected fluid and pressures used to inject may not be sufficient enough to be the sole cause of seismic activity in the area. However, the argument can be made that this is an area of induced seismicity because the earthquakes that caused this event could be induced by SWD well activities. The 4.9M earthquake was only the fifth the area had experienced from 2010-2014 and the pattern of earthquakes of 4.3-5.8 magnitude are shown to occur along the outer margins of the current earthquake zone (Fig. 11). The locations of high magnitude events could be in response to increased shear stresses being generated by areas much farther away.

AOI 3 did not have any seismic activity. This area could be used as an analog to reduce the number of earthquakes by slowly decreasing the amount of fluid injected. It could also be an analog for proper disposal practices because minimal pressure was used in the injection process. If any of these earthquakes have been induced, a gradual decrease in volume should be practiced rather than a complete cease in injection. The disposal volumes seen in 2012-2015 are similar to that of AOI 2. With its location along the outer margins of the study area, and its position along a known fault, a large earthquake is very possible if smaller events continue to the east.

The seismic activity seems to be confined to areas of lower magnetic susceptibility. This holds true for the study area, as well as for seismic activity in central Oklahoma (Fig. 11). The western portion of Kay County is an exception to this observation. The confining of seismic activity to magnetic lows could be related to the physical properties and/or changes in pore pressure within injection zones of injection wells atop magnetic highs. The magnetic high in Barber and Harper Counties has a slight trend to the northeast were a series of injection wells stretch its entire length. The wells injecting with elevated pressures along this trend are frequent and could be a factor in confining seismic activity within the magnetic lows.

The fracture pattern of the Arbuckle Group in the study area likely follows the same northeast-southwest trend seen on magnetic maps. A northwest-southeast trend of cross cutting faults has been reported along the length of the Nemaha Uplift and is interpreted in NewMag aeromagnetic maps, but is not detected within the sedimentary section of the Sedgwick Basin. Gay (2009) has sighted over 90 cases were structure maps of oil and gas fields, interpreted by outside parties, correlate with shear zones found on aeromagnetic maps. Figure 8 is just one area in Kay County, along the Nemaha Uplift that depicts this relationship. The locations of faults mapped in sedimentary units in AOI's 1 and 2 are also consistent with magnetically mapped shear zones and fault blocks.

The upper Arbuckle Group is the primary zone of disposal for the study area. This group is heterogeneous, and consists of complex stacks of reservoir and non-reservoir lithologies at various frequency and thickness scales. "The Arbuckle in Kansas can be viewed as having three end-member reservoir architectures, representing fracture-, karst-, and matrix-dominated architectural systems, with numerous possible variations between these end-member architectures" (Franseen and others, 2003). The end members described by Franseen (2003) were intended for the Cotter and Jefferson City Dolomite formations, located in the upper Arbuckle. SWD well locations have northeast-southwest trends directly within and west of the Argonia-Pretty Prairie Suture zone. A similar northeast-southwest trend is seen along the Pratt-Joy sutures but do not yield the same well counts, volumes, or injection pressures as the latter. This contrast could depict how the Arbuckle Group has specific end-member reservoir properties and heterogeneous lithologies across the study area. As a working hypothesis, injection practices should change with the location of the well in relation to injection interval properties. Recently, (Holubnyak and others, 2016) began modeling the reservoir quality of the Arbuckle Group in the Wellington Field, Sumner County, Kansas for CO_2-brine sequestration. The proposed injection interval for the project is within the lowest formations of the Arbuckle Group. This injection interval is much deeper than any injection intervals in the Oklahoma portions of the study area, and an unknown number in the Kansas study area but is likely to be deeper as well. Although modeling of Arbuckle Group was not a possibility in this study, it is a method that must be used for a full understanding of the migration habits of fluid in the injection reservoir, pressure regimes, and physical properties of reservoir rock and confining units.

A significant drawback to the study's interpretation is the lack of analysis on in-situ reservoir properties in response to pressures used to inject a specified volume and a full lithologic understanding of the Arbuckle Group's various lithologic boundaries. Small scale field studies, like that of (Holubnyak and others, 2016), are likely to yield precise conclusions to the validity of safe storage and disposal practices. Although magnetic data is dependent on lithology, a relationship between lithology type and magnetic reading was not obtained. Lithology types and ages presented by (Van Schmus and others, 1993), (Sims, 1990), and the Kansas Geologic Survey varied in magnetic reading across similar rock types. What can be seen are several large tectonic boundaries, separating presumed Precambrian terranes (Gay, 1986) (Fig.9). Of these tectonic boundaries, the Argonia and Pretty Prairie sutures coincide with areas of elevated earthquake activity in that may be related to SWD activities, but naturally occurring seismic activity cannot be ruled out as a possibility. The Midcontinent Rift and the Southern Oklahoma Aulacogen are two separate phases of extensive volcanism that may be reactivating and influencing the current seismic activity. Comparisons between the intraplate tectonics of the New Madrid seismic zone and Oklahoma-Kansas seismic zone can be made. The New Madrid seismic zone is situated within the Reelfoot Rift (Hildenbrand and Hendricks, 1995), while the study area, as well as the seismically active zone in central Oklahoma, lies between the MCR and the Oklahoma Aulacogen (Fig. 6). Moment tensors (focal mechanisms) by

Herrmann and Canas (1978) describe thrust and strike-slip fault movement in the New Madrid seismic zone, while the Oklahoma-Kansas seismic zone includes normal, strike-slip, transpressional, and transtensional movement. The Garvin and the surrounding counties in south-central Oklahoma are historically active with over 90% occurring within this zone since 1977 (Luza, 2008). The area’s active seismic past could be an explanation for the genesis of earthquakes in Oklahoma; however, no disposal well information was examined for this explanation. Seismicity can propagate and cause earthquakes elsewhere and is thought to be the case for AOI 2. Seismic propagation from central Oklahoma may account for the seismic adjustment in the study area. However, the variety of fault types found in the study area and the large increase of SWD volume and injection pressures seen in 2010-2015 probably accentuated seismic activity in the area.

CONCLUSIONS

By comparing the locations, volumes, and pressures of SWD wells to earthquake epicenters along magnetically mapped shear zones, areas with increased likelihood for seismic activity are characterized by SWD wells using elevated pressures to inject large volumes of waste water (>1.0 MMBBL). Magnetic variations correspond to areas of major lithologic changes and are interpreted as deep seated ductile shear zones, along which faults in the overlying sedimentary section and earthquake hypocenters lie. Intraplate seismicity exists in the New Madrid seismic zone and is similar to the study area being within a failed rift zone, but moment tensors seen in the study area and the amount of fluid disposed into the subsurface are significant differences between the two areas of intraplate seismicity. AOI’s 1 and 2 could both represent areas of induced seismic activity. AOI 3 shows no seismic activity in 2010-2016, and could be used to outline a plan to gradually reduce SWD well volumes in locations with seismic activity. Shear zones on the margins of seismically active zones are more likely to experience large magnitude earthquakes than areas within the center of the seismically active zone. AOI 3 has similar disposal volumes as AOI 2 and is located along the outer margin of the seismically active zone which may make it susceptible to a large earthquakes; however, injection pressures are all gravity driven in AOI 3 (one exception in 2010: 13 PSI being used). Large earthquakes (4.0-5.8M) allow the seismically active zone to migrate and expand along zones of weakness by inducing smaller earthquakes. Current injection wells operating around seismically active zones should reduce pressures and volume until seismic activity is reduced significantly. The process of selecting SWD locations needs to be backed by sound geologic knowledge of the injection formation. This includes the lithology of the injection interval, porosity and permeability measurements, in-situ reservoir pressures, and theoretical models detailing the favorable rates of injection without increasing pore pressure. Other injection wells in operation around the proposed injection location would need to be taken into account. As lucrative shale plays emerge, advancements in technologies used in hydraulic fracturing operations need to be accompanied by safe, effective, and efficient advancements in the disposal of waste water.

REFERENCES

REFERENCES

Adkison, W.L., 1972, Stratigraphy and structure of middle and upper Ordovician rocks in the Sedgwick Basin and adjacent Areas, South-Central Kansas: Kansas Geological Survey, paper 702.

Ake, J., Mahrer, K., O'connell, D., Block, L., 2005, Deep –injection and closely monitored induced seismicity at Paradox Valley, Colorado: Bulletin of the Seismological Society of America, v. 95, n. 2, p. 664-683.

Andrews, M.C., Mooney, W.D., and Meyer, R.P., 1985, The relocation of microearthquakes in the northern Mississippi Embayment: Journal of Geophysical Research, v. 90, no. B12, p. 10223-10236.

Armbruster, J.G., Steeples, D.W., Seeber, L., 1989, The 1989 earthquake sequence near Palco, Kansas: A possible example of induced seismicity (abstract): Seismological Research Letters, v. 60, no. 4, p. 141.

Bartram, J.G., Imbt, W. C., Shea, E.F., 1950, Oil and gas in Arbuckle and Ellenburger formations, midcontinent region: American Association of Petroleum Geologists, Bulletin, v. 34, p. 682-700.

Bickford, M.E., Sides, J.R., Cullers, R.L., 1981b, Chemical evolution of magmas in the Proterozoic terrane of the St. Francois Mountains, southeastern Missouri; 1, Field, petrographic, and major element data: Journal of Geophysical Research, v. 86, p. 10365-10386.

Bickford, M.E., Van Schmus, W.R., Karlstrom, K.E., Mueller, P.A., Kamenov, G.D., 2015. Mesoproterozoic-trans-Laurentian magmatism: a synthesis of continent wide age distributions, new SIMS U-Pb ages, zircon saturation temperatures, and Hf and Nd isotopic compositions. Precambrian. v. 265, p. 286–312.

Blair, K.P., Berendsen, P., 1988, Subsurface structural geology of the Nemaha tectonic zone, Kansas [abstract]: Geological Society of America, South-central Section Meeting Abstracts with Programs, v. 20, n.2, p. 91.

Cole, V.B., 1975, Subsurface Ordovician-Cambrian rocks in Kansas: Kansas Geological Survey, Subsurface Geology Series 2, p. 18.

Darold, A.P., Holland, A.A., Morris, J.K., and Gibson, A.R., 2015, Oklahoma Earthquake Summary Report 2014: Oklahoma Geological Survey, Open-File Report (OF1-2015).

Denson, R.E., 1966, Basement rocks in adjoining parts of Oklahoma, Kansas, Missouri, and Arkansas [Ph.D. thesis]: Austin, University of Texas.

Domrois, S.L., 2013, The midcontinent exposed: Precambrian basement topography, and fault-and-fold zones, within the cratonic platform of the United States [Thesis]: University of Illinois at Urbana-Champaign.

Ellsworth, W.L., 2013, Injection-induced earthquakes: Science, v. 341, p. 142, DOI: 10.1126/science.1225942.

Franseen, E.K., Byrnes, A.P., Cansler, J.R., Steinhauff, D.M., Carr, T.R., 2004, The geology of Kansas-Arbuckle Group: Current research in earth sciences, Kansas Geological Survey Bulletin 250, part 2, p. 43.

Friess, J.P., 2005. The southern terminus of the Nemaha tectonic zone, Garvin County, Oklahoma: Shale Shaker, v. 56, n. 2.

Gay, S.P. Jr., 1986, Relative timing of tectonic events in newly recognized Precambrian terranes in south-central Kansas, U.S.A., as determined by residual aeromagnetic data: Basement Tectonics Proceedings, v. 6, p. 153-167.

Gay, S.P. Jr., 1989, "Graniteville-type" Proterozoic igneous intrusions mapped in southeast Kansas: Geophysics in Kansas, Kansas Geological Survey Bulletin v. 226, p. 229-243.

Gay, S.P. Jr., 1999, Strike-Slip, compressional thrust-fold nature of the Nemaha system in eastern Kansas and Oklahoma: American Association of Petroleum Geologists, Midcontinent Section Meeting, Geoscience for the 21st Century, p. 39-50.

Gay, S.P. Jr., 2009, Reactivation tectonics: The evidence and the consequences, Technical Publication, v. 3.

Ham, W.E., Denson, R.E., Merritt, C.A., 1964, Basement rocks and structural evolution of southern Oklahoma: Oklahoma Geological Survey Bulletin 95, p. 302.

Herrmann, R.M., and Canas, J.A., 1978, Focal mechanisms studies in the New Madrid seismic zone: Bulletin of Seismological Society of America, v/. 68, p. 1095-1102.

Hildenbrand, T.G., Hendricks, J.D., 1995, Geophysical setting of the Reelfoot Rift and relations between rift structures and the New Madrid seismic zone: U.S. Geological Survey professional paper; 1538, v. E, p. 1-30.

Holland, A.A., 2015, Preliminary Fault map of Oklahoma, Oklahoma Geological Survey, Open-File Report OF3-2015.

Holtkamp, S.G., Brudzinski, M.R., Currie, B.S., 2015, Regional detection and monitoring of injection-induced seismicity: Application to the 2010-2012 Youngstown, Ohio, seismic sequence: American Association of Petroleum Geologists, v. 99, n. 9, p. 1671-1688.

Holubnyak, Y., Watney, W., Birdie, T., Rush, J., Fazelalavi, M., 2016, Reservoir modeling of CO2 injection in Arbuckle saline aquifer at Wellington Field, Sumner County, Kansas: Kansas Geological Survey, University of Kansas Center for Research, Open-File Report 2016-29.

Kansas Corporation Commission, 2016, Database of saltwater disposal/enhanced oil recovery wells in Kansas: Rene Stucky (accessed January 2016).

Kansas Geologic Survey, 2016, Kansas earthquake database: http://www.kgs.ku.edu/Geophysics/Earthquakes/historic.html (accessed January 2016).

Kelly, T.E., Merriam, D.F., 1964, Structural development of the Sedgwick Basin, south-central Kansas: Kansas Academy of Science, v. 67, n. 1.

Keranen, K.M, Savage, H.M., Abers, G.A., Cochran, E.S., 2013, Potentially induced earthquakes in Oklahoma, USA- links between waste water injection and the 2011 MW 5.7 earthquake sequence: Geology, v. 41, no. 6, p. 699–702.

Latham, L.R., Newill, R.J., Wallin, E.T., 1988, U-Pb geochronology of southern Missouri: Geological Society of America Abstracts with Programs, v. 20, p. 122.

Luza, K.V., 2008, Earthquakes of Oklahoma, Oklahoma Geological Survey. Educational Publication n.9.

McBee, W. Jr., 2003, Nemaha strike-slip fault zone, AAPG Mid-Continent section meeting Oct 13, 2003; Search and Discovery Article 10055.

McNamara, D.E., Benz, H.M., Herrmann, R.B., Bergman, E.A., Earle, P., Holland, A., Baldwin, R., Gassner, A., 2015, Earthquake hypocenters and focal mechanisms in central Oklahoma reveal a complex system of reactivated subsurface strike-slip faulting, Geophysics Research Letters, v. 42, p. 2742-2794.

Murray, K.E., 2014, Class II underground injection control well data for 2010-2013 by geologic zones of completion, Oklahoma: Oklahoma Geological Survey, Open-File Report (OF1-2014).

Murray, K.E., 2015, Class II saltwater disposal for 2009-2014 at the annual-, state-, and county- scales by geologic zones of completion, Oklahoma: Oklahoma Geological Survey, Open-File Report (OF5-2015).

Murray, K.E., Holland, A.A., 2014, Inventory of class II underground injection control volumes in the midcontinent: Oklahoma City Geological Society, v 65, is. 2, p 98-106.

Nelson, B.K., DePaolo, D.J., 1984, 1700-Myr greenstone volcanic successions in southwestern North America and isotopic evolution of the Proterozoic mantle: Nature, v. 312, p. 746-754.

Oklahoma Corporation Commission, 2016, Database of all underground injection control wells in Oklahoma: http://www.occeweb.com/og/ogdatafiles2.htm (accessed January 2016).

Pearce, J.A., Harris, N.B.W., Tindle, A.G., 1984, Trace element discrimination diagrams for the tectonic interpretation of granitic rocks: Journal of Petrology, v. 25, p. 956-983.

Pratt, T., 1989, Major Proterozoic basement features of the eastern Midcontinent of North America revealed by recent COCORP profiling: Geology, v. 17, p. 505-509.

Raleigh, C.B., Healy, J.H., Bredehoeft, J.D., 1976, An experiment in earthquake control at Rangely, Colorado: Science. V. 191, p. 1230-1236.

Roy, R.F., Blackwell, D.D., Birch, F., 1968, Heat generation of plutonic rocks and continental heat flow provinces: Earth and Planetary Science Letters, v. 5, p. 1-12.

Sass, J.H, 1981, Heat flow from the crust of the United States, *in* Touloukian, Y.S., Judd, W.R., and Roy, R.F., Physical properties of rocks and minerals: New York, McGraw-Hill, Cindas Data Series on Material Properties, p. 503-548.

Sides, J.R., Bickford, M.E., Shuster, R.D., Nusbaum, R.L., 1981, Calderas in the Precambrian terrane of the St. Francois Mountains, Southeastern Missouri: Journal of Geophysical Research, v. 86, p. 10349-10364.

Snyder, F.G., 1968, Tectonic History of the midcontinent United States: University of Missouri and Rolla Journal, no. 1, p. 65-77.

Sweeney, R.E., Hill, P.L., 2005, Nebraska, Kansas, and Oklahoma aeromagnetic and gravity maps and data: a web site for distribution of data. U.S. Geological Survey Data Series DS-138, v. 1, Report 2005.

Thomas, J.J., Shuster, R.D., Bickford, M.E., 1984, A terrane of 1,350- to 1,450-m.y.-old silicic volcanic and plutonic rocks in the buried Proterozoic of the mid-continent and in the Wet Mountains, Colorado: Geological Society of America Bulletin, V. 95, p. 1150-1157.

United States Geological Survey, 2017, Earthquake catalog: accessed March, 2017. https://earthquake.usgs.gov/earthquakes/search/

Van Schmus, W.R., Bickford, M.E., 1993, Transcontinental Proterozoic provinces (Chapter 4); *in*, Precambrian: Conterminous U.S., J. C. Reed, Jr., M. E. Bickford, R. S. Houston, P. K. Link, D. W. Rankin, P. K. Sims, and W. R. Van Schmus, (eds.): Geological Society of America, The Geology of North America, v. C-2, p. 171-334.

Van Schmus, W.R., Bickford, M.E., Zietz, I., 1987, Early and middle Proterozoic provinces in the central United States, *in* Kroner, A., ed., Proterozoic lithosphere evolution: Washington, D.C., American Geophysical Union, Geodynamics Series, v. 7.

Van Schmus, W.R., Green, J.C., Halls, H.C., 1982, Geochronology of Keweenawan rock of the Lake Superior region; A summary, *in* Wold, R.J., and Hinze, W.J., Tectonic history of the Lake Superior Basin: Geological Society of America Memoir 156, p. 165-171.

Yarger, H.L., 1985, Kansas basement study using spectrally filtered aeromagnetic data, *in* Hinze, W.J., The utility of regional gravity and magnetic anomaly maps: Society of Economic Geophysicists, p. 213-232.

APPENDIX

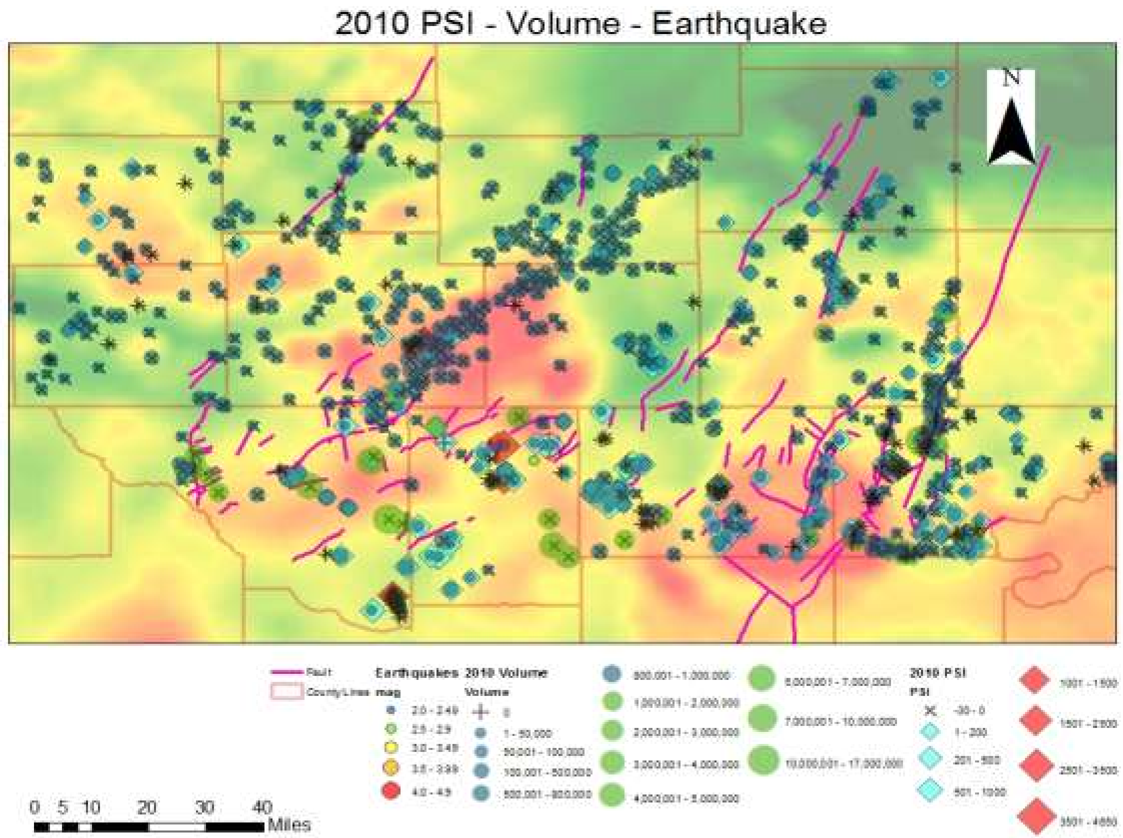

Appendix 1a: Study area in 2010. One earthquake detected in Alfalfa County, Oklahoma. The green circles indicate wells disposing 1MMBBL. Red diamonds indicate wells injecting with >1000 PSI. Figure 24a: Injection is at its highest in 2010. Six wells are injecting >1MMBBl of waste water. Note these wells are operating on gravity drain. Aeromagnetic map from Sweeney and Hill (2005). Higher magnetic readings are red, yellow are median magnetic readings, and greens are low magnetic readings.

2011 PSI - Volume - Earthquake

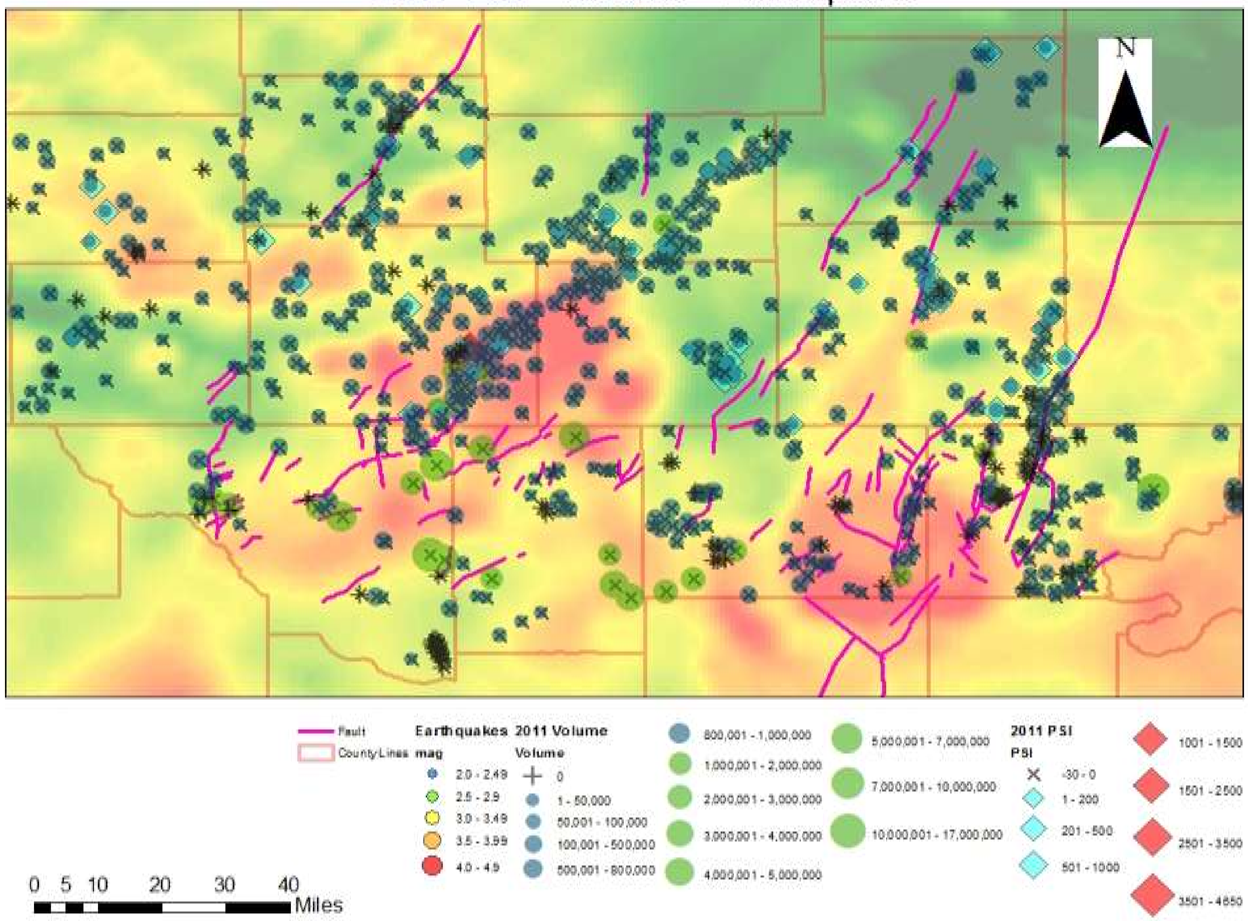

Appendix 1b: Study area in 2011. The Oklahoma SWD wells did not record PSI. The green circles indicate wells disposing 1MMBBL. Red diamonds indicate wells injecting with >1000 PSI. Figure 24a: Injection is at its highest in 2010. Six wells are injecting >1MMBBl of waste water. Note these wells are operating on gravity drain. Aeromagnetic map from Sweeney and Hill (2005). Higher magnetic readings are red, yellow are median magnetic readings, and greens are low magnetic readings.

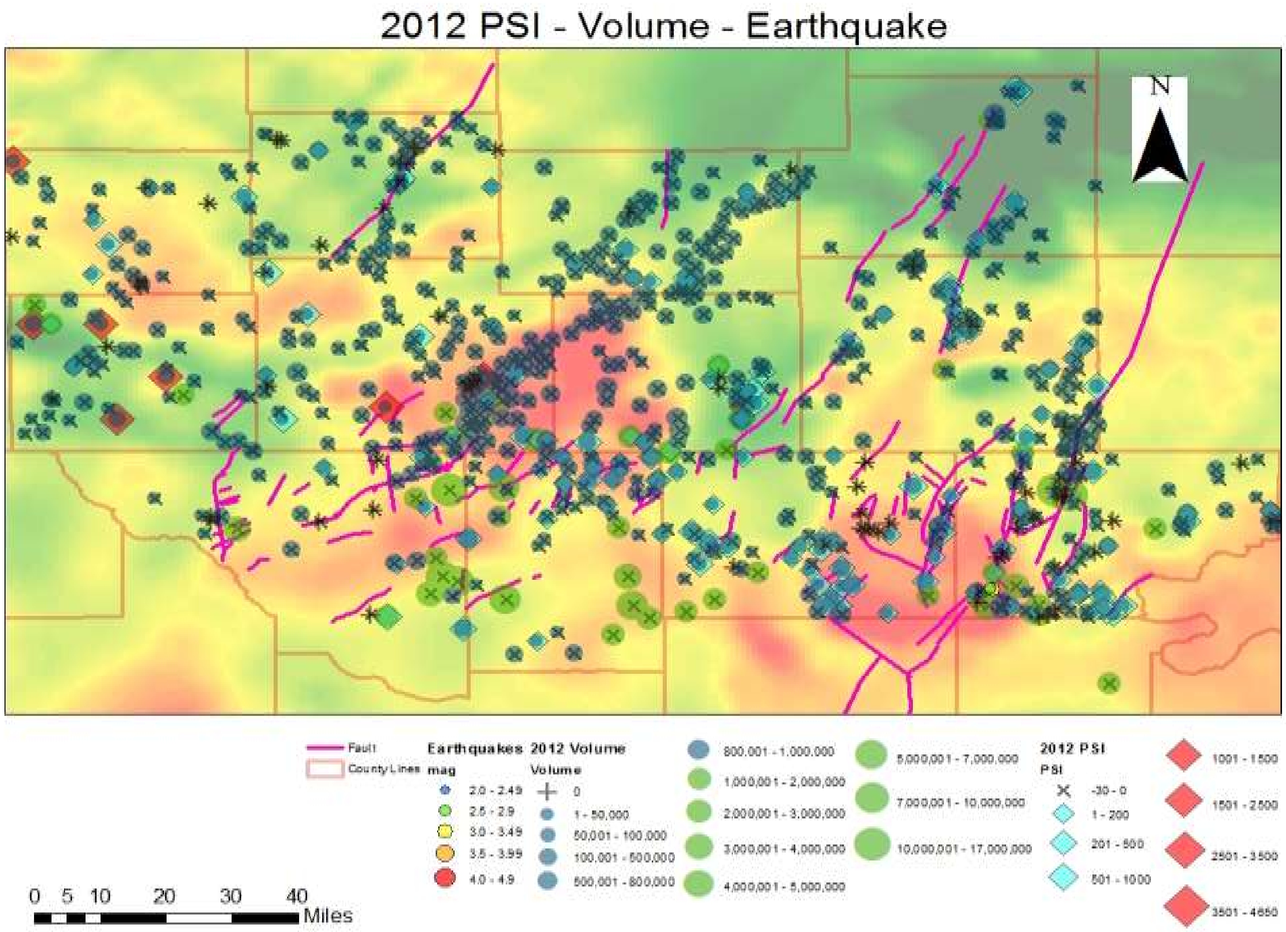

Appendix 1c: Study area in 2012. Notice the increase number of disposal wells in the center of the map compared to the previous two years. A set of earthquakes in SW Kay County, Oklahoma. . The green circles indicate wells disposing 1MMBBL. Red diamonds indicate wells injecting with >1000 PSI. Figure 24a: Injection is at its highest in 2010. Six wells are injecting >1MMBBl of waste water. Note these wells are operating on gravity drain. Aeromagnetic map from Sweeney and Hill (2005). Higher magnetic readings are red, yellow are median magnetic readings, and greens are low magnetic readings.

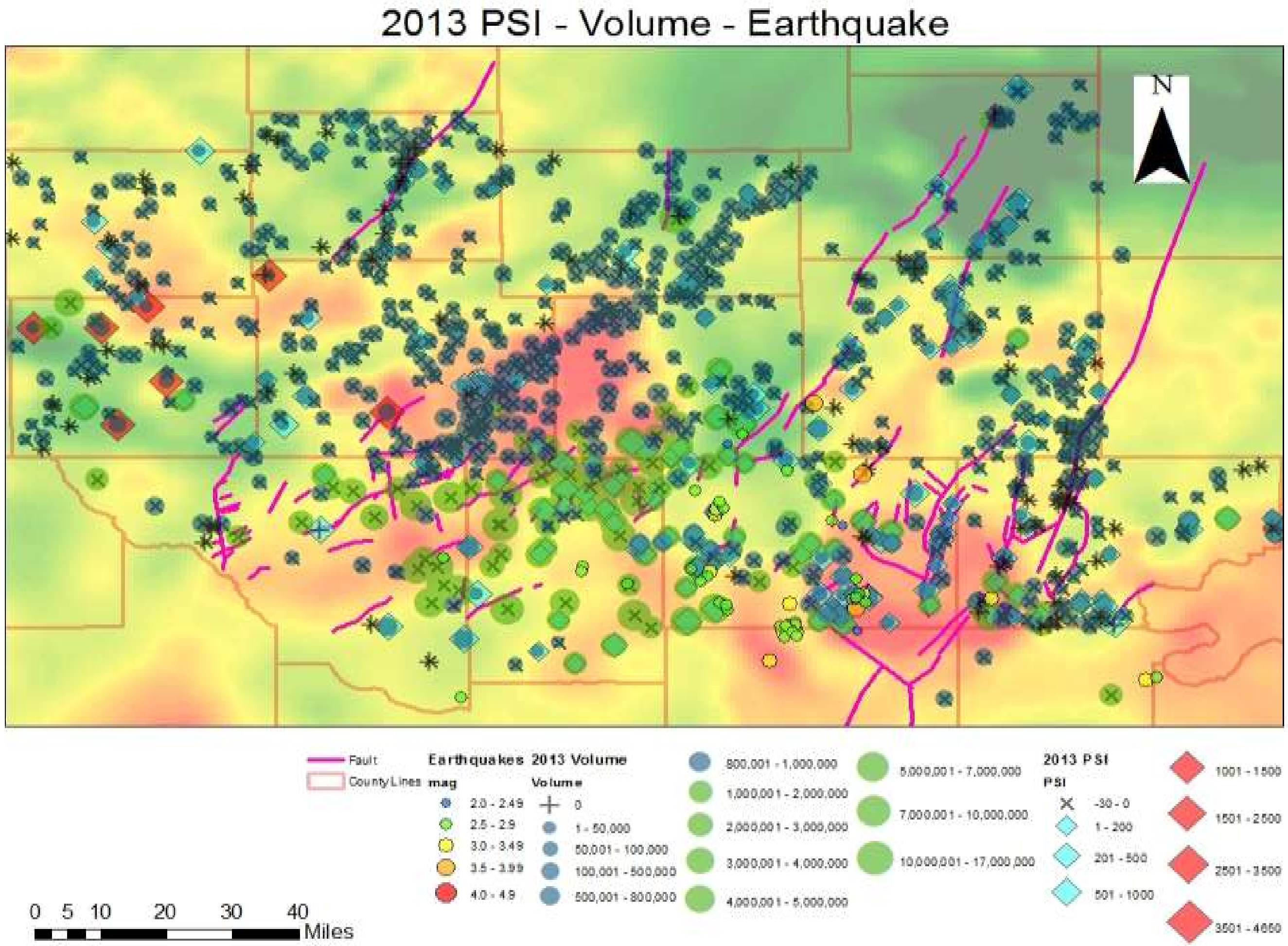

Appendix 1d: Study area in 2013. Where well presence increased in 2012, volumes increased in 2013. The green circles indicate wells disposing 1MMBBL. Red diamonds indicate wells injecting with >1000 PSI. Figure 24a: Injection is at its highest in 2010. Six wells are injecting >1MMBBl of waste water. Note these wells are operating on gravity drain. Aeromagnetic map from Sweeney and Hill (2005). Higher magnetic readings are red, yellow are median magnetic readings, and greens are low magnetic readings.

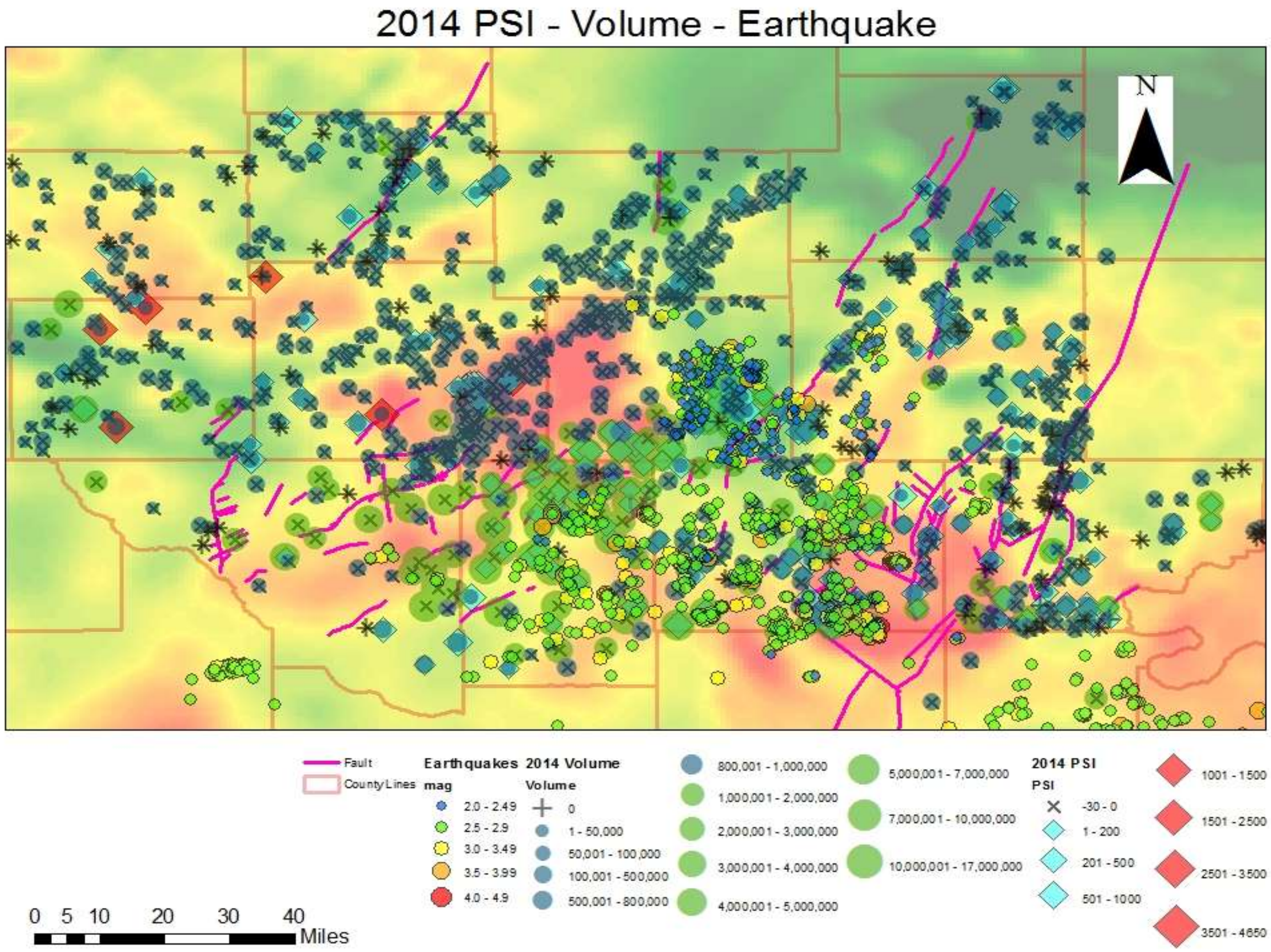

Appendix 1e: Study area in 2014. Total volume disposed is at its highest (849.7 MMBBL). 2014 earthquake total -1647 events. The green circles indicate wells disposing >1MMBBL. Red diamonds indicate wells injecting with >1000 PSI. Figure 24a: Injection is at its highest in 2010. Six wells are injecting >1MMBBl of waste water. Note these wells are operating on gravity drain. Aeromagnetic map from Sweeney and Hill (2005). Higher magnetic readings are red, yellow are median magnetic readings, and greens are low magnetic readings.

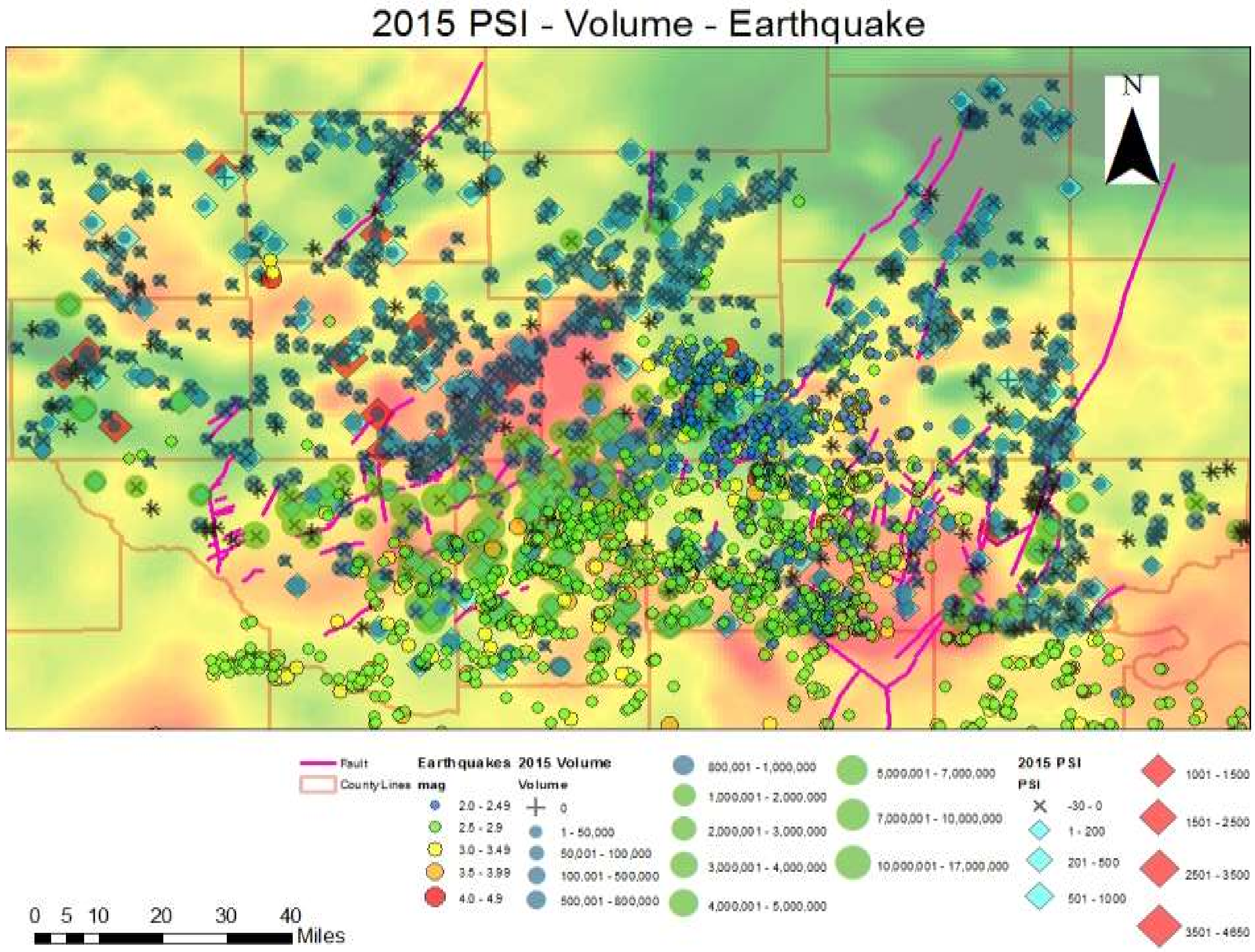

Appendix 1f: Study area in 2015. Total volume disposed decreases (763.4 MMBBL). Earthquakes increase to 3327 events. The green circles indicate wells disposing >1MMBBL. Red diamonds indicate wells injecting with >1000 PSI. Figure 24a: Injection is at its highest in 2010. Six wells are injecting >1MMBBl of waste water. Note these wells are operating on gravity drain. Aeromagnetic map from Sweeney and Hill (2005). Higher magnetic readings are red, yellow are median magnetic readings, and greens are low magnetic readings.

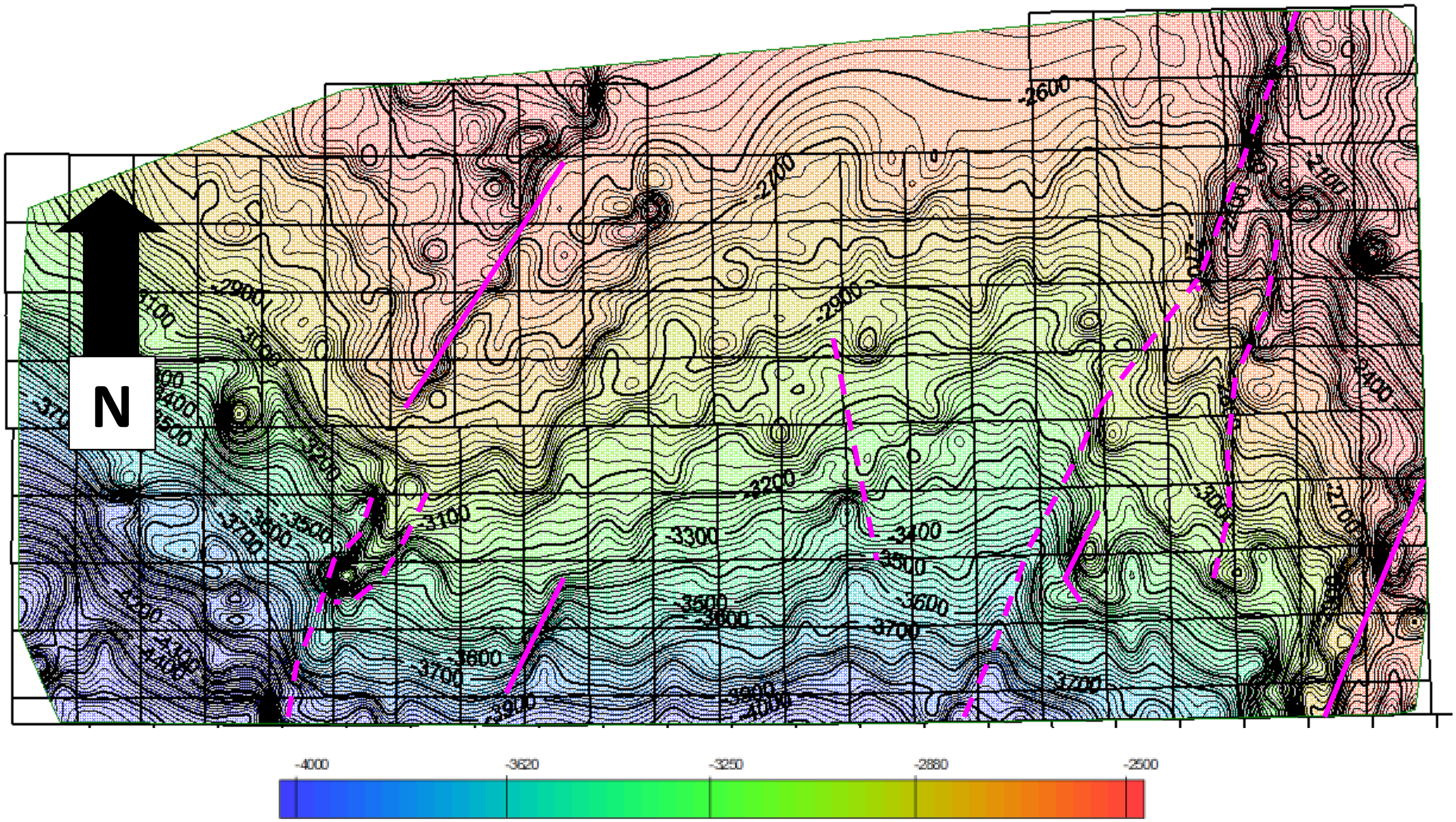

Appendix 2: Top of Simpson structure in Kansas counties. Solid pink lines are faults of high certainty, dashed pink lines are approximated fault positions. Contour interval: 20 ft.

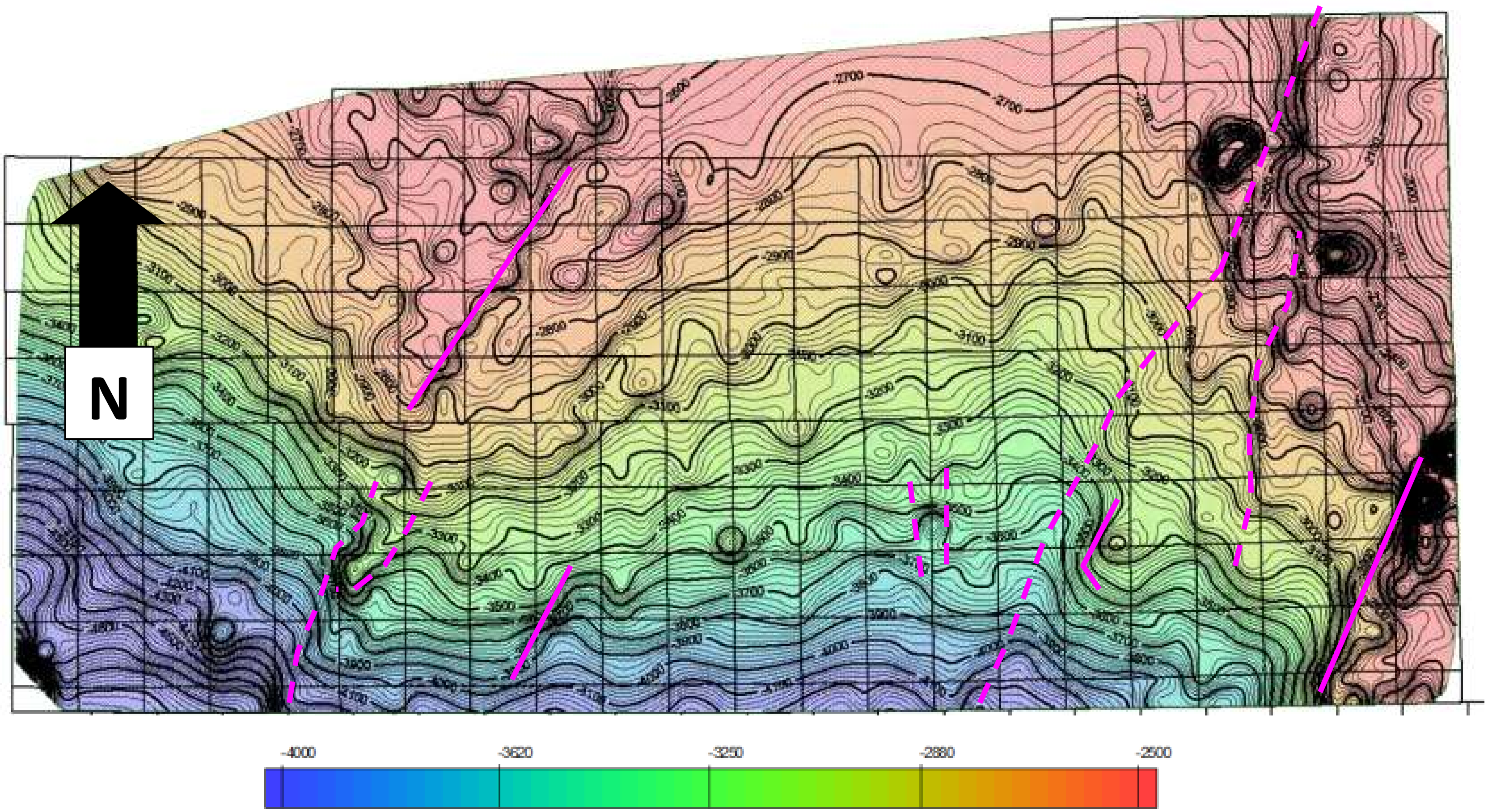

Appendix 3: Top of Arbuckle structure map. Solid pink lines are faults of high certainty, dashed pink lines are approximated fault positions. Contour interval: 20 ft.

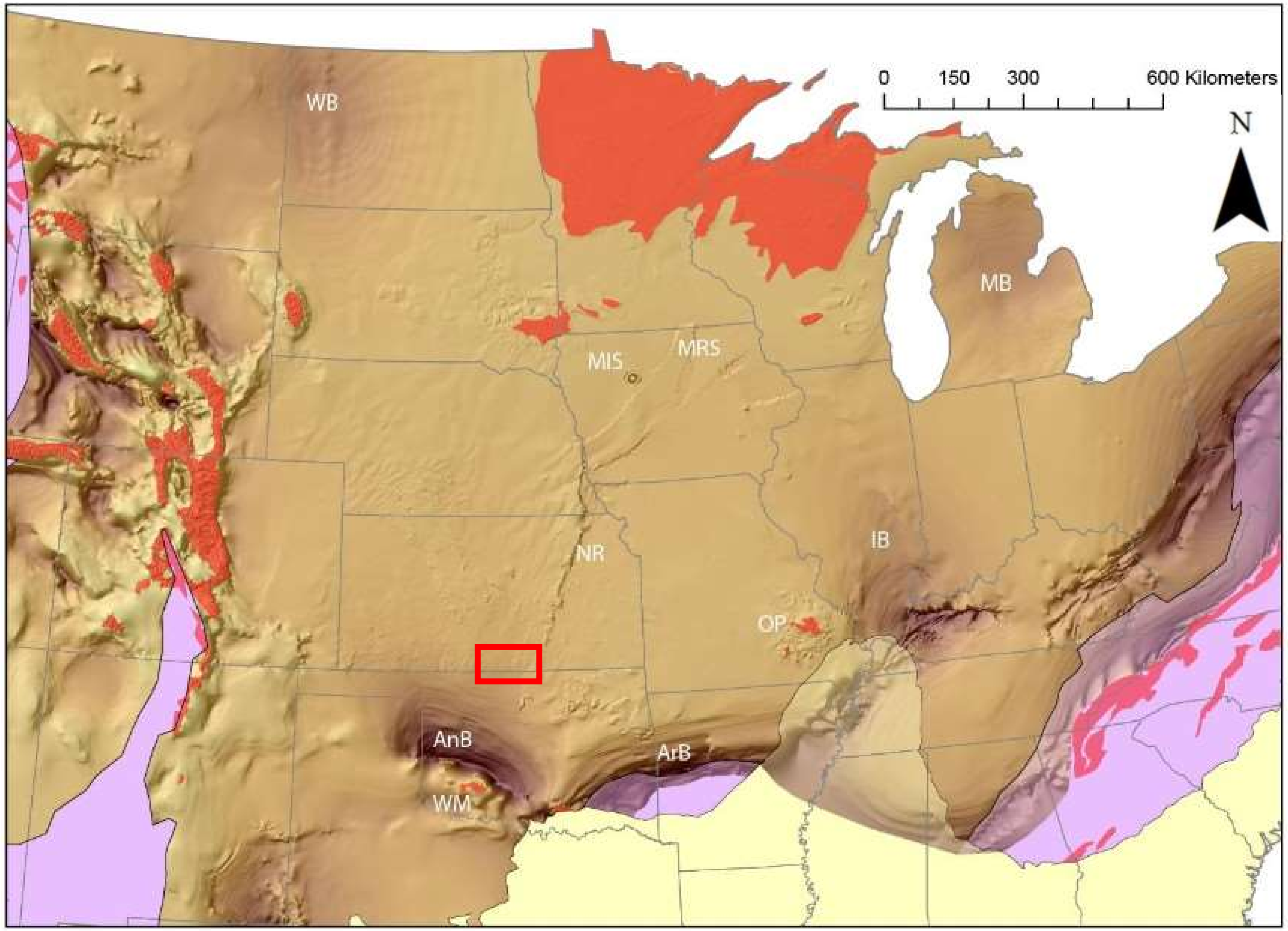

Figure 3.2: Precambrian shaded relief map of the Midcontinent, with overlays of the Cordillera, Appalachians, and Ouachitas in purple, the coastal plain in yellow, and Precambrian outcrops in red. MIS=Manson Impact Structure, MRS=Midcontinent Rift System, NR=Nemaha Ridge, and WM=Wichita Mountains.

Appendix 4: Study area in red. (Domrois, 2013)

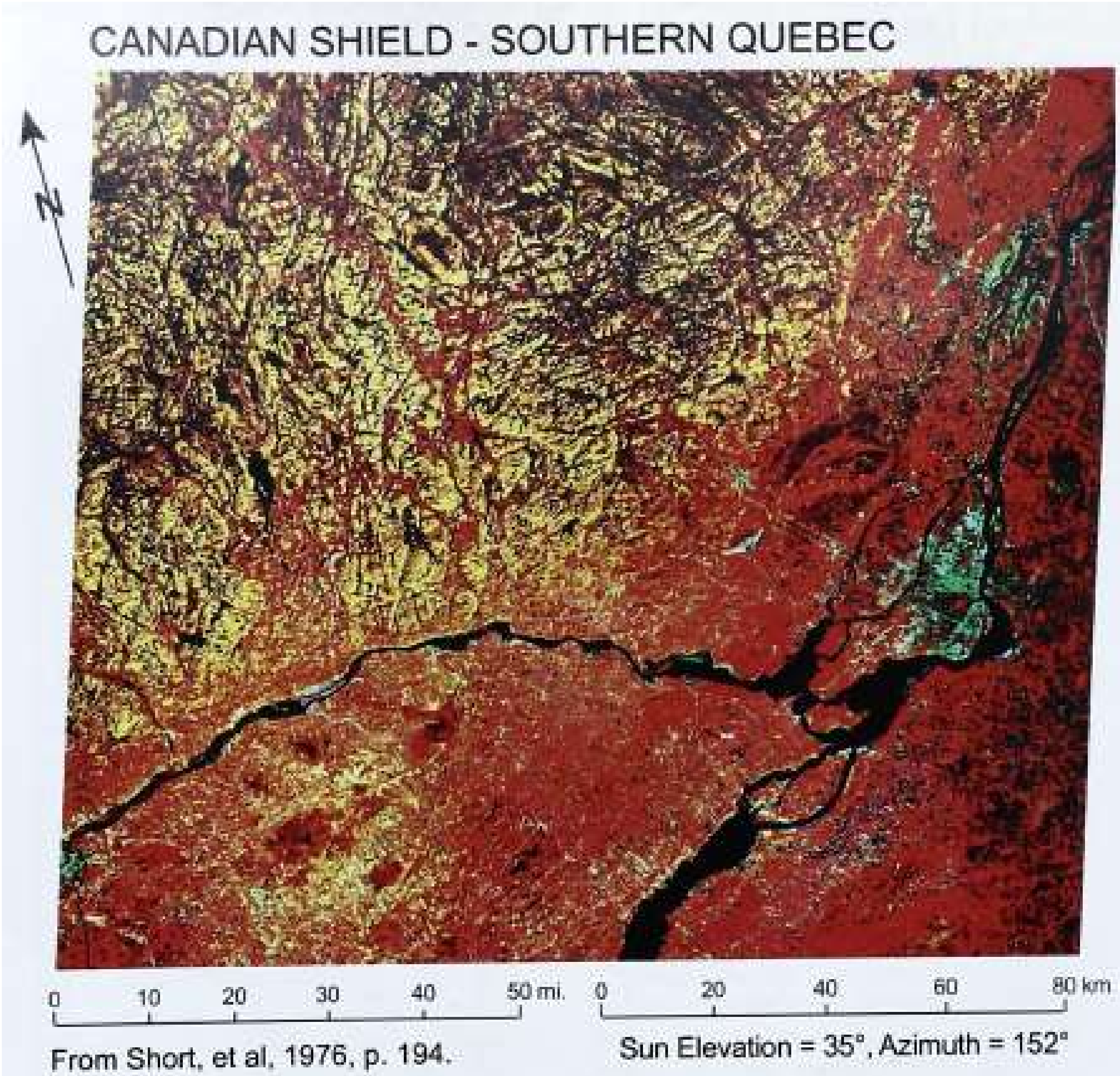

Appendix 5: Landsat image of the Canadian Shield in southern Quebec. Yellow tones in the north-northwest contain abundant basement fractures, which are lacking in the Paleozoic onlap of the Ontario Basin to the south (red tones) (Gay, 2009).

GUYANA SHIELD: SOUTH AMERICA (Venezuela - Brazil)

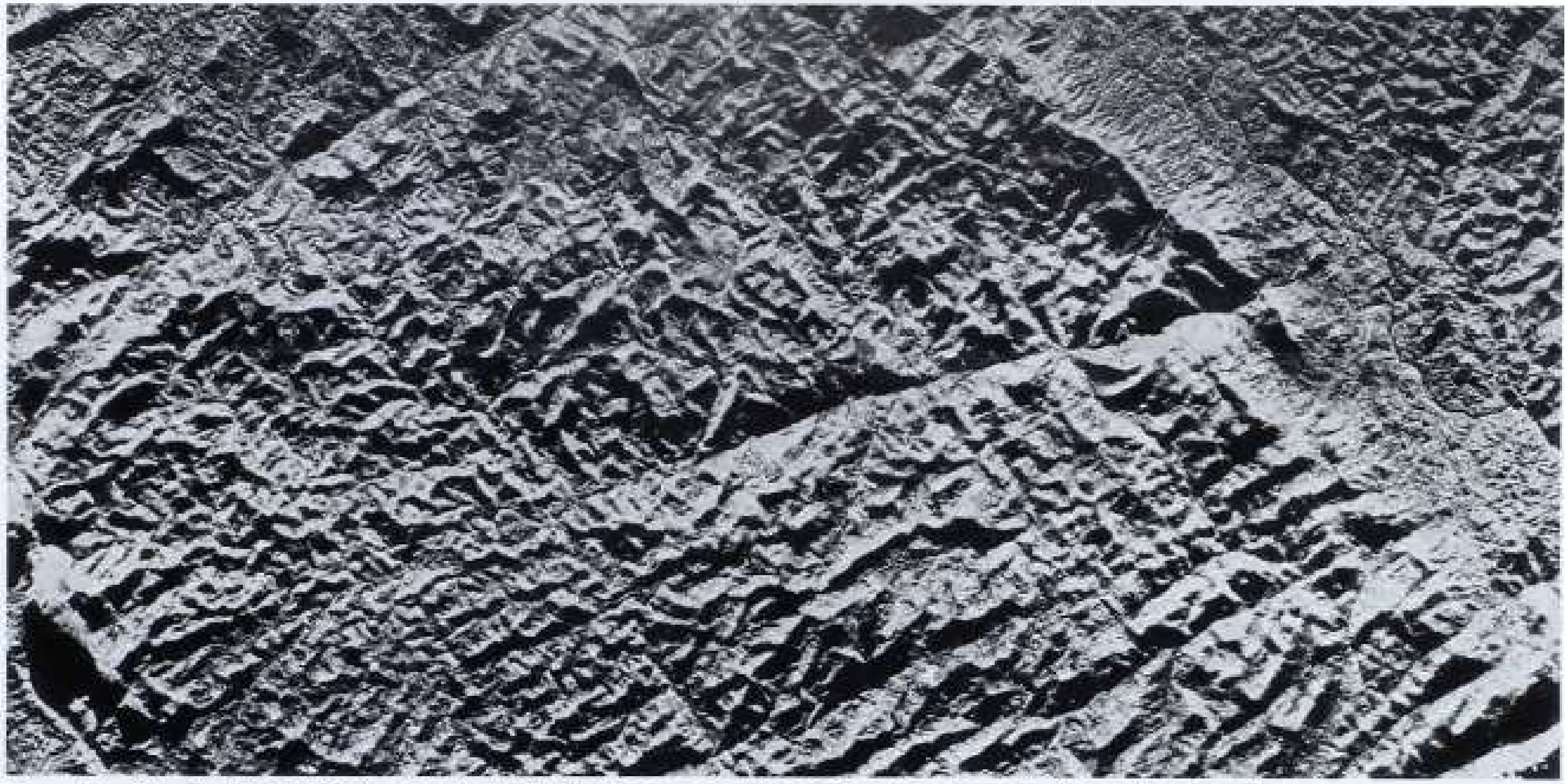

From the Stanford Earth Scientist, April 1972. Image courtesy of Homer Jensen. Aero Service Corp.

Appendix 6: SLAR (Side-looking airborne radar) image of the Guyana Shield in South America. Four facture directions fall into 2 orthogonal sets (Gay, 2009).

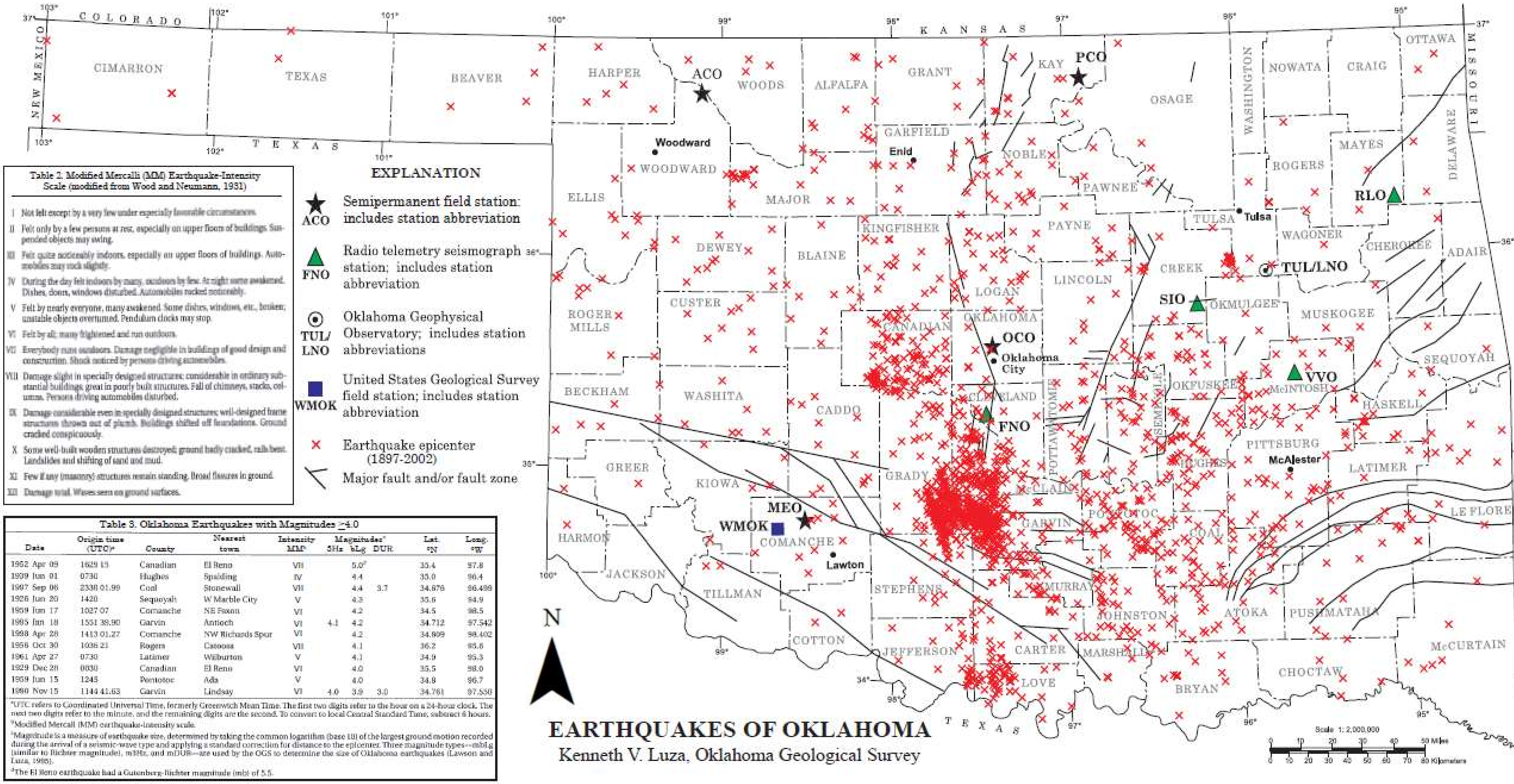

Table 2. Modified Mercalli (MM) Earthquake-Intensity Scale (modified from Wood and Neumann, 1931)

I	Not felt except by a very few under especially favorable circumstances.
II	Felt only by a few persons at rest, especially on upper floors of buildings. Suspended objects may swing.
III	Felt quite noticeably indoors, especially on upper floors of buildings. Automobiles may rock slightly.
IV	During the day felt indoors by many, outdoors by few. At night some awakened. Dishes, doors, windows disturbed. Automobiles rocked noticeably.
V	Felt by nearly everyone, many awakened. Some dishes, windows, etc., broken; unstable objects overturned. Pendulum clocks may stop.
VI	Felt by all; many frightened and run outdoors.
VII	Everybody runs outdoors. Damage negligible in buildings of good design and construction. Shock noticed by persons driving automobiles.
VIII	Damage slight in specially designed structures; considerable in ordinary substantial buildings, great in poorly built structures. Fall of chimneys, stacks, columns. Persons driving automobiles disturbed.
IX	Damage considerable even in specially designed structures; well-designed frame structures thrown out of plumb. Buildings shifted off foundations. Ground cracked conspicuously.
X	Some well-built wooden structures destroyed; ground badly cracked, rails bent. Landslides and shifting of sand and mud.
XI	Few if any (masonry) structures remain standing. Broad fissures in ground.
XII	Damage total. Waves seen on ground surfaces.

Table 3. Oklahoma Earthquakes with Magnitudes ≥4.0

Date	Origin time (UTC)[a]	County	Nearest town	Intensity MM[b]	Magnitudes[c] 3Hz	bLg	DUR	Lat. °N	Long. °W
1952 Apr 09	1629 15	Canadian	El Reno	VII		5.0[d]		35.4	97.8
1939 Jun 01	0730	Hughes	Spalding	IV		4.4		35.0	96.4
1997 Sep 06	2338 01.99	Coal	Stonewall	VII		4.4	3.7	34.676	96.498
1926 Jun 20	1420	Sequoyah	W Marble City	V		4.3		35.6	94.9
1959 Jun 17	1027 07	Comanche	NE Faxon	VI		4.2		34.5	98.5
1995 Jun 18	1551 38.90	Garvin	Antioch	VI	4.1	4.2		34.712	97.542
1998 Apr 28	1413 01.27	Comanche	NW Richards Spur	VI		4.2		34.909	98.402
1956 Oct 30	1036 21	Rogers	Catoosa	VII		4.1		36.2	95.8
1961 Apr 27	0730	Latimer	Wilburton	V		4.1		34.9	95.3
1929 Dec 28	0030	Canadian	El Reno	VI		4.0		35.5	98.0
1959 Jun 15	1245	Pontotoc	Ada	V		4.0		34.8	96.7
1990 Nov 15	1144 41.63	Garvin	Lindsay	VI	4.0	3.9	3.0	34.761	97.550

[a] UTC refers to Coordinated Universal Time, formerly Greenwich Mean Time. The first two digits refer to the hour on a 24-hour clock. The next two digits refer to the minute, and the remaining digits are the second. To convert to local Central Standard Time, subtract 6 hours.

[b] Modified Mercalli (MM) earthquake-intensity scale.

[c] Magnitude is a measure of earthquake size, determined by taking the common logarithm (base 10) of the largest ground motion recorded during the arrival of a seismic-wave type and applying a standard correction for distance to the epicenter. Three magnitude types—mbLg (similar to Richter magnitude), m3Hz, and mDUR—are used by the OGS to determine the size of Oklahoma earthquakes (Lawson and Luza, 1995).

[d] The El Reno earthquake had a Gutenberg-Richter magnitude (mb) of 5.5.

Appendix 7: Earthquakes of Oklahoma 1897-2002. (Luza, 2008)

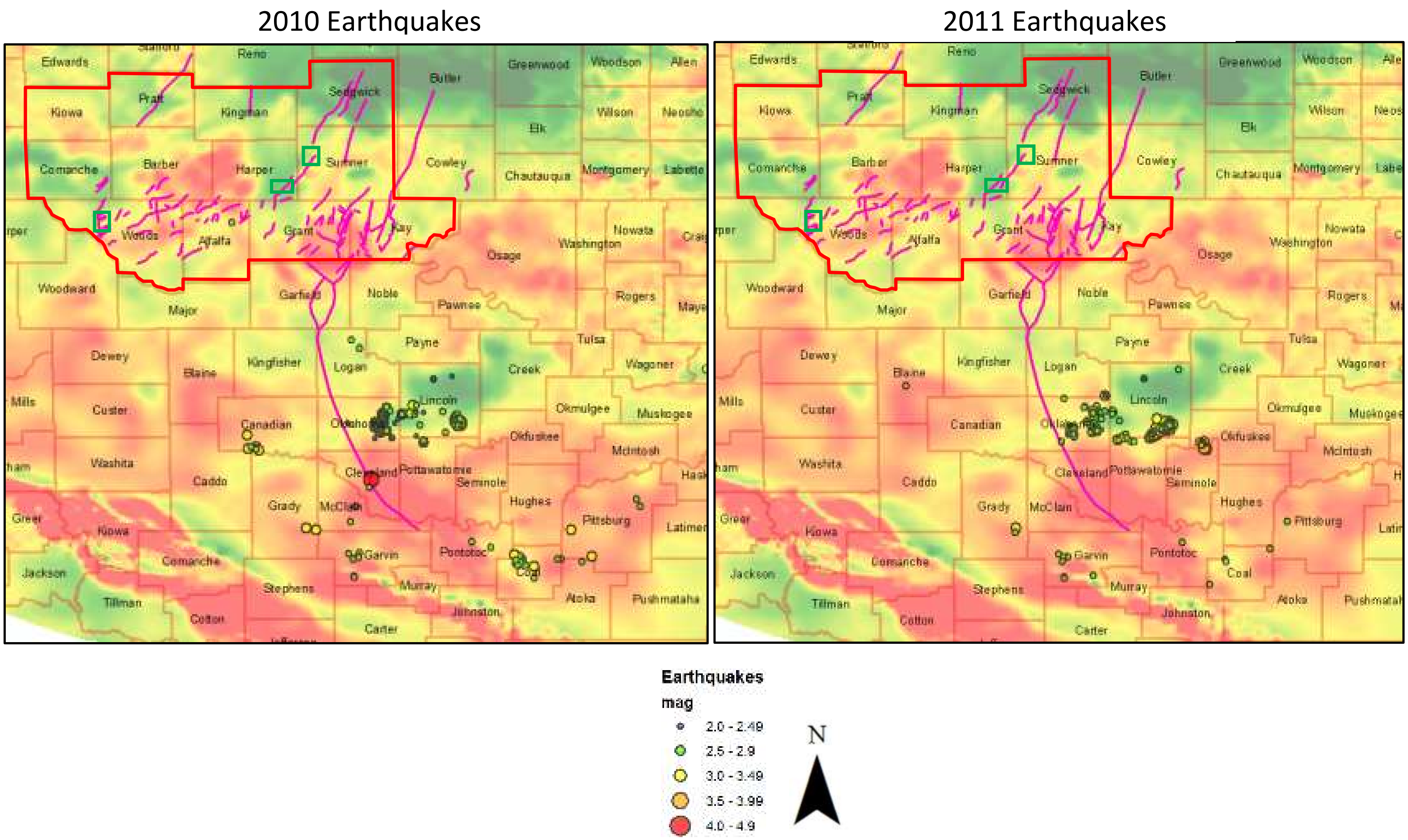

Appendix 8: Comparison of earthquakes south of the study area. Study area in red. AOI's are outlined in green. Faults in pink. Figure 24a: Injection is at its highest in 2010. Six wells are injecting >1MMBBl of waste water. Note these wells are operating on gravity drain. Aeromagnetic map from Sweeney and Hill (2005). Higher magnetic readings are red, yellow are median magnetic readings, and greens are low magnetic readings.

2012 Earthquakes

2013 Earthquakes

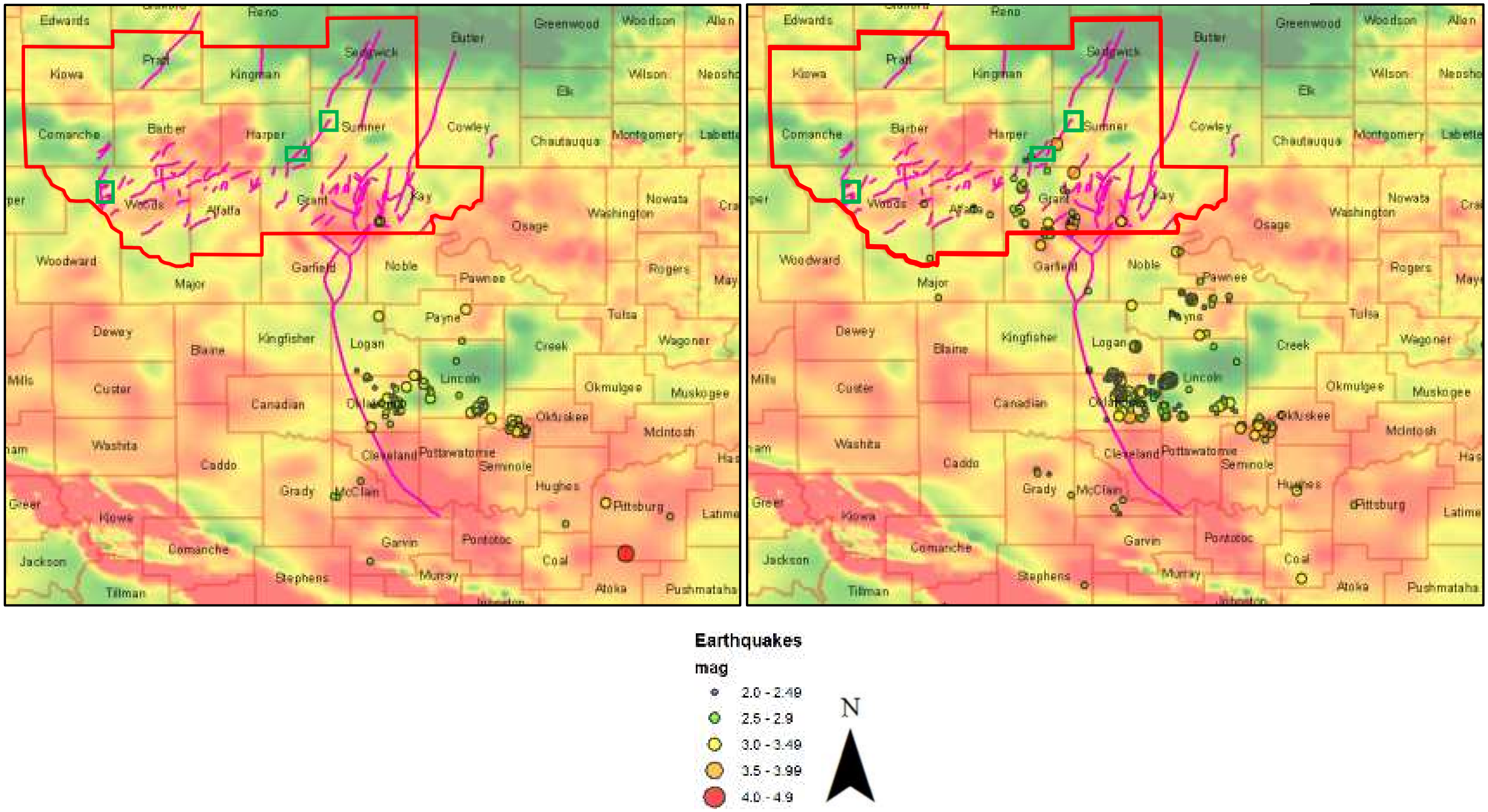

Appendix 9: Comparison of earthquakes south of the study area. Study area in red. AOI's are outlined in green. Faults in pink. Figure 24a: Injection is at its highest in 2010. Six wells are injecting >1MMBBl of waste water. Note these wells are operating on gravity drain. Aeromagnetic map from Sweeney and Hill (2005). Higher magnetic readings are red, yellow are median magnetic readings, and greens are low magnetic readings.

2014 Earthquakes

2015 Earthquakes

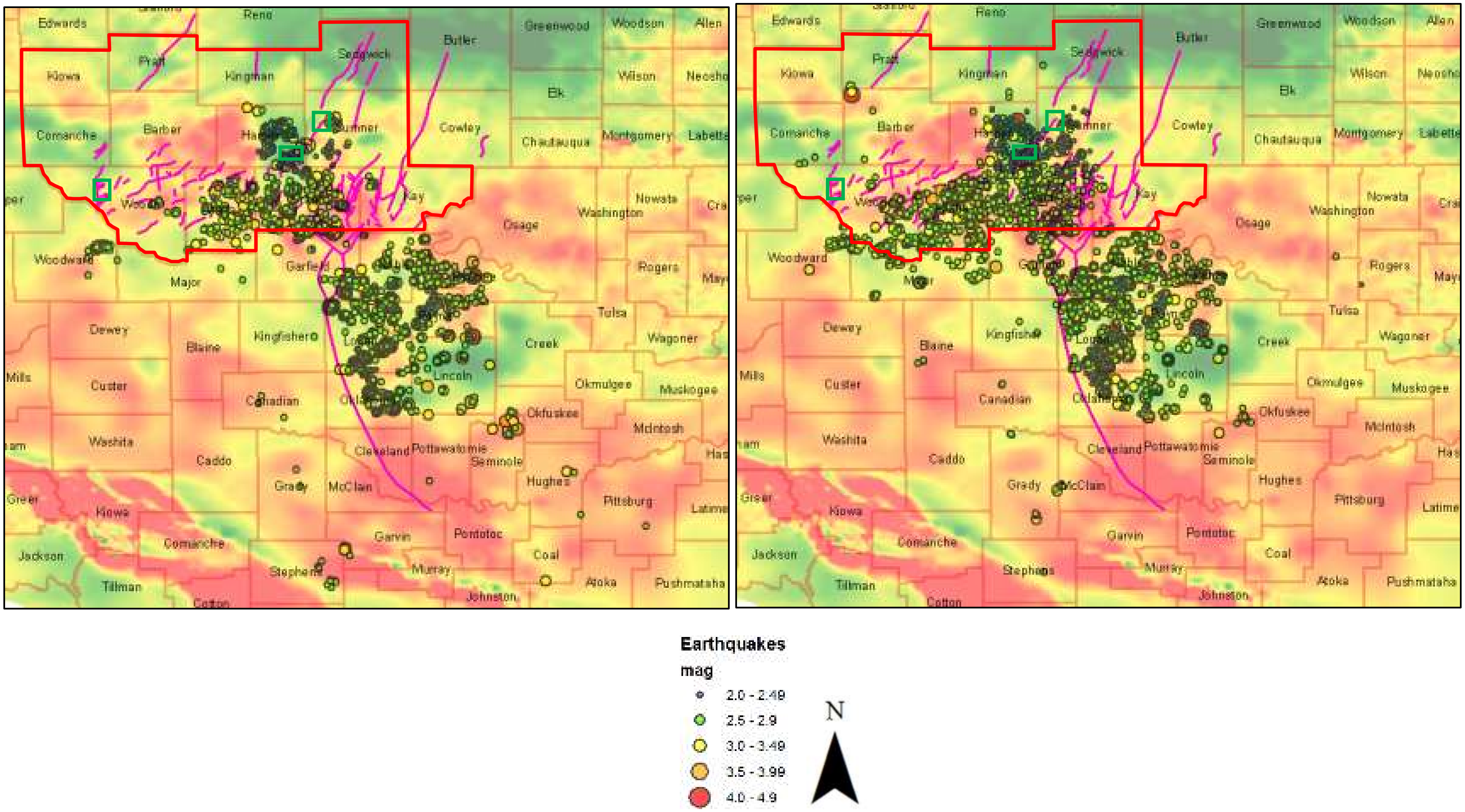

Appendix 10: Comparison of earthquakes south of the study area. Study area in red. AOI's are outlined in green. Faults in pink. Figure 24a: Injection is at its highest in 2010. Six wells are injecting >1MMBBl of waste water. Note these wells are operating on gravity drain. Aeromagnetic map from Sweeney and Hill (2005). Higher magnetic readings are red, yellow are median magnetic readings, and greens are low magnetic readings.

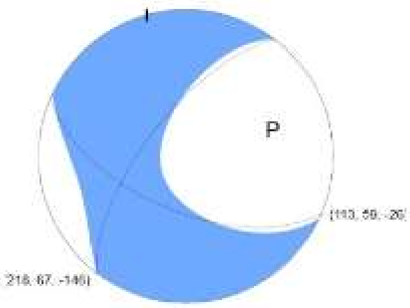

a) Transpressional fault

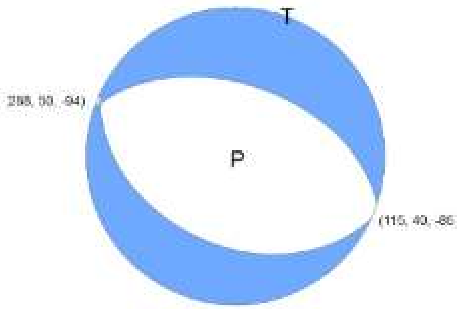

b) Normal fault

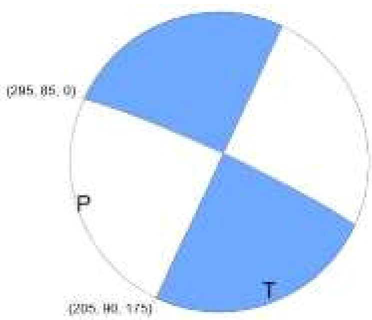

c) Strike - Slip fault

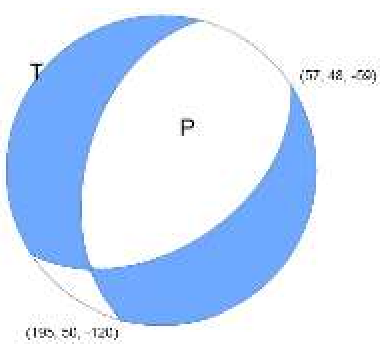

d) Transtensional fault

Appendix 11: Moment tensor types depicted in the study area.